

LINEAR LIBRARY  
C01 0068 4732



**Use of water-soluble phosphine ligands in  
heterogeneous hydroformylation catalysis:  
application to long-chain 1-alkenes**

A thesis submitted to the  
University of Cape Town  
in fulfilment of the requirements for the degree of  
MASTER OF SCIENCE

by

JUDITH G O DU TOIT  
*BSc(Hons) Cape Town*

Department of Chemistry  
University of Cape Town  
Rondebosch  
7700  
South Africa

January 1994

The University of Cape Town has been given  
the right to reproduce this thesis in whole  
or in part. Copyright is held by the author.

The copyright of this thesis vests in the author. No quotation from it or information derived from it is to be published without full acknowledgement of the source. The thesis is to be used for private study or non-commercial research purposes only.

Published by the University of Cape Town (UCT) in terms of the non-exclusive license granted to UCT by the author.

## **Acknowledgements**

## ACKNOWLEDGEMENTS

I would like to extend my sincere thanks to:

My supervisor, Associate Professor Klaus Koch for his expert guidance.

The Head of Department, Professor Luigi Nassimbeni for making the facilities of the department available.

SASOL for their financial assistance and encouragement over the last two years.

Pieter de Koning, proof-reader and fellow explorer; TG, DA, RJ, FW, NC, CS and the rest of the Chemistry Department for making my time at UCT lively and enjoyable.

My parents and family for their absolute support and understanding.

# **Table of Contents**

# TABLE OF CONTENTS

<b>ACKNOWLEDGEMENTS</b>	<b>i</b>
<b>TABLE OF CONTENTS</b>	<b>iii</b>
<b>ABSTRACT</b>	<b>viii</b>
<b>CHAPTER 1 – INTRODUCTION</b>	<b>1</b>
<b>1.1 Hydroformylation Catalysts</b>	<b>4</b>
Simple cobalt carbonyl catalysts	5
Tertiary-phosphine modified cobalt carbonyl systems	7
Modified rhodium catalysts	8
<i>The proposed catalytic cycle</i>	
Nature and choice of ligand	11
<i>Electronic donor-acceptor properties</i>	
<i>Cone angle</i>	
Other metal catalysts	14
<b>1.2 Cobalt versus Rhodium</b>	<b>15</b>
<b>1.3 Catalyst Deactivation</b>	<b>16</b>
<b>1.4 Homogeneous versus Heterogeneous Catalysis</b>	<b>17</b>
Supported catalysts	18
Catalysts in biphasic systems	20
<i>Catalysts in the aqueous phase</i>	
<i>Supported aqueous phase catalysts</i>	

<i>Phase transfer agents</i>	
<b>1.5 Objectives of the project</b>	<b>25</b>
<b>CHAPTER 2 – METHODS AND PREPARATION</b>	<b>28</b>
<b>2.1 Synthesis and Characterisation</b>	<b>30</b>
Preparation of ligands	30
<i>tripotassium salt of tri(m-sulfonatophenyl)phosphine, TPPTS</i>	
<i>tripotassium salt of tri(m-sulfonatophenyl)phosphine oxide, TPPOTS</i>	
<i>sodium diphenylphosphinebenzene-m-sulfonate, TPPMS</i>	
Preparation of metal complexes	37
<i>carbonylhydridotris(triphenylphosphine) rhodium(I), RhH(CO)(PPh<sub>3</sub>)<sub>3</sub></i>	
<i>carbonylhydridotris[tri(m-sulfonatophenyl)phosphine] rhodium(I), RhH(CO)(TPPTS)<sub>3</sub></i>	
<b>2.2 Experimental</b>	<b>43</b>
General	43
Synthesis	46
<b>2.3 Characterisation and Quantification of Products of Catalysis</b>	<b>50</b>
Theory of quantitative <sup>13</sup> C NMR Spectroscopy	53
<i>Precautions taken to ensure suitable conditions for quantitative</i>	
Results and discussion	59
<i>Characterisation of products by <sup>13</sup>C NMR spectroscopy</i>	
<i>Measurement of T<sub>1</sub> values for the application of quantitative spectroscopy</i>	
<i>Comparison of quantitative results using GC and <sup>13</sup>C NMR</i>	
<b>CHAPTER 3 – CATALYTIC HYDROFORMYLATION REACTIONS</b>	<b>68</b>
<b>3.1 Reaction Procedure</b>	<b>70</b>
<b>3.2 Hydroformylation Reactions</b>	<b>71</b>

Two-phase hydroformylation reactions	71
<i>Rhodium catalytic species prepared in situ</i>	
<i>Heterogeneous hydroformylation using a synthesised catalyst precursor</i>	
Homogeneous hydroformylation	84
<b>CHAPTER 4 – CATALYST SPECIATION</b>	<b>86</b>
<b>4.1 Rhodium Speciation</b>	<b>89</b>
Rhodium(III) complexes	89
<i>chloro-aqua species</i>	
<i>phosphine complexes</i>	
Rhodium(I) complexes	92
<i>phosphine complexes</i>	
<b>4.2 Phosphorous NMR Spectroscopy of Rhodium Complexes</b>	<b>93</b>
Factors affecting rhodium-phosphorous coupling constants	93
<i>Differences in coupling in rhodium(I) and rhodium(III) complexes</i>	
<i>Effect of the nature of the ligand trans to phosphine</i>	
<b>4.3 Speciation Experiments</b>	<b>96</b>
Tertiary-phosphine rhodium complexes formed in aqueous solution	98
<i>System 1</i>	
<i>System 2</i>	
<i>System 3</i>	
Distribution of species under hydroformylation conditions	113
<sup>31</sup> P NMR spectrum of the synthesised catalytic precursor,	
RhH(CO)(TPPTS) <sub>3</sub>	113
<b>4.4 Conclusion</b>	<b>116</b>

<b>CHAPTER 5 - DISCUSSION</b>	<b>118</b>
<b>5.1 Two-phase Hydroformylation Reactions</b>	<b>120</b>
Rhodium catalytic species prepared <i>in situ</i>	120
<i>Influence of chain-length on activity</i>	
<i>Influence of rhodium concentration</i>	
<i>Effect of excess phosphine ligand</i>	
<i>Conclusion</i>	
Heterogeneous hydroformylation using synthesised catalyst precursor	132
<b>5.2 Homogeneous Hydroformylation</b>	<b>134</b>
<b>5.3 Conclusion</b>	<b>135</b>
<b>REFERENCES</b>	<b>137</b>

# **Abstract**

## Abstract

The two-phase rhodium–tri(*m*-sulfonatophenyl)phosphine (Rh–TPPTS) system for the hydroformylation of 1-octene, 1-decene, and 1-dodecene to the corresponding aldehydes, has been investigated. Due to the two distinct phases – the catalytic species in the aqueous phase and the products and reactants in the organic phase – the separation of the catalyst was easily facilitated. A comparison was made of the activity, selectivity towards linear aldehydes, and catalyst lifetime of two systems where *i*) the active catalytic species were generated *in situ* from rhodium trichloride (RhCl<sub>3</sub>·3H<sub>2</sub>O) and excess phosphine ligand (TPPTS) under mild hydroformylation conditions (5 MPa H<sub>2</sub>/CO (1:1); 100 °C); and *ii*) where the rhodium(I) complex, RhH(CO)(TPPTS)<sub>3</sub> is used as the catalyst precursor. The former system was found to be superior in activity and selectivity to that of the latter, achieving fairly high conversions of *ca.* 60% for the hydroformylation of 1-octene, with *n:iso* ratios of up to 16:1 for a catalyst composition a Rh:P ratio of 1:30. Unfortunately low conversions of *ca.* 10% for the hydroformylation of 1-decene and *ca.* 4% for that of 1-dodecene resulted under the same conditions. While the reasons for the drastic decrease in conversion for C<sub>10</sub> and C<sub>12</sub> alkenes is not completely clear, this poor conversion is attributed to the extremely low solubility of the long-chain 1-alkenes in the aqueous phase. Under certain optimum conditions (Rh:P ≥1:20), virtually no leaching of rhodium into the organic phase was detected.

A <sup>31</sup>P NMR spectroscopic study was undertaken in an attempt to ascertain the nature and distribution of rhodium tertiary-phosphine complexes in the aqueous phase before and after the mixture was subjected to standard hydroformylation conditions.

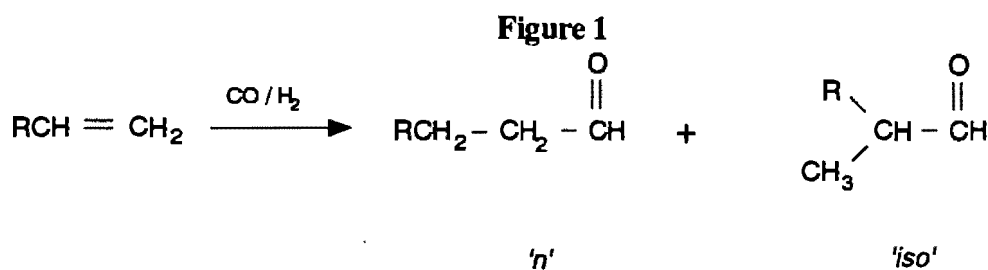
# **Chapter 1**

## **Introduction**

# Chapter 1

## Introduction

One of the oldest and most common homogeneous catalytic reactions of olefins is hydroformylation, the addition of carbon monoxide (CO) and hydrogen (H<sub>2</sub>), to produce an aldehyde which may be linear or branched:

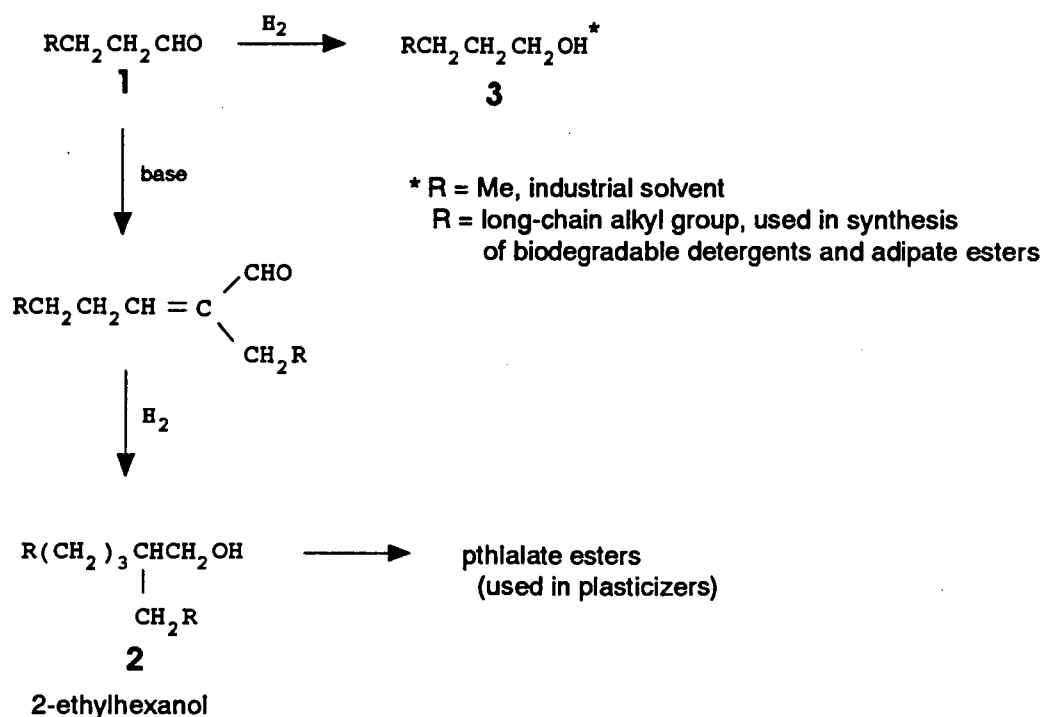


In the absence of isomerisation of the alkene substrate there are two possible aldehyde products depending on the orientation of the H-CHO addition across the double bond of the alkene. With a terminal alkene as substrate, anti-Markovnikov addition of H and CHO leads to the production of the linear (*'n'*) aldehyde while Markovnikov addition results in the branched (*'iso'*) product (Figure 1). In all but a few specialised cases the linear (normal) isomer is the preferred commercial product and thus the normal:branched (*n:iso*) ratio is an extremely important parameter in industrial hydroformylation processes.

Hydroformylation is now one of the largest commercial processes based on homogeneous catalysis by transition metal complexes and its uses have grown steadily.<sup>1</sup> This success is due largely to the availability of inexpensive raw materials, in particular propene and synthesis gas (CO/H<sub>2</sub>). A principal example of hydroformylation is the manufacture of butyraldehyde (butanal) from propene. Synthesis gas has been produced on a large scale for many years as a source of hydrogen for ammonia and methanol production mainly by reforming methane, although other processes involving heavy oil residuum partial oxidation and coal gasification have been commercialised in recent years. Butanal (1) is then either converted to 2-ethylhexanol (2) via an aldol condensation/hydrogenation sequence, or directly hydrogenated to n-butanol (3), as depicted in Scheme 1.<sup>2</sup>

### Scheme 1

Synthesis of important commercial products from linear aldehydes



Since the *iso*-isomer has considerably fewer end uses and hence a much lower commercial value, high *n:iso* ratios are particularly important in the industrial hydroformylation of propene.

A second major application of hydroformylation is the synthesis of long-chain alcohols from terminal olefins of higher molecular weight, ( $C_7$  and greater), such as 1-octene, with subsequent or concurrent hydrogenation.<sup>3</sup> Again selectivity to the *n*-isomer is an important consideration in this process design since the linear products are especially useful and valuable in the synthesis of biodegradable detergents and for the production of adipate esters. The latter serve as high temperature lubricants and as plasticizers.

## 1.1 Hydroformylation Catalysts

In 1938 Roelen at Ruhrchemie AG, discovered that cobalt-containing heterogeneous catalysts effected the addition of carbon monoxide (CO) and hydrogen ( $H_2$ ) to ethylene, to yield aldehydes and ketones.<sup>4</sup> It was soon recognised that the actual catalytic species was a soluble cobalt carbonyl species formed by reductive carbonylation of cobalt oxide, with the reaction taking place in the homogeneous liquid phase. This reaction was soon developed into an industrial synthesis of aldehydes and alcohols.

In the development of both homogeneous and heterogeneous hydroformylation catalysts, the areas of primary concern are:

- percentage of olefin conversion to the corresponding alcohol or aldehyde and selectivity of the reaction to the linear product.
- molar ratio of normal to iso alcohols or aldehydes (*n:iso*).

- separation of the catalyst from the reaction medium containing the hydroformylation products.
- stability and lifetime of the catalyst.
- catalyst reactivation.

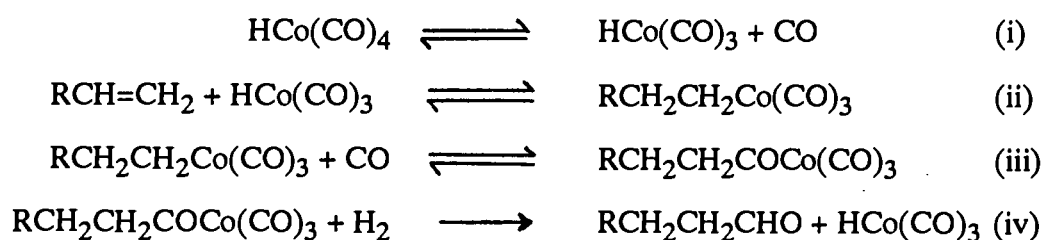
Three types of homogeneous transition metal complexes are used in industrial hydroformylation processes. In order of both their present commercial importance, and historic development these are:

- i) hydrido cobalt carbonyl complex,  $[\text{HCo}(\text{CO})_4]$
- ii) tertiary-phosphine hydrido cobalt carbonyl species, [e.g.,  $\text{CoH}(\text{CO})(\text{PPh}_3)_3$ ]
- iii) tertiary-phosphine hydrido rhodium(I) carbonyl species, [e.g.,  $\text{RhH}(\text{CO})(\text{PPh}_3)_3$ ]

### 1.1.1 Simple cobalt carbonyl catalysts

Processes using unmodified cobalt carbonyl catalysts (*i.e.*, no added inert ligands), were first commercially operational by the late 1940s, and still constitute the major percentage, in terms of capacity, of today's hydroformylation plants.<sup>5</sup> Typically temperatures in the range 140-180 °C with pressures ranging from 20-35 MPa are employed which results in a mixture (roughly 3:1) of both linear and branched alcohols or aldehydes.

The main steps in this mechanism first elucidated by Breslow and Heck,<sup>6</sup> are as follows:



where step (ii) involves the  $\beta$ -hydrogen transfer to the coordinated olefin, step (iii) the insertion of CO to form the acyl, and step (iv) acyl cleavage by hydrogen. All of these proposed steps in the catalytic cycle are reversible, with the possible exception of the acyl complex to form the aldehyde (step iv). Step (ii) is the olefin insertion into a metal-hydride bond, the reverse being  $\beta$ -hydride elimination to form an M-H bond and olefin metal complex. Since the reaction is reversible, isomerism can result, producing alkane products.

These simple cobalt carbonyl catalysts are reasonably satisfactory for industrial hydroformylation processes, but several problems do exist. The carbonyls  $\text{HCo}(\text{CO})_4$  and  $\text{Co}_2(\text{CO})_8$  are unstable and volatile, and easily decompose with the formation of cobalt metal. These properties make them difficult to separate from aldehyde products during the product purification and catalyst recycling steps. Other disadvantages include the loss of about 15 % of the alkene by hydrogenation, and the formation of ketone and condensation by-products. Equally seriously, the severe reaction conditions (temperature: 140-180 °C; pressure: 20-35 MPa) impose economic penalties for the construction and operation of the high-pressure reactor. More significantly, the limited selectivity for the desired linear aldehyde and alcohol increases the consumption of starting materials and requires large distillation facilities for product purification. Also, if the normal-isomer is the required product, a normal:branched (*n:iso*) of 3 or 4 to 1, which is the best achievable value using such processes, leaves much room for improvement.

The first important breakthrough in overcoming these disadvantages occurred in the early sixties, when Slauch and Millineaux working in Shell Oil's laboratories,<sup>7</sup> discovered that the addition of tertiary-phosphine ligands to the cobalt carbonyl system led to complexes (*e.g.*,  $\text{CoH}(\text{CO})(\text{PPh}_3)_3$ ), which catalysed the direct

synthesis of linear alcohols, even from internal olefins, and did not depend on high carbon monoxide pressures for their stability.

### 1.1.2 Tertiary-phosphine modified cobalt carbonyl systems

Compared to the unmodified systems, cobalt carbonyl hydroformylation catalysts containing alkyl tertiary-phosphines are more stable - requiring  $H_2/CO$  pressures of as low as 0.5-1 MPa with temperatures in the range of 100-180 °C. Due to their increased stability at lower pressures and higher temperatures, conditions which are typically used for the hydrogenation of alkenes, this system tends to give rise to alcohols rather than aldehydes under hydroformylation conditions. Unfortunately their activity is lower than that of the simple cobalt carbonyl catalyst.

The presence of the phosphine ligand is important in the stabilization of the catalyst during product recovery, as well as in its ability to direct the reaction to the formation of the desired product, *i.e.* the *n*-isomer. The increased stability of the complex can be attributed to electronic effects (electron donor-acceptor properties) of the phosphine ligand, while the increased linear selectivity is due to the steric hindrance imposed by the bulky phosphine ligands which preferentially direct the addition of the H and CHO groups in an anti-Markovnikov manner, which results in the production of a linear aldehyde. This results in an increase in the desired *n:iso* ratio.

Since both selectivity and stability of the catalyst are favoured by a large excess of phosphine ligand, it has been suggested that molten triphenylphosphine (m.p. 79 °C) is the ideal solvent for the reaction. However, a large excess of ligand unfortunately decreases the rate of reaction. Thus for practical operation a compromise between reaction rate and reaction selectivity must be made. As far as the nature of the

tertiary-phosphine ligand is concerned, of those tested,<sup>5</sup> triphenylphosphine appears to be optimal in terms of reaction rate, selectivity and also of cost.

### 1.1.3 Modified rhodium catalysts

Research in industrial laboratories in the 1950s showed that many rhodium complexes catalyse the hydroformylation of olefins under very mild conditions.<sup>3</sup> Despite their high activity however, the simple rhodium compounds were not very attractive as they yielded mostly branched aldehydes. It was later found that the addition of phosphine ligands such as triphenylphosphine or triphenylphosphite gave active catalysts with excellent selectivity for the desired linear aldehydes, and activities  $10^2$ - $10^4$  times that of their cobalt analogues. A further advantage were the lower pressure and temperature conditions required for operation (1.5-2.5 MPa and 80-120 °C respectively). This modified-rhodium technology was successfully put into commercial production by Union Carbide in 1976.<sup>8</sup>

Simultaneously with the commercial development, Wilkinson and his co-workers studied the mechanism of hydroformylation with  $\text{RhH}(\text{CO})(\text{PPh}_3)_3$  as a catalyst.<sup>9</sup> These studies have produced a good understanding of the role of the catalyst in the hydroformylation and hydrogenation of alkenes. Under hydroformylation conditions, tertiary-phosphine rhodium complexes all seem to give rise to the hydridocarbonyldi(tertiaryphosphine)rhodium species,  $\text{RhH}(\text{CO})(\text{PPh}_3)_2$ . This is one of the key intermediates in these systems.

The commercial catalyst may be prepared by reaction of high-surface-area metallic rhodium (such as rhodium on charcoal) with synthesis gas in the presence of triphenylphosphine or triphenylphosphite. In the presence of this catalyst, propene reacts with synthesis gas at 1-2 Mpa and *ca.* 100 °C to yield the linear aldehyde,

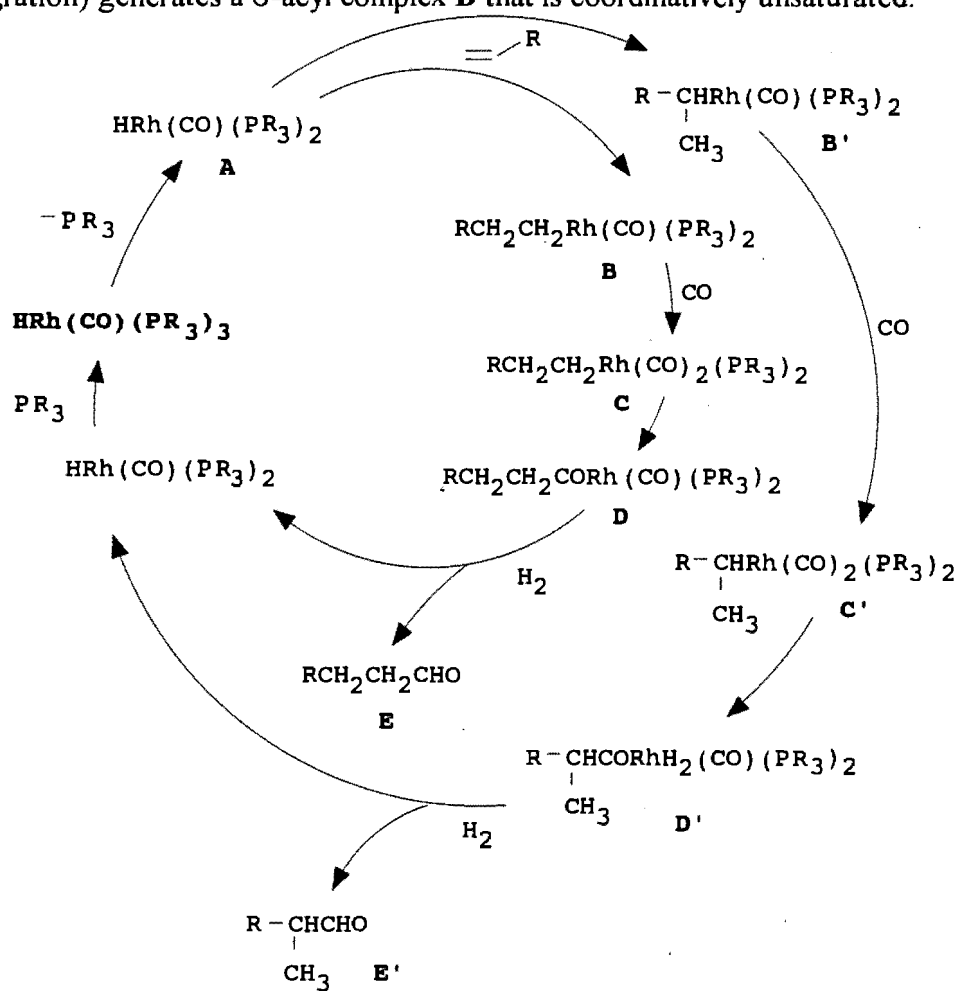
*n*-butyraldehyde predominantly. Little or no aldehyde is hydrogenated to C<sub>4</sub> alcohols, although some olefin is lost through hydrogenation to propane. The selectivity to the desired linear aldehyde is very high, > 90 %, when excess phosphine ligand is present.<sup>3</sup>

### 1.1.3.1 *The proposed catalytic cycle*

The catalytic cycle for the hydroformylation of olefins has not been elucidated fully, but the available evidence of the rhodium system based on RhH(CO)(PPh<sub>3</sub>)<sub>3</sub>, is consistent with the suggested cycle outlined in Scheme 2.<sup>3</sup> The mechanism of hydroformylation with the modified rhodium catalysts is quite similar to that of the cobalt catalyst. Many of the intermediates isolated in the course of mechanistic studies at atmospheric pressure,<sup>10</sup> have also been observed by infrared studies at pressures typical of commercial operations.<sup>11</sup> The immediate catalytic precursor is HRhCO(PPh<sub>3</sub>)<sub>3</sub>. This compound is much more stable than HCo(CO)<sub>4</sub>, but requires the presence of some excess ligand for stabilisation during the catalytic cycle.

As in the cobalt system, the complex undergoes reversible phosphine ligand dissociation at rates dependent on the nature and concentration of the ligand, and the temperature employed. Such dissociation results in a coordinatively unsaturated square-planar trans-bisphosphine-monocarbonyl hydride complex **A**, that can bind the olefin. The  $\alpha$ -olefin enters the vacant coordination site in **A**, and inserts into the Rh-H bond to form a coordinated linear (**B**) or branched alkyl (**B'**) group. It is at this stage that the phosphine ligand concentration has the greatest influence in affecting the *n*:*iso* ratio of the aldehydes produced. If the olefin  $\pi$ -complex bears two large phosphine ligands (resulting from the high concentration of the phosphine ligand), crowding in the coordination sphere of the metal will favour formation of the *n*-alkyl derivative **B**, via anti-Markovnikov addition of H and the formyl group CHO. If however, one of the phosphine ligands has been replaced by a much

smaller carbon monoxide (CO) ligand, there will be space to form, via Markovnikov addition of H and CHO, the more bulky *iso*-alkyl group B'. The alkyl metal complex B is coordinatively unsaturated and readily binds another CO ligand to give the dicarbonyl complex C (or C'). Carbon monoxide (CO) insertion (or alkyl migration) generates a  $\sigma$ -acyl complex D that is coordinatively unsaturated.



**Scheme 2**

Simplified proposed catalytic cycle for hydroformylation using a triphenylphosphine-modified rhodium catalyst.<sup>3</sup>

Oxidative addition of hydrogen ( $H_2$ ) is postulated to follow, which is the only step in the cycle that involves a change in oxidation state of the metal and thus is probably rate-determining. This is followed by reductive elimination of the acyl group to yield the linear or branched aldehyde, **E** and **E'** respectively, and regenerate the catalytically active rhodium hydride.

The major uncertainties in this proposed mechanism concern the number of phosphine and CO ligands in the intermediates.

As in other homogeneous catalytic systems, many different catalyst precursors can be used since the catalytically active species is probably generated under reaction conditions. These include rhodium metal on carbon,  $Rh_4(CO)_{12}$ ,  $Rh_2O_3$ ,  $RhCl_3 \cdot 3H_2O$ ,  $acacRh(CO)_2$ ,  $RhCl(CO)(PPh_3)_3$  and  $RhH(CO)(PPh_3)_3$ . In cases where one starts with a higher oxidation state of rhodium, reduction by hydrogen ( $H_2$ ), and carbon monoxide (CO) takes place under reaction conditions.

#### 1.1.4 Nature and choice of ligand

Trialkylphosphines do not participate directly in the catalytic cycle in the sense that they remain associated with the transition metal and do not appear as part of the product(s). Although these ligands do not contribute directly to the products of the catalysed reaction, they play a vital role in determining the activity and selectivity of the catalyst system. The ligand can influence the behavior of a transition-metal catalyst by modifying the steric and/or electronic environment at the active site.

In an attempt to separate electronic and steric effects in trivalent-phosphine ligands, Tolman has proposed two parameters,<sup>12</sup> the first based on the electron donor-

acceptor properties of the phosphine ligands, and the second based on size and thus the steric effect of the ligand.

#### *1.1.4.1 Electronic donor-acceptor properties - the electronic parameter, $\nu$*

Trialkylphosphines play a major role in increasing the stability of the catalytic system which permits low pressure and temperature operation. It has been suggested that the enhanced stability of the transition-metal phosphine complex is due to the fact that the tertiary-phosphine is a poorer  $\pi$ -acceptor than CO, and thus leaves more  $\pi$ -acceptor electron density available to the carbonyl ligands.<sup>13</sup> Equally important are the greater  $\sigma$ -donor properties of the tertiary-phosphine ligand. The overall result therefore is the increased electron density in the metal-carbonyl bonding orbitals thereby increasing the strength of the metal-carbonyl coordination. The resulting transition-metal complexes are considerably more stable with tertiary-phosphine substitution, permitting hydroformylation catalysis at low CO/H<sub>2</sub> pressures.

Oswald and coworkers recently showed that electronic effects of phosphorous ligands are an important factor in rhodium hydroformylation.<sup>14</sup> It is suggested that strongly basic  $\sigma$ -bonding trialkylphosphine ligands are advantageous compared to triarylphosphine ligands from the viewpoint of product removal, complex stability, and ligand degradation. Although the total aldehyde product selectivity (*n+iso*) is high, the resulting *n:iso* ratio is relatively low. Oswald concludes that the electronic and acceptor characteristics are important factors in determining the equilibria and dissociation of the catalytic complexes (species) present. This information in turn can be used for the determination of catalytic activity and selectivity of the catalytic system.

#### 1.1.4.2 Cone angle - the steric parameter, $\sigma$

To estimate the steric requirements of tertiary-phosphine ligands, Tolman developed the cone-angle concept, as portrayed in Figure 1, which has found wide application in studies of steric effect.

The increased steric crowding resulting from a substituted tertiary-phosphine causes the catalytic complex to exhibit a marked preference for terminal over internal alkenes when forming  $\pi$ -complexes. Similarly in all subsequent ligand migration reactions in the cycle, transition states leading to the least substituted alkyl or aryl complex are much more favoured. It is the steric effect in these modified systems which is mainly responsible for the higher *n:iso* ratios of the alcohols or aldehydes produced. Of the trialkylphosphine ligands used in this study the maximum influence was apparently achieved with a ligand cone angle of *ca.*  $130^\circ$  ( $\text{PEt}_3$ :  $132^\circ$ ,  $\text{PPh}_3$ :  $145^\circ$ ) and there was little or no improvement by increasing the cone angle by using bulkier trialkylphosphine ligands. Pruett and Smith<sup>15</sup> observed that the use of bulky ortho-substituted triaryl phosphite ester ligands such as tris-(*o*-phenoxyphenyl)phosphite leads to a reduced aldehyde linearity *i.e.*, a decreased *n:iso* ratio.

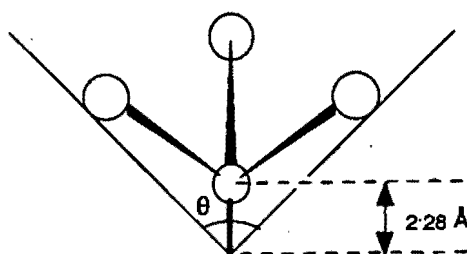


Figure 1

Tolman's 'cone angle' ( $\sigma$ ) for a symmetrical phosphorous ligand of the type  $\text{PR}_3$ <sup>13</sup>

However, more recently Van Leeuwen and Roobeek<sup>16,17</sup> showed that bulky ligands such as tris-(*o*-*tert*-butylphenyl)phosphite, have an increased activity for the hydroformylation of both linear-internal and branched-internal olefins. They suggested that for steric reasons, only two highly bulky ligands could be coordinated to the same rhodium atom. Therefore such ligands could serve to increase the coordinative unsaturation of rhodium and thus lead to higher catalytic activity for the hydroformylation of internal olefins.

A number of coordinatively unsaturated rhodium carbonyl complexes of bulky and highly basic trialkylphosphine ligands are described by Otsuka and coworkers<sup>18</sup> and by Freeman and Young.<sup>19</sup> Young patented the use of some of these trialkylphosphine compounds as improved rhodium catalyst ligands for the hydroformylation of internal and terminal mono-branched olefins under pressure.

However, apart from electronic and steric effects, the ligand can also influence the physical properties of a metal complex which can be important in the design of a catalyst system. For example, the solubility of a tertiary-phosphine in either a polar or non-polar solvent may be increased by introduction of appropriate functional groups on the ligand.

### 1.1.5 Other metal catalysts

A comparison of the relative hydroformylation activity of transition metals which readily form metal carbonyl complexes<sup>20</sup>, demonstrates the following trend:

	Rh	>	Co	>	Ru	>	Mn	>	Fe	>	Cr, Mo, W, Ni
relative activity	10 <sup>3</sup> -10 <sup>4</sup>		1		10 <sup>-2</sup>		10 <sup>-4</sup>		10 <sup>-6</sup>		0

Apart from rhodium and cobalt, other transition-metal complexes used to achieve hydroformylation are: ruthenium complexes such as  $\text{Ru}(\text{CO})_3(\text{PPh}_3)_2$ , platinum-tin catalysts<sup>21-23</sup> where  $\text{PtH}(\text{CO})(\text{SnCl}_3)(\text{PPh}_3)_2$  appears to act similarly to  $\text{RhH}(\text{CO})(\text{PPh}_3)_3$ , and  $\text{PtH}(\text{Ph}_3\text{PO})-(\text{Ph}_2\text{POH})(\text{PPh}_3)$  which is made from  $\text{Pt}(\text{COD})_2$ ,  $\text{PPh}_3$ , and  $\text{Ph}_2\text{POH}$ .<sup>24</sup> The latter system yields ketones when under high pressure.

## 1.2 Cobalt versus Rhodium

In order to compare rhodium and cobalt as hydroformylation catalysts, some data relating to the industrial operation of three catalytic systems is shown in Table 1.<sup>5</sup>

	Co	Co + PR <sub>3</sub>	Rh + PPh <sub>3</sub>
Temp. (°C)	140-180	160-200	80-120
Pressure (MPa)	25-35	5-10	1.5-2.5
Co/Rh : alkene (%)	0.1-1.0	0.5-1.0	10 <sup>-2</sup> -10 <sup>-3</sup>
<i>n:iso</i> ratio	3-4:1	8-9:1	12-15:1
Aldehydes (%)	ca. 80	—	ca. 96
Alcohols (%)	ca. 10	ca. 80	—
Alkanes (%)	ca. 1	ca. 15	ca. 2
Product	ca. 9	ca. 5	ca. 2

**Table 1**

Comparison of Three Major Hydroformylation Processes

On going from left to right across the table there is a marked decrease in the energy requirement of the catalytic system, in terms of both milder operating conditions and greater product selectivity. The generally high alkane level in the modified cobalt systems is compensated, to some extent, by the feasibility of a one-step process to alcohols. On the other hand if the aldehydes is the desired product, then a one-step process to the alcohol can be a disadvantage. The advantage of lower energy requirements of the modified systems have aided their growth in industry in recent years.

In practice cobalt is often preferable to rhodium as a hydroformylation catalyst for liquid olefin substrates. With higher molecular weight substrates the separation of the catalyst and products is a difficult operation and the potential cost due to rhodium losses in a liquid phase reaction is prohibitively high. Thus cobalt is favoured due to its lower cost. Rhodium based systems however, as shown in the table, are orders of magnitude more active than cobalt, which provides an incentive for the development of a heterogeneous system where the adventitious loss of the catalyst due to separation difficulties is low, and the catalytic lifetime high.

### **1.3 Catalyst Deactivation**

The catalyst can be degraded in a number of ways during hydroformylation reactions leading to a significant decrease in activity. Catalyst life is impaired by intrinsic poisons such as strong acid, hydrogen cyanide (HCN), and sulfur as H<sub>2</sub>S or C(S)O. Hydrogen sulfide forms rhodium sulfide compounds which besides being catalytically inactive, make rhodium recovery from the spent catalyst more difficult. Feed stream purification however, circumvents this potential problem.

Intrinsic deactivation is another cause of impairment of catalyst life. This phenomenon is evident in systems which have been under hydroformylation conditions for a long period of time. Recent studies have shown that the deactivation involves insertion of rhodium into a P-C bond of triphenylphosphine.<sup>25</sup> Insertion of olefin into the metal hydride bond produces a metal alkyl complex, which reductively eliminates an alkyldiphenylphosphine.

Fortunately, traces of oxygen in the system do not deactivate the catalyst since any oxygen reacts with the vast excess of the trialkylphosphine to form inert trialkylphosphine oxide.

#### **1.4 Homogeneous versus Heterogeneous Catalysis**

The advantages of homogeneous catalysis as described above are well recognised, but a major impediment to the more generalised use of homogeneous systems revolves around the problem of separation of the products from the catalyst especially when the catalyst is expensive or toxic. The difficulty in separation is particularly relevant when dealing with long-chain alkenes due to their high boiling points, since the simplest separation method is distillation of the products from the reaction medium, resulting in extensive decomposition of the homogeneous rhodium catalyst.

A convenient means of avoiding the separation difficulty is by 'heterogenising' the system, thus hopefully combining the virtues of both homogeneous (high activity and selectivity at fairly low temperatures and pressures) and heterogeneous (easy and efficient separation of the products from the catalyst) systems.

'Heterogenisation' of the homogeneous hydroformylation catalysts has become the subject of intense study in recent years,<sup>26-34</sup> and a number of comparisons have been made between heterogenised catalysts and their homogeneous precursors.

In these heterogeneous systems, the reactants and catalyst exist in different phases. Most commonly, solid catalysts are used with gaseous or liquid reactants, sometimes both. Other combinations are possible but less often encountered.

Introducing a separate phase however, immediately complicates the mechanism. Interfacial phenomena such as diffusion, absorption, and adsorption which all play critical roles in establishing the rate, now become important. Features such as the rates and energetics of adsorption, the structure of the active surface, and the nature of reactive intermediates are more complex than those for reactions occurring in the bulk fluid phase.

Thus in every important application of heterogeneous catalysis there is much controversy on the exact details of the chemistry involved due to the complex nature of the system.

A number of methods have subsequently been developed for the 'heterogenisation' of the homogeneous hydroformylation system and will be discussed below.

#### **1.4.1 Supported catalysts**

One of the major advances in catalytic chemistry in the past 25 years has been the development of transition metal catalysts chemically bonded to solid supports. Such supports may be inorganic oxides such as silica, alumina, metal oxides and zeolites<sup>34-43</sup> or organic polymers<sup>44-49</sup> such as polystyrene. Such supported or

anchored catalysts are presumed to combine the virtues of both homogeneous and heterogeneous catalysts. Association of different metals in hydroformylation catalysts, especially cobalt and rhodium clusters, has been a recent topic of intensive attention in order to obtain higher conversions and improved selectivities.<sup>47</sup>

Unfortunately this method has not been very successful in providing industrially viable catalysts. Problems encountered have included leaching of the metal into the solvent; lowered activity and selectivity (comparable at best to purely homogeneous analogues); and oxidation of the phosphorous atoms.<sup>50-55</sup>

Recently, in attempts to combine the features of homogeneous and heterogeneous systems in one configuration, supported liquid phase catalysts (SLPCs) have been employed.<sup>56</sup> Such catalysts are prepared by dissolving a transition metal complex in a high boiling-point solvent and impregnating a porous support material such as alumina or silica with this solution. This method showed comparable activity and selectivity for the hydroformylation of hexene to the conventional supported catalyst.

Recently an interesting family of heterogeneous supported catalysts, denoted supported aqueous phase catalysts (SAPC's), designed to facilitate chemical reactions at the interface of two liquids, have been reported.<sup>30,34-37</sup> These SAP catalysts consist of a water-soluble organometallic complex dissolved in a film of water which is supported on a high-surface-area hydrophilic solid. It has been suggested that during catalysis the complex  $[(\text{RhH}(\text{CO})(\text{TPPTS})_3)]$  remains dissolved in the aqueous phase and catalyses the reaction at the aqueous-organic phase interface.

These systems represent a breakthrough in terms of a heterogeneous system for the hydroformylation of long-chain olefins, as the solubility of the olefin in the aqueous

phase, which is a definite problem in the two-phase system, does not seem to be a limiting factor in the SAPC system.<sup>34</sup> The *n:iso* ratios however, in the hydroformylation of 1-octene with the supported aqueous phase catalyst, was poorer than in the biphasic system.

The use of ion-exchange resins for the support of a variety of homogeneous catalysts have also been the subject of some study. It has been reported that coordination of a cationic ligand leads to unusually high solubilities of the transition-metal complex in polar solvents (*e.g.* water).<sup>45</sup> Baird and coworkers found that the adsorption of a cationic amphos - rhodium(1) complex (amphos =  $\text{Ph}_2\text{PCH}_2\text{CH}_2\text{NMe}_3^+\text{I}^-$ ), on a strong acid cation-exchange resin resulted in the formation of a novel supported catalyst for the hydrogenation and hydroformylation of olefins.<sup>45</sup> Although no leaching of the catalytic metal was reported, the selectivity to aldehydes was poor.

#### 1.4.2 Catalysts in biphasic systems

The most obvious two-phase system for catalytic reactions involving alkenes, is to have the catalyst in an aqueous solution in which the reactant (alkene), as well as the products (corresponding aldehydes or alkanes), are insoluble.

Over the past decade the interest in "homogeneous" catalysis using water-soluble transition-metal complexes has increased significantly. Water solubilisation of organometallic compounds is generally achieved via coordination of water-soluble ligands, usually tertiary-phosphines which contain highly polar functional groups such as amino, carboxylic acid, hydroxide or sulfonate groups. Unfortunately hydroxyl-containing ligands often do not exhibit greatly advanced water-solubility, while phosphines containing amino and carboxyl groups are soluble only in acid and

basic media respectively.<sup>27</sup> A review article<sup>28</sup> describes a large number of compounds prepared from such phosphines, in some cases comparing catalytic activities of their complexes with those of the more typical, un-functionalised phosphines. Compounds containing sulfonated triphenylphosphine have also been extensively studied.<sup>29,33,34</sup>

One reason for this increased interest, is the commercialisation (in 1984) of butanal production from propene using a water-soluble rhodium complex.<sup>29</sup> The rhodium-based catalyst contains ligands that ensure hydrophilic properties of the catalytic complex; coordination of the ligands maintains the rhodium in the aqueous phase, while the local environment of the metal remains hydrophobic in character. It is suggested<sup>30</sup> that the hydroformylation of propene occurs homogeneously in the aqueous phase and the butanal so produced, forms a second phase because of its fairly low solubility in water. The relative solubilities of the long-chain 1-alkene substrates in the aqueous phase may become a limiting factor, if indeed the reaction does occur as postulated at the aqueous/organic interface.

It must also be taken into account that reactions which occur at an interface (aqueous/organic phases) can differ from those occurring in the bulk fluid phase as a result of the different orientation of molecules at the interface. The geometrical arrangement at the interface can lead to alterations in reaction rate, equilibrium and selectivity.

#### *Catalysis in the aqueous phase*

Since the early works of Barbie,<sup>57</sup> Grignard,<sup>58</sup> and later by Ziegler,<sup>59</sup> water has been considered undesirable in organometallic reactions. Exceptions are oxidation and hydration reactions in which water can act as a reagent. However, about 30 years ago, olefin hydrogenation was carried out in water in the presence of Co(II) salts and excess CN<sup>-</sup>. This catalytic system has since been studied intensely, and

apparently the water molecule does not play any role in the catalytic cycle, especially in the elementary step of metal-carbon cleavage.<sup>60,61</sup>

In 1973, the first attempt to carry out a transition-metal (rhodium, palladium or platinum)-catalytic reaction in aqueous solution in the presence of alkylphosphines, was reported.<sup>62</sup> The alkylphosphine had hydroxymethyl substituents and was thus slightly water-soluble. These complexes however did not catalyse hydrogenation or hydroformylation of alkenes in water. In spite of the disappointing result, one could expect that the water should not interfere with the organometallic catalytic system, as the water molecule is a 'hard' base whereas reaction intermediates in conventional organometallic catalysis often have a 'soft' character. Moreover, from a purely experimental point of view, it is known that reactions catalysed by Rh, Pd or Pt can be carried out without great care regarding the purity of solvents or reagents (*i.e.* the water content of the solvents is not required to be zero).<sup>62</sup>

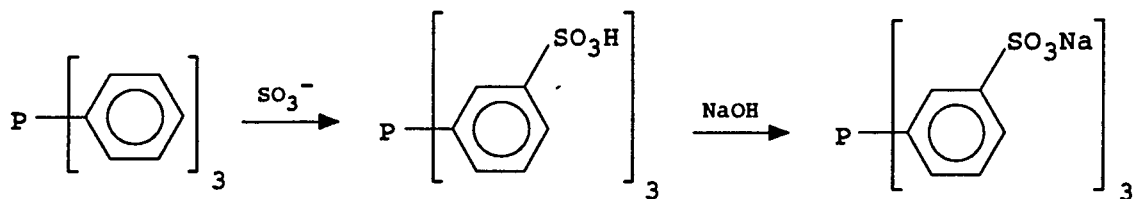
Thus theoretical, as well as experimental considerations indicated that a hydroformylation reaction could be carried out in the presence of water.

In 1974, the trisodium salt of tri(*m*-sulfophenyl)phosphine was prepared by sulfonation of triphenylphosphine with oleum followed by neutralisation,<sup>29,63</sup> as shown in Scheme 3. This ligand is used in the highly successful catalytic system commercialised by Rhône-Poulenc.

The mono-substituted sulfonated triphenylphosphine, sodium salt of (*m*-sulfophenyl)diphenylphosphine was prepared as early as 1958 by J. Chatt,<sup>64</sup> by sulfonation of triphenylphosphine. This ligand is however, much less soluble in water than the trisulfonated equivalent (80 gdm<sup>-3</sup> at 20°C instead of 1100 gdm<sup>-3</sup>).<sup>29</sup>

## Scheme 3

Synthetic route for the trisodium salt of tri(*m*-sulfophenyl)phosphine



A number of other water-soluble ligands and their metal complexes have been synthesised, and their catalytic activity in the hydroformylation of alkenes examined. These include the cationic water-soluble amphos group – [(2-diphenyl phosphinoethyl)trimethylammonium iodide,  $\text{Ph}_2\text{PCH}_2\text{CH}_2\text{NMe}_3^+\text{I}^-$ ] and the respective cobalt and rhodium metal complexes, synthesised by M.C. Baird and coworkers.<sup>26,65,66</sup> The properties of these complexes as hydroformylation catalysts were studied as two-phase systems, and when adsorbed onto strong cation exchange resins. The two-phase system using the rhodium catalyst showed reasonable activity to aldehydes with a fairly high *n:iso* ratios (*ca.* 9:1). However some leaching of the rhodium was observed.

Research work has also been carried out on the catalytic activity of a dinuclear rhodium catalyst – the dinuclear thiolato bridged  $\text{Rh}_2(\mu\text{-SR})_2(\text{CO})_2\text{L}_2$  – where the phosphate ligand is trisulfonated triphenylphosphine (TPPTS).<sup>31</sup> Fairly high rates and good selectivity in linear aldehydes were obtained for the hydroformylation of 1-hexene.

A carboxylated triphenylphosphine has been studied by M.J.H. Russel<sup>32</sup> and, with the use of phase transfer agents for the hydroformylation of longer chain 1-alkenes ( $C_{10}$ ,  $C_{12}$ ), has shown high activity and selectivity for the production of linear aldehydes, although it is accompanied by a certain amount of leaching of the metal into the organic phase.

The use of the monosulfonated triphenylphosphine (TPPMS) in the rhodium catalyst  $RhH(CO)(TPPMS)_3$ ,<sup>33</sup> was demonstrated by Wilkinson and co-workers, for the hydroformylation of 1-propene and 1-hexene. The yields of, and the selectivity for the appropriate linear aldehyde were comparable to those obtained by the homogeneous hydroformylation system in the presence of excess phosphine and under the conditions of high temperature and pressure. However, again in this case some loss of the rhodium complex to the organic phase was noted.

#### *Phase-transfer agents*

The use of phase-transfer agents in order to increase the percentage conversion of alkenes to aldehydes has been demonstrated in the two-phase system for the hydroformylation of 1-dodecene, using a rhodium carboxylated-triphenylphosphine catalyst.<sup>32</sup> This method effectively promotes the reaction rate by enabling the alkene to diffuse efficiently into the aqueous phase and the aldehyde product back into the organic phase, presumably by inducing micelle formation.<sup>32</sup> However, use of the phase-transfer agent certainly has the disadvantage of promoting an interphase transfer of the catalytic metal as well, leading to catalyst loss. Another potential problem is the formation of an emulsion which again results in separation difficulties. This method was shown to be successful in terms of increased activity, but was unfortunately accompanied by a significant increase in rhodium catalyst leeching into the organic phase.

## 1.5 Objectives of the Project

The complexity of the heterogeneous reaction systems outlined previously suggests that the design of an industrial plant for the hydroformylation of high-molecular weight alkenes would be non-trivial.

However, due to the commercial value of high-molecular weight aldehydes and alcohols, the idea of utilising a water-soluble catalyst in the heterogeneous hydroformylation of long-chain alkenes is very attractive. As side products in certain industrial reactions, these long-chain alkenes can be converted to commercially valuable reagents for use in the synthesis of biodegradable detergents, lubricants and plasticisers.

The objective of this study was to design a simple and possibly industrially feasible heterogeneous catalytic system for the hydroformylation of long-chain 1-alkenes, based on the well-known homogeneous hydroformylation catalyst precursor,  $\text{RhH}(\text{CO})(\text{PPh}_3)_3$ .

It was decided to utilise a two-phase heterogeneous system where the catalyst is found in the aqueous phase and the reactants and products in the organic phase, thereby facilitating easy separation of the catalyst from the reactants. Rhodium was chosen as the catalytic metal due to its superior activity, and the tri(*m*-sulfophenyl)phosphine salt (TPPTS) as the functionalised phosphine ligand. Coordination of the ligand to the metal renders the catalytic complex water-soluble.

An '*in situ*' catalyst preparation method was chosen for simplicity reasons, as opposed to a system utilising a pre-synthesised catalytic precursor e.g.  $\text{RhH}(\text{CO})(\text{TPPTS})_3$ . The active catalytic species are generated *in situ* from rhodium

trichloride ( $\text{RhCl}_3 \cdot 3\text{H}_2\text{O}$ ) and excess phosphine ligand (TPPTS) by the action of  $\text{CO}$  and  $\text{H}_2$  under pressure. The simplicity and adaptability of this system are important industrial advantages.

Rhône-Poulenc and Ruhrchemie have successfully implemented the heterogeneous rhodium-TPPTS system for the production of n-butanol on an industrial scale. However, this has not as yet, been successfully applied to the hydroformylation of long-chain 1-alkenes.

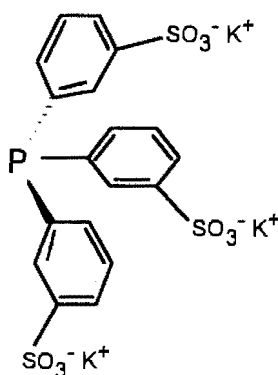


**Figure 2**

Schematic diagram of trisulfonated triphenylphosphine

In summary, the main objectives of this study were to use the catalytic system described above:-

- i)* to investigate the feasibility of applying this heterogeneous system, using TPPTS as the phosphine ligand and rhodium as the catalytic metal, for the hydroformylation of long-chain 1-alkenes ( $\text{C}_8 - \text{C}_{12}$ ).
- ii)* optimisation of the conditions of temperature and pressure.
- iii)* optimisation of the ratios; rhodium : phosphine ligand : olefin

*iv)* to study the catalytic species found in the aqueous phase in order to address the nature of the heterogeneous system and to draw a comparison with the homogeneous system

Thus with a view to the production of industrially valuable linear-aldehydes, the implementation of this heterogeneous hydroformylation system has considerable potential, and may have far-reaching consequences.

## **Chapter 2**

### **Preparation and Methods**

## Chapter 2

### Preparation and Methods

In this chapter the synthesis and characterisation by  $^{31}\text{P}$  and  $^{13}\text{C}$  NMR spectroscopy of some water-soluble phosphine ligands and certain corresponding metal complexes, will be discussed. These include the tripotassium salt of tri(*m*-sulfonatophenyl)phosphine (TPPTS), and the corresponding rhodium complex, carbonylhydrido tris[tri(*m*-sulfonatophenyl)phosphine] rhodium(I) ( $\text{RhH}(\text{CO})(\text{TPPTS})_3$ ) which are used in future catalytic studies.

As attempts made to obtain commercially synthesised TPPTS from Rhône-Poulenc were unsuccessful, the ligand in this study was prepared using a recently patented method by Ruhrchemie,<sup>67</sup> with slight modification. The synthesis of TPPTS however, proved less than straightforward with the main difficulty involving the separation of the pure compound from the complex mixture of sulfonated products. Experimental details of the synthesis of the following ligands and metal complexes are given in Section 2.2.

Secondly, the use of  $^{13}\text{C}$  nuclear magnetic resonance spectroscopy as a sensitive qualitative and quantitative analytical tool for the analysis of hydroformylated products, will be discussed. This was implemented as a complimentary qualitative and quantitative analytical technique with gas chromatography.

## 2.1 Synthesis and Characterisation

### 2.1.1 Preparation of ligands

As the main objective of this study is the utilisation of water-soluble phosphine ligands in order to render the rhodium catalytic complex water-soluble, a number of phosphine ligands for this purpose were synthesised and characterised.

*Tripotassium salt of tri(m-sulfonatophenyl)phosphine, TPPTS*

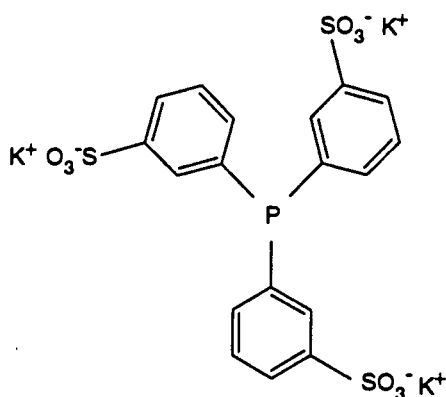
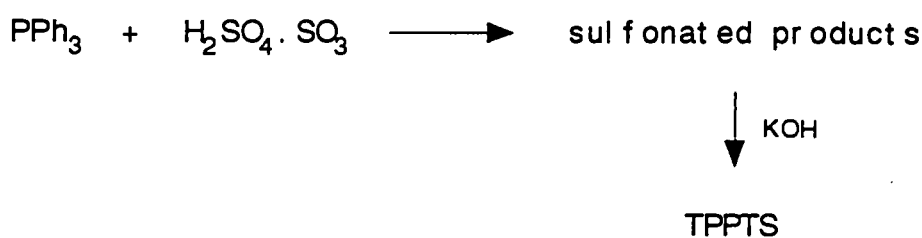


Figure of TPPTS

TPPTS was first prepared by sulfonation of triphenylphosphine with oleum followed by neutralisation, in 1974 by E.G. Kuntz.<sup>29,67</sup> Since then the synthesis of this ligand has been improved, and the method patented.<sup>67</sup>



Experimental details of the synthetic route are given in Section 2.3.2.1.

Sulfonation of triphenylphosphine with oleum, under nitrogen, over a period of 24 hours resulted in a complex mixture of sulfonated products including mono-, di- and tri-sulfonated phosphines; mono-, di- and tri-sulfonated phosphine oxides; and di- and tri-sulfonated phosphine sulfides, as well as the unsulfonated starting material. After careful hydrolysis at 0 °C the strongly acidic solution was extracted with tris(isooctyl)amine in toluene. This resulted in the extraction of the sulfonated triphenylphosphine derivatives into the organic phase. In order to separate the required product, TPPTS, from the complex mixture, an exhaustive re-extraction process was implemented using a potassium hydroxide solution. The different sulfonated species are extracted into the aqueous phase corresponding to certain pH values as outlined in Table 2.1.<sup>67</sup>

A wide distribution of products was therefore obtained which resulted in the disadvantage of resulting low yields of TPPTS, as well as the difficulty of attaining a high purity material.

The aqueous phase was collected over the pH range of 5.5 to 6.5 and dried on a rotary evaporator. After a number of attempts for the purification of the TPPTS ligand, which is not discussed in the patent, the best method was found to be precipitation of the resultant brown solid from a concentrated solution in water with ethanol.

The product obtained was analysed by <sup>13</sup>C and <sup>31</sup>P NMR spectroscopy. The <sup>31</sup>P NMR spectrum of the recrystallised product shows a very characteristic single peak for P(*m*-C<sub>6</sub>H<sub>4</sub>SO<sub>3</sub>K)<sub>3</sub> at  $\delta_P = -2.9$  ppm, as shown in Figure 2.1, and confirms that sulfonation of the triphenylphosphine is complete. The <sup>13</sup>C spectrum of P(*m*-

$C_6H_4SO_3K)_3$  is shown in Figure 2.2 and confirms that the sulfonate group is in the *meta* position. See Table 2.2 (at the end of this section) and the Experimental Section, 2.2.

**Table 2.1**

Composition of extracted products at their respective pH values as reported in the patent<sup>67</sup>

pH	Molar percentage of extracted products					
	DS <sup>1</sup>	TS <sup>2</sup>	ODS <sup>3</sup>	OTS <sup>4</sup>	SDS <sup>5</sup>	STS <sup>6</sup>
4.02	–	–	–	1	–	–
5.00	–	1.5	1	2	–	–
5.25	–	3	1	1	–	–
5.50	–	9	–	1	–	–
5.75	–	15	–	–	–	1
6.00	–	15.5	–	–	–	1
6.25	3	6	–	–	–	–
6.75	12	1.5	–	–	–	–
7.00	8	–	–	–	1	–
7.54	4.5	–	–	–	–	–

<sup>1</sup> triphenylphosphine-disulfonate salt, TPPDS

<sup>2</sup> triphenylphosphine-trisulfonate salt, TPPTS

<sup>3</sup> triphenylphosphineoxide-disulfonate salt, TPPODS

<sup>4</sup> triphenylphosphineoxide-trisulfonate salt, TPPOTS

<sup>5</sup> triphenylphosphinesulfide-disulfonate salt, TPPSDS

<sup>6</sup> triphenylphosphinesulfide-trisulfonate salt, TPPSTS



A significant amount of the corresponding phosphine oxide,  $P(O)(m-C_6H_4SO_3K)_3$  which is characterised by a single peak at  $\delta_p = 37.3$  ppm in the  $^{31}P$  spectrum as shown in Figure 2.3, did appear in the fractions at pH values of less than 5.5, but by extremely careful addition of the potassium hydroxide solution in order to obtain the exact range required, this problem of contamination was minimized.

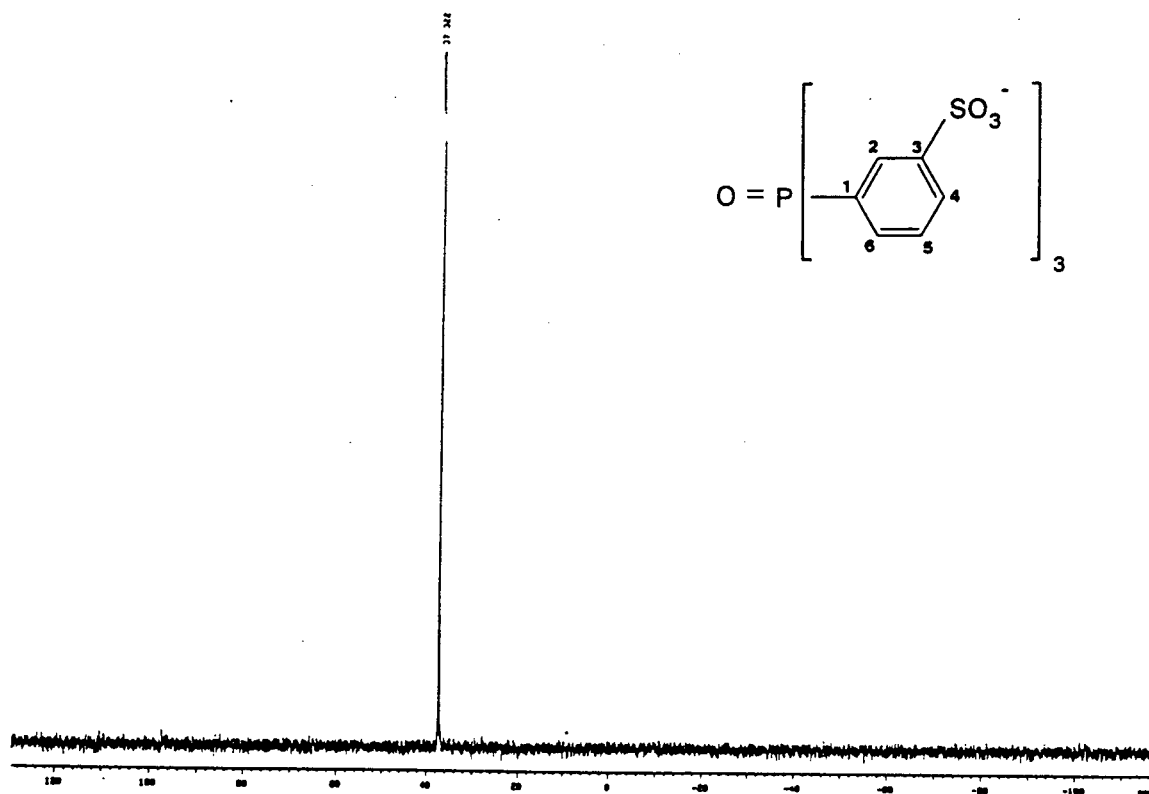
The  $^{13}C$  spectrum of the phosphine oxide shown in Figure 2.4 shows an increase in the  $J(P-C)$  coupling constant for  $C_1$  from 9.8 Hz to 109.7 Hz, the latter coupling constant being in the range characteristic of a phosphorous(V) complex, thus confirming the assignment to that for the phosphine oxide.

In the hope of increasing the yield of TPPTS, the reaction time was extended in order to allow more complete substitution by the sulfonate group. It was found that a reaction time of 48–60 hours resulted in a marked improvement of up to 50% of the yield. The amount of oleum added was also adjusted in the hopes of increasing the degree of substitution of the sulfonate group but this showed no marked effect on the yield. The final yields of pure TPPTS obtained lay in the range of 25–35%.

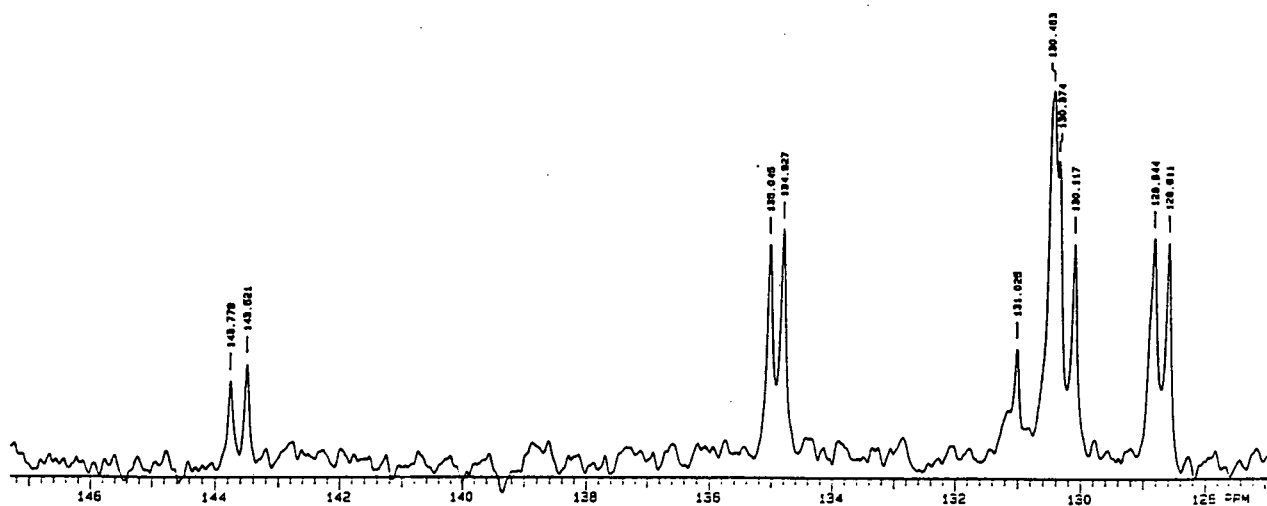
The synthesis of the benzylisothiuronium salt derivative of TPPTS was attempted in order to characterise the compound more fully, but this product was not crystalline despite repeated attempts at crystallisation. However the microanalytical data (%C and %H) of the TPPTS ligand was good, and the  $^{13}C$  and  $^{31}P$  NMR spectra indicated that the product was relatively pure.

#### *Tripotassium salt of tri(m-sulfonatophenyl)phosphine oxide, TPPOTS*

TPPOTS was separated and purified for use in catalytic speciation studies. The pH fraction of 4.5–5.2 was taken and the same steps followed for the purification and analysis of TPPTS as outlined above, were undertaken.

**Figure 2.3**

$^{31}\text{P}$  NMR spectrum of tri(*m*-sulfonatophenyl)phosphine oxide salt, TPPOTS, in  $\text{D}_2\text{O}$

**Figure 2.4**

$^{13}\text{C}$  NMR spectrum of tri(*m*-sulfonatophenyl)phosphine oxide salt, TPPOTS, in  $\text{D}_2\text{O}$

The  $^{31}\text{P}$  NMR spectrum showed a single characteristic peak at  $\delta_{\text{P}} = 37.3$  ppm. The  $^{13}\text{C}$  NMR spectrum as discussed above, is assigned in detail in Table 2.2.

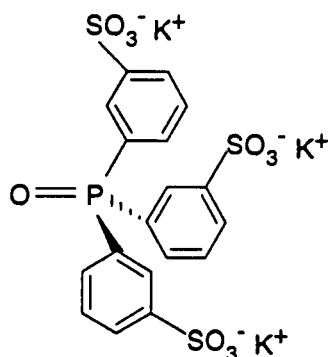


Figure of TPPTOS

*Sodium diphenylphosphinobenzene-*m*-sulfonate, TPPMS*

This ligand was synthesised by following the method laid out by S. Arhland *et al.*<sup>64</sup> who prepared TPPMS as early as 1958. The first use of TPPMS in heterogeneous catalytic hydroformylation studies was reported by G. Wilkinson and co-workers in 1977,<sup>33</sup> using a rhodium complex prepared by an exchange reaction between  $\text{PPh}_3$  and TPPTS.

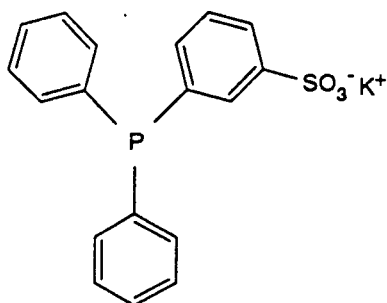


Figure of TPPMS

Sodium diphenylphosphinobenzene-*m*-sulfonate, TPPMS, was prepared by dissolving triphenylphosphine in a mixture of oleum and sulfuric acid. The reaction

was deemed complete when the addition of one drop of water gave a clear solution, due to the relative solubilities of  $\text{PPh}_3$  (insoluble in water) and TPPTS (soluble in water). The solution was then neutralised with sodium hydroxide which resulted in precipitation of the desired product as white shiny plates.

The  $^{31}\text{P}$  NMR spectrum consisted of a single peak at  $\delta_{\text{P}} = -3.3$  ppm which is a 0.5 ppm downfield shift from the singlet of the sulfonated phosphine, TPPTS. The product was characterised as the benzylisothiuronium derivative. See Section 2.3.2.3 for experimental details.

### 2.1.2 Preparation of metal complexes

*Synthesis of carbonylhydridotris(triphenylphosphine) rhodium(I),  $\text{RhH}(\text{CO})(\text{PPh}_3)_3$*

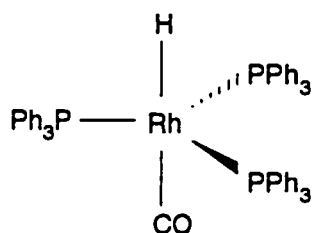


Figure of  $\text{RhH}(\text{CO})(\text{PPh}_3)_3$

Carbonylhydridotris(triphenylphosphine) rhodium(I) was first prepared from  $\text{RhCl}(\text{CO})[\text{P}(\text{C}_6\text{H}_5)_3]_2$  by reduction with hydrazine in ethanolic suspension.<sup>69</sup> More recently, single-step syntheses have been reported with the use of a potassium hydroxide/alcohol mixture as an effective reducing system.<sup>70</sup>

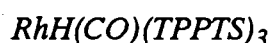


This method involves the addition of ethanolic rhodium trichloride solution to a refluxing solution of triphenylphosphine in ethanol, followed by the rapid, successive addition of aqueous formaldehyde and an ethanolic potassium hydroxide solution. The bright yellow crystalline product was then washed with ethanol, water, ethanol and finally n-hexane. An important factor in this synthesis is achieving and maintaining homogeneous conditions wherever possible by the efficient stirring and rapid, successive additions of the reagents.<sup>70</sup> Experimental details of the synthesis are described in Section 2.3.2.4.

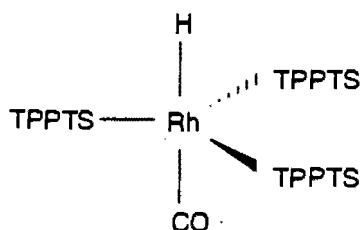
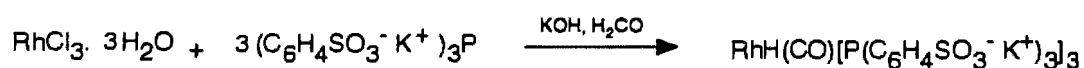
The <sup>31</sup>P NMR spectrum of RhH(CO)(PPh<sub>3</sub>)<sub>3</sub> shows a doublet at δ<sub>P</sub> = 41.6 ppm with *J*(Rh–P) = 155.4 Hz, which suggests a trigonal bipyramidal structure with the three phosphorous atoms in the equatorial plane and H and CO in axial positions, see Table 2.3 at the end of this section. A singlet at δ<sub>P</sub> = 29.4 ppm arises which as yet remains unassigned.

The IR spectrum shows bands at 2036 cm<sup>-1</sup>, attributed to ν(RhH) and at 1917 cm<sup>-1</sup> attributed to ν(CO) which agree with those given in the literature.<sup>70</sup> (ν = stretching frequency).

*Synthesis of carbonylhydridotris[tri(m-sulfonatophenyl)phosphine] rhodium(I),*



The method followed for the synthesis of water-soluble carbonylhydrido tris[tri(*m*-sulfonatophenyl) phosphine] rhodium(I) was similar to that used for the preparation of the analogous carbonylhydrido-tris(triphenylphosphine) rhodium(I) by Ahmed and coworkers mentioned above.

Figure of  $\text{RhH}(\text{CO})(\text{TPPTS})_3$ 

As with the synthesis of  $\text{RhH}(\text{CO})(\text{PPh}_3)_3$ , the success of this reaction was assumed to be dependent on the maintenance of homogeneous conditions. This assumption was shown to be correct as no success was achieved when the reaction was initially attempted in ethanol, since homogeneous conditions were not obtained due to the extremely poor solubility of the TPPTS ligand in ethanol.

By using water as the solvent, homogeneous conditions were achieved while following a similar synthetic route. An aqueous rhodium trichloride solution was added to a refluxing solution of TPPTS in water, and followed by the addition of aqueous formaldehyde and an aqueous solution of potassium hydroxide in rapid succession. The bright yellow product was filtered and washed with ice-cold water in order to remove excess starting material and resulting TPPOTS, and then with ethanol, and dried *in vacuo*. The yield (ca. 40 %) was low due to loss of the product during the washings. See Section 2.3.2.5 for experimental details.

The product was characterised by  $^{13}\text{C}$  and  $^{31}\text{P}$  NMR spectroscopy. Figure 2.5 shows the  $^{31}\text{P}$  NMR spectrum of  $\text{RhH}(\text{CO})(\text{TPPTS})_3$  dissolved in  $\text{D}_2\text{O}$ . A doublet

at  $\delta_P = 45.9$  ppm with  $J(\text{Rh-P}) = 155.5$  Hz suggests a similar structure to that of the complex  $\text{RhH}(\text{CO})(\text{PPh}_3)_3$ , viz., a trigonal bipyramidal structure with the three phosphorous atoms in the equatorial plane and H and CO in axial positions. The  $^{31}\text{P}$  NMR results and assignments are in agreement with those reported in literature.<sup>34</sup>

A significant amount of the excess phosphine ligand (TPPTS) was oxidised to the phosphine oxide by rhodium(III) chloride during the reaction, as shown by the characteristic singlet at  $\delta_P = 36.95$  ppm in the  $^{31}\text{P}$  NMR spectrum (Figure 2.5). The phosphine oxide remained uncoordinated to the rhodium metal. The doublet arising at  $\delta_P = 28.93$  ppm with  $J(\text{Rh-P}) = 100.17$  Hz remains unassigned, but is discussed further in Chapter 4.

Tables 2.2 and 2.3 summarise some  $^{13}\text{C}$  and  $^{31}\text{P}$  NMR data comprising chemical shifts and coupling constants where applicable, for the ligands and metal complexes described above. The respective NMR spectra are shown in Figures 2.1 to 2.5.

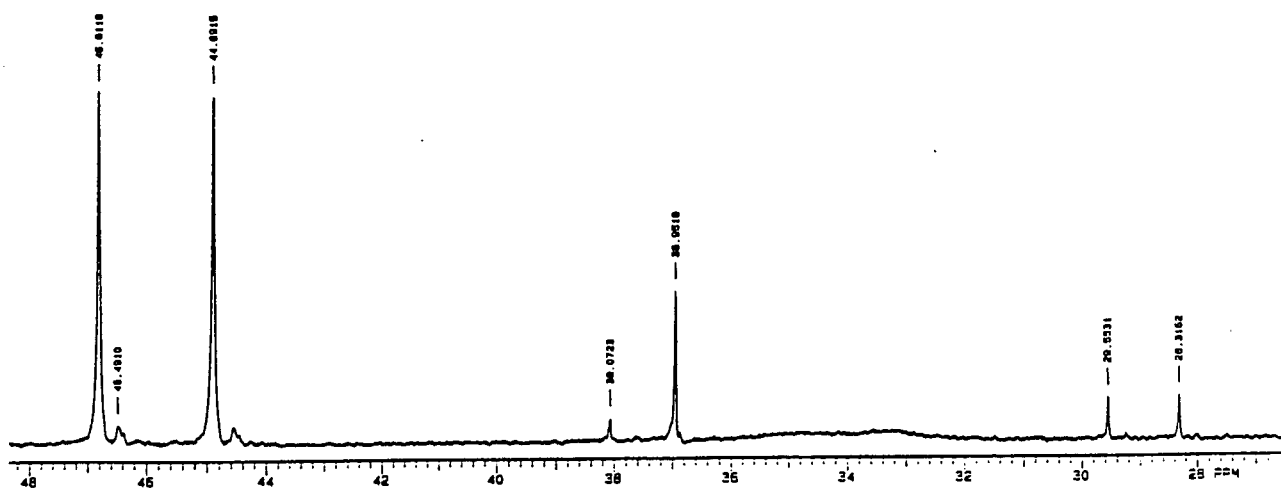
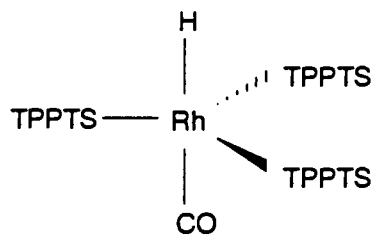


**Figure 2.5**

$^{31}\text{P}$  NMR spectrum of  $\text{RhH}(\text{CO})(\text{TPPTS})_3$ , in  $\text{D}_2\text{O}$

**Table 2.2**<sup>13</sup>C NMR data for the sulfonated phosphine ligands, TPPTS and TPPOTS, in D<sub>2</sub>O

Compound	$\delta_C^a$ ( $J_{P-C}$ ) <sup>b</sup>					
	C <sub>1</sub>	C <sub>2</sub>	C <sub>3</sub>	C <sub>4</sub>	C <sub>5</sub>	C <sub>6</sub>
TPPTS	136.6 (9.8)	136.4 (16.5)	143.1 (8.0)	126.6 (0)	129.7 (5.8)	130.3 (23.7)
TPPOTS	129.9 (109.7)	134.9 (11.0)	143.7 (13.0)	130.5 (0)	130.2 (12.9)	128.7 (11.7)

<sup>a</sup> chemical shifts are in ppm relative to internal TMS.<sup>b</sup> P–C coupling constants given in Hz, in brackets under the chemical shift.**Table 2.3**<sup>31</sup>P NMR data for some ligands and rhodium complexes

Compound	$\delta_P^a$	$J_{Rh-P}$ (Hz) <sup>b</sup>
<i>Ligand</i>		
TPP	-1.5	—
TPPMS	-3.3	—
TPPTS	-2.9	—
TPPTOS	37.3	—
<i>Complex</i>		
RhH(CO)(PPh <sub>3</sub> ) <sub>3</sub>	45.9	155.5
RhH(CO)(TPPTS) <sub>3</sub>	41.6	155.5

<sup>a</sup> chemical shifts are in ppm relative to external 85 % H<sub>3</sub>PO<sub>4</sub> / D<sub>2</sub>O<sup>b</sup> Rh–P coupling constants given in Hz, where applicable

## 2.2 Experimental

### 2.2.1 General

All reagents were analytically pure and generally supplied by Aldrich Chemical Company. Rhodium was used as  $\text{RhCl}_3 \cdot 3\text{H}_2\text{O}$  which was on loan from Johnson and Matthey. Unless otherwise stated solvents used were Analytical Reagent grade. Glass-distilled water was used throughout.

Microanalyses were performed by Mr P. Benincaasa, on a Heraeus Universal Combustion Analyser, Model CHN-Rapid, at the Department of Chemistry, University of Cape Town.

Melting points were measured on a Linkam hot stage with a Nikon SM2-10 microscope.

Infrared (IR) spectra were recorded as either NUJOL mulls or as neat liquids using NaCl pressed discs, on a Perkin-Elmer 983 Infrared spectrophotometer.

$^{13}\text{C}$  and  $^{31}\text{P}$  NMR spectra were recorded on a Varian VXR-200 pulse Fourier transform spectrometer operating at 50.309 MHz and 80.984 MHz respectively. Some  $^{31}\text{P}$  NMR spectra were also recorded on a high resolution Varian Unity 400 pulse Fourier transform spectrometer operating at 161.903 MHz. Unless stated otherwise,  $^{13}\text{C}$  NMR spectra were run at a frequency of 50.309 and  $^{31}\text{P}$  at a frequency of 161.903 MHz. Chemical shifts are reported in parts per million (ppm) relative to the internal standard, tetramethylsilane (TMS) for  $^{13}\text{C}$  spectra and the external standard, 85 % orthophosphoric acid ( $\text{H}_3\text{PO}_4$ ) for  $^{31}\text{P}$  NMR spectra. Unless otherwise stated,  $\text{D}_2\text{O}$  or a 50:50 solution of  $\text{D}_2\text{O}/\text{H}_2\text{O}$  was used as the solvent. All

$^{13}\text{C}$  and  $^{31}\text{P}$  spectra are proton decoupled unless stated otherwise, where {H} denotes proton decoupling. Coupling constants,  $J$  values, are given in hertz (Hz).

Gas chromatograms were recorded on a Carlo Erba 4200 Gas Chromatograph equipped with a SP 4290 integrator and using a flame ionisation detector. High purity gases were used (99.99 % purity). The carrier gas was further purified over molecular sieve prior to entering the chromatograph. A 30 m SUPELCOWAX™ 10 fused silica capillary column (0.31 mm ID, 0.50  $\mu\text{m}$  film thickness) was used in all the experimental GC work. In order to ensure unambiguous characterisation of the hydroformylated products, the fused silica capillary column was initially installed in-line with a VG Micromass 16M mass spectrometer, and the assignments of applicable mixtures were made. In most cases a temperature program appropriate for the sample being analysed, was employed.

### Catalytic reactions

All hydroformylation reactions took place in a homebuild batch stainless-steel reactor, shown in Figure 2.6, of volume 215 ml, equipped with a heating mantle and stirrer. An inserted teflon cup prevented contact of  $\text{CO}/\text{H}_2$  with the steel. The temperature was controlled by a UNITEMP thermostat equipped with thermocouple.

The 1:1 carbon monoxide/hydrogen mixture, (49 %  $\text{CO}$ , 51 %  $\text{H}_2$ ), was supplied by Fedgas and used without further purification. The stirring rate was kept constant at 215 rpm, unless otherwise stated. The catalytic mixture was placed in a teflon cup and stirred by means of a teflon-coated magnetic stirrer bar at a constant rate. The reaction sequence was initiated by sealing the reactor and purging the entire system first for 30 minutes with nitrogen and then with the synthesis gas mixture. The synthesis gas pressure was then increased to 5 MPa and the reaction heated to the

required temperature (100°C unless otherwise stated) over a period of about one hour, after which the pressure was readjusted to the required value.

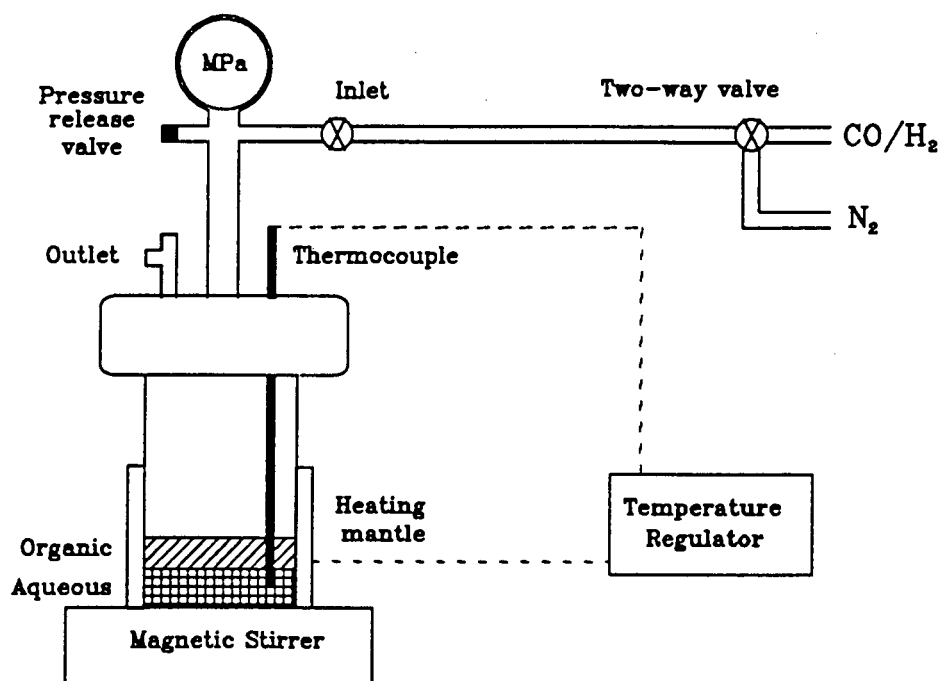


**Figure 2.6**

Schematic representation of stainless-steel reactor

The reaction was left stirring for the required time (24 hours unless otherwise stated) and then cooled to between 0 and 5 °C, and the pressure released. Due to the presence of two phases (aqueous phase containing the catalytic species and the organic phase containing the reactants and products), the separation of the catalyst was easily achieved with the use of a separating funnel. In most cases, the organic

phase was completely clear which indicated negligible leaching of the rhodium from the aqueous phase into the organic phase. The aqueous phase, containing the catalytic species, was washed twice with toluene or benzene in order to remove all remaining (dissolved) organic reactants or products, and then used, if required, for further catalytic reactions.

The reaction products in the organic phase were analysed qualitatively and quantitatively by gas chromatography and quantitative  $^{13}\text{C}$  NMR spectroscopy.

### 2.3.2 Synthesis

#### 2.3.2.1 Synthesis of the tripotassium salt of tri(*m*-sulphophenyl)phosphine, TPPTS

Triphenylphosphine (10 g, 38 mmol) was placed under nitrogen in a 500 ml two-necked, round-bottomed flask, equipped with a calcium chloride drying tube. Oleum (120 ml, 25–35%  $\text{SO}_3$ ) was added dropwise via a dropping funnel to the vigorously stirred mixture over a period of approximately one hour, while the temperature was kept constant at 0 °C. The reaction was then stirred under nitrogen and at room temperature (20–25 °C) for 48 hours. The reaction was quenched by adding the mixture dropwise, under careful temperature control, to ice (250 ml). The resulting clear, pale brown solution was further purified by the extraction-reextraction technique .

#### Extraction-reextraction

The strongly acidic sulfonation mixture was added to trioctylamine (50 ml in 150 ml toluene) in a 1000 ml separating funnel. After the sulfonated products were extracted into the organic phase, a re-extraction process using a potassium hydroxide solution (50 % w/v), was used to separate the tri(*m*-

sulphonatophenyl)phosphine salt, TPPTS, from other sulfonated products, which included mono- and di-sulfonated phosphines, phosphine oxides and phosphine sulphides. Water (100 ml), plus the necessary quantities of the potassium hydroxide solution were added sequentially to the organic mixture in order to give the required pH value, which was measured using a PHM62 standard pH meter with glass electrode.

Fractions were collected at sequential pH intervals, evaporated to dryness on a Büchi rotary evaporator and the residue examined by  $^{31}\text{P}$  NMR spectroscopy. The required product, TPPTS, was found to occur mostly in the pH region of 5.5 – 6.5, which corresponded to the results obtained in the patent.<sup>67</sup>

The fractions in the pH range of 5.5 – 6.5 were collected and evaporated to dryness on a rotary evaporator, which yielded a yellow-brown solid. The product was then further purified by dissolving the solid in a minimum amount of water and precipitating the white-powder, tris(*m*-sulphonatophenyl)phosphine with ethanol and then drying it *in vacuo*.

$\text{P}(\text{C}_6\text{H}_4\text{SO}_3^-\text{K}^+)_3$  (7.2 g, 30.6 %) (Found: C, 34.9; H, 2.4;  $\text{C}_{18}\text{H}_{12}\text{P}(\text{SO}_3\text{K})_3$  requires C, 35.1; H; 2.0%)

$\delta_{\text{P}}$  -2.866 (s).

$\delta_{\text{C}}$  126.648 (1C, s, 4-C), 129.7425 (1C, d,  $J^3$  5.79, 5-C), 130.344 (1C, d,  $J^2$  23.65, 6-C), 136.4375 (1C, d,  $J^2$  16.45, 2-C), 136.6025 (1C, d,  $J^1$  9.760, 1-C), 143.1015 (1C, d,  $J^3$  7.999, 3-C)

### 2.3.2.2 Synthesis of tris(*m*-potassiumsulphatophenyl)phosphine oxide, TPPOTS

The same experimental route was followed as used for the preparation of TPPTS, discussed above. The fractions of pH 4.5–5.2 were separated and the resultant product purified by precipitation from the minimum amount of water with ethanol.

$\delta_P$  37.322 (s)

$\delta_C$  128.7275 (1C, d,  $J^2$  11.722, 6-C), 129.9345 (1C, d,  $J^1$  109.7, 1-C), 130.2455 (1C, d,  $J^3$  12.92, 5-C), 130.463 (1C, s, 4-C), 134.936 (1C, d,  $J^2$  10.967, 2-C), 143.65 (1C, d,  $J^3$  12.98, 3-C)

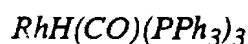
### 2.3.2.3 Synthesis of sodium diphenylphosphinobenzene-m-sulfonate, TPPMS

Triphenylphosphine (10 g, 38 mmol) was added slowly with cooling, to oleum, (20 ml 25–30 %  $SO_3$ ) in a 500 ml two-necked round-bottomed flask. The phosphine dissolved and the solution was heated under reflux for two hours at 100 °C. The solution was then tested periodically for completion by adding one drop of water until a test drop gave a clear solution. The strongly acidic solution was poured into water (200 ml) and neutralised with a saturated NaOH solution (ca. 80 ml). When cool the product separated as shiny, white leaves. This may be contaminated by crystals of sodium sulphate if the solution is allowed to stand for too long or is cooled in ice. The product was then filtered and extracted with water. The aqueous extract was evaporated to a volume of ca. 20 ml and left overnight in a refrigerator. The resulting white shiny plate-like crystals were filtered and washed with cold diethyl ether and recrystallised from ethanol. The yield was fairly low at 4.5 g but comparable to literature values.<sup>64</sup>

TPPMS 4.5 g(33%);  $\delta_P$  (80.984 MHz) -3.3 ppm)

TPPMS was characterised as its benzylisothiuronium salt, m.p. 146–149 °C (Found: C, 61.5; H, 4.9; N, 5.5.  $C_{25}H_{25}N_2S_2P$  requires C, 61.4; H, 4.95; N, 5.5 %)

### Synthesis of carbonylhydridotris(triphenylphosphine) rhodium(I),



A solution of rhodium trichloride trihydrate (0.261 g, 0.990 mmol) in hot ethanol (20 ml) was added to a vigorously stirred, refluxing solution of triphenylphosphine

(2.652 g, 10.11 mmol) in ethanol (100 ml), in a 500 ml two-necked round-bottomed flask. After 30 seconds, aqueous formaldehyde (10 ml, 40% w/v solution) and potassium hydroxide [0.80 g in hot ethanol (20 ml)], were added rapidly and sequentially to the orange reaction mixture. The mixture was heated under reflux for 10 minutes and then allowed to cool to room temperature. The bright yellow crystalline product was filtered, washed successively with ethanol, water, ethanol and finally hexane, and dried *in vacuo*.

$\text{RhH}(\text{CO})(\text{PPh}_3)_3$  (0.734 g, 80.8 %), m.p. 110–112 °C, (Found: C, 70.6; H, 5.1;  $\text{C}_{55}\text{H}_{46}\text{OP}_3\text{Rh}$  requires C, 71.90; H, 5.05%);  $\nu_{\text{max}}/\text{cm}^{-1}$  2036 (RhH) and 1917 (CO);  $\delta_{\text{P}}$  (80.984 MHz,  $\text{CDCl}_3$ ) 41.5814 (3P, d,  $J^1_{\text{RhP}}$  155.4).

### 2.3.2.5 Synthesis of carbonylhydridotris[tri(*m*-sulfonatophenyl)phosphine]rhodium(I), $\text{RhH}(\text{CO})(\text{TPPTS})_3$

A solution of rhodium trichloride trihydrate (0.052 g, 0.20 mmol) in hot water (5 ml) was added to a vigorously stirred, boiling solution of tris(*m*-potassiumsulphatophenyl)-phosphine, (TPPTS), (1.23 g, 1.99 mmol) in water (20 ml), in a 100 ml two-necked, round-bottomed flask. After 30 seconds, aqueous formaldehyde (3 ml, 40% w/v solution) and a solution of potassium hydroxide [(0.16 g) in hot water (5 ml)] were added rapidly and successively to the orange reaction mixture. The mixture was heated under reflux for 10 minutes and then allowed to cool to room temperature. The bright yellow crystalline product was filtered, washed successively with ice-cold water and then with ethanol, and dried *in vacuo*.

$\text{RhH}(\text{CO})(\text{TPPTS})_3$  0.17 g (43%)

$\delta_{\text{P}}$ (80.984 MHz) 45.8517 (3P, d,  $J^1_{\text{RhP}}$  155.5 Hz)

$\nu_{\text{max}}/\text{cm}^{-1}$  1986 (RhH) and 1922 (CO).

### 2.3 Characterisation and Quantification of Products of Catalysis

The principal method initially implemented for the analysis of the products resulting from hydroformylation reactions was gas chromatography (GC). Initially a packed column was used but as it did not effect efficient separation of the linear and branched aldehyde isomers, a capillary column was installed which achieved good separation. However, the assignments of the resulting peaks were ambiguous and as standards of odd-carbon-number linear and branched aldehydes could not easily be obtained, this method could not be entirely relied upon. Due to this problem of assignment, the column was installed in a GC-MS (gas chromatograph-mass spectrometer) from which probable assignments were made.

Figure 2.7 shows the gas chromatogram (using the capillary column) of a mixture of products resulting from the hydroformylation of 1-octene.

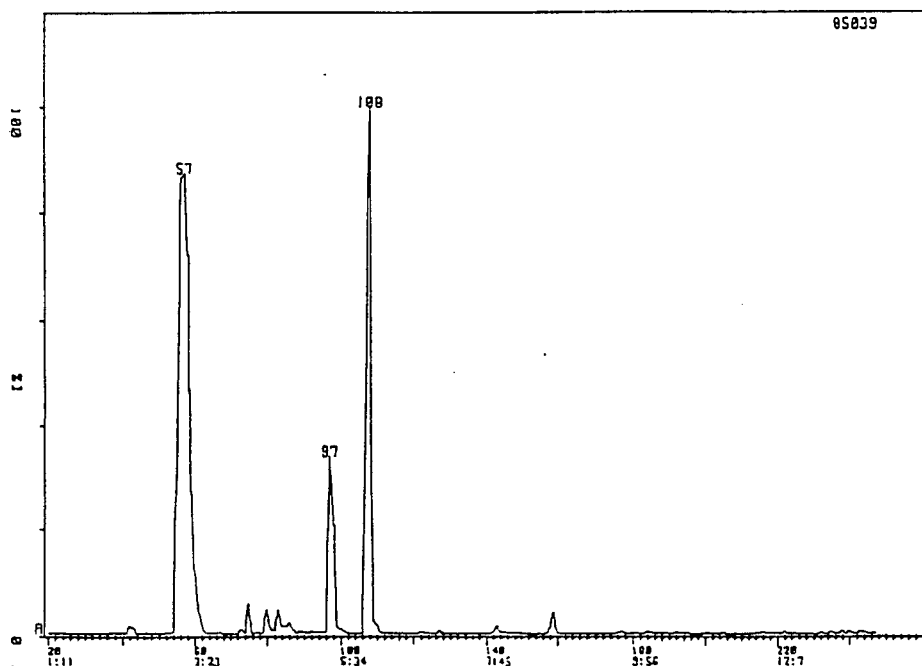


**Figure 2.7**

Gas chromatogram for products of the hydroformylation of 1-octene

The corresponding mass spectrum for each of the three major peaks are shown in Figures 2.8, 2.9 and 2.10 respectively. With the use of accumulated literature mass spectra data for similar compounds, the assignments 1-octene, *iso*-nonanal and *n*-nonanal, corresponding to the peaks 57, 97, and 108 respectively in the chromatogram, were made.

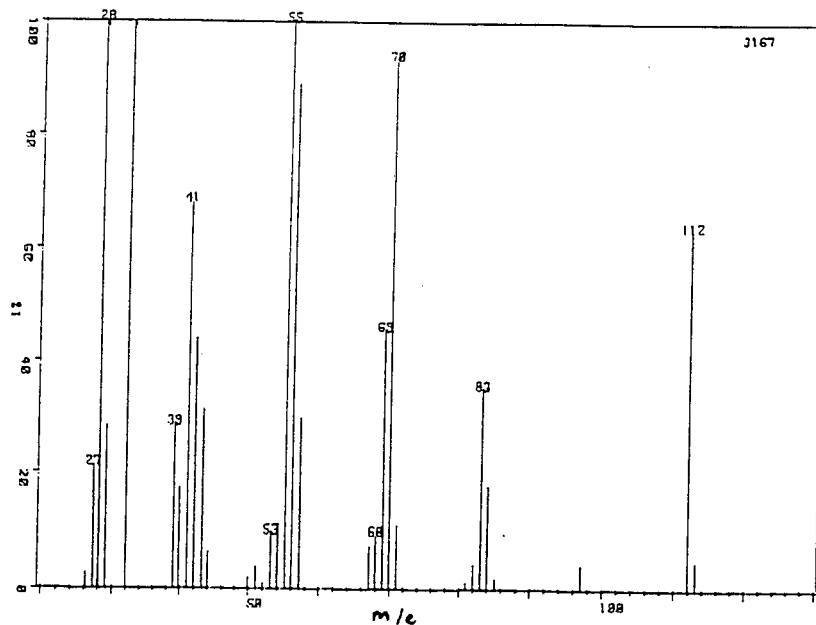


Figure 2.8

Mass spectrum corresponding to peak 57 in the gas chromatogram – assigned to 1-octene

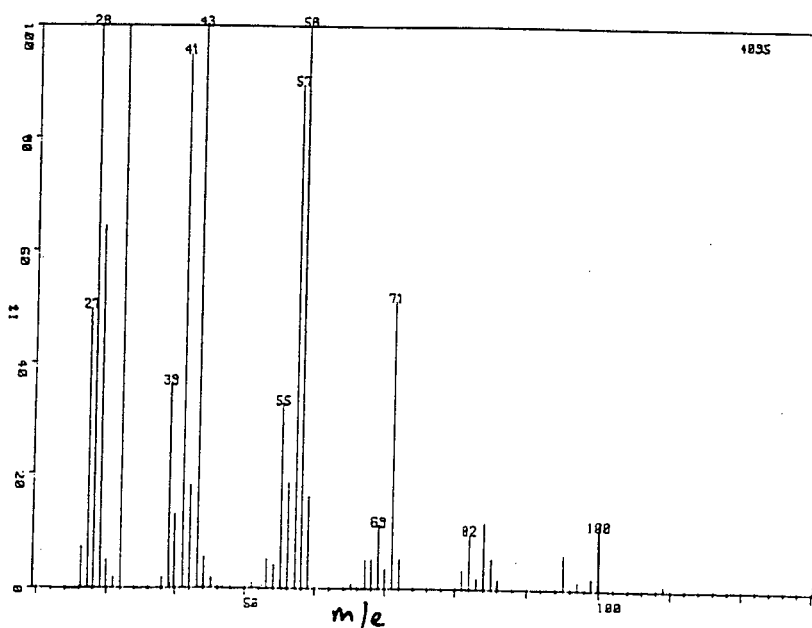
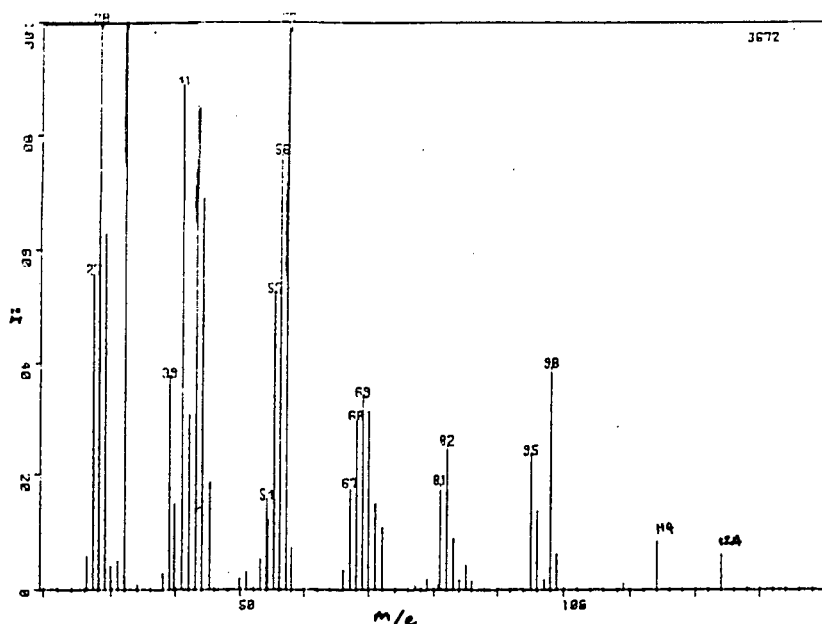


Figure 2.9

Mass spectrum corresponding to peak 97 in the gas chromatogram – assigned to *iso*-nonanal



**Figure 2.10**

Mass spectrum corresponding to peak 108 in the gas chromatogram – assigned to *n*-nonanal

However, in order to substantiate this characterisation of the hydroformylation products we resorted to the use of  $^{13}\text{C}$  NMR spectroscopy in conjunction with GC–mass spectroscopy.  $^{13}\text{C}$  NMR spectroscopy is a powerful technique which gives unambiguous structural information of alkene and aldehyde isomers which result from the hydroformylation reactions.

It was also decided to implement  $^{13}\text{C}$  NMR spectroscopy as a *quantitative* analytical tool for the comparison of the results obtained from the two analytical techniques viz. GC and  $^{13}\text{C}$  NMR. Care had to be exercised in the NMR experimental design, taking into account the factors affecting quantitative measurements, viz. the differences in spin relaxation times ( $T_1$ ) of carbons in different environments, and nuclear Overhauser enhancement (nOe). This is discussed in detail in Section 2.3.1.1.

Characterisation of the products by  $^{13}\text{C}$  NMR, and the quantitative comparison of GC/GC-MS and NMR results obtained from the integration of the peak areas are discussed further in Section 2.3.2.

### 2.3.1 Theory of quantitative $^{13}\text{C}$ NMR spectroscopy

The practicality of the  $^{13}\text{C}$  nucleus as a source of quantitative analytical information for complex mixtures of substances containing carbon compounds, has arisen with the advent of highly sensitive detection techniques such as pulsed Fourier transform NMR.  $^{13}\text{C}$  NMR spectroscopy can be particularly applicable in the analysis of mixtures containing molecules which differ principally in the structural relationship of their functional groups.<sup>74</sup>

Despite potential difficulties in obtaining meaningful peak integrations, the superior spectral dispersion of  $^{13}\text{C}$  NMR makes it suitable for quantitative analysis.<sup>72</sup> This leads to a well resolved spectrum in which each component is represented by a number of peaks which are not affected by, or interfere with, peaks due to other components.

#### 2.3.1.1 *Precautions taken to ensure suitable conditions for quantitative $^{13}\text{C}$ NMR spectroscopy*

$^{13}\text{C}$  NMR as a quantitative method, where peak areas are proportional to the number of nuclei, can be accurate and fairly simple to use if the following factors are taken into account: *a*) the differences in spin lattice relaxation times ( $T_1$ ), which may be the cause of inaccurate quantitative measurements, and *b*) the nuclear Overhauser enhancement which is induced by decoupling of the protons.

a) Spin lattice relaxation time measurements

Since the values of  $T_1$  for  $^{13}\text{C}$  nuclei can vary over several orders of magnitude (milliseconds to seconds) even within the same molecule, a different equilibrium will be set up by the train of pulses for each  $^{13}\text{C}$  environment, depending on the ratio of  $T_1$  to the pulse repetition rate  $\tau$  and also upon the strength and duration of the pulsed radiofrequency (RF) magnetic field.

The Inversion-Recovery method<sup>73,74</sup> – one of the oldest and simplest pulse sequences is one of the most common methods for the measurement of  $T_1$  values.

The pulse sequence is schematically depicted in figure 2.11.

*Inversion recovery method*

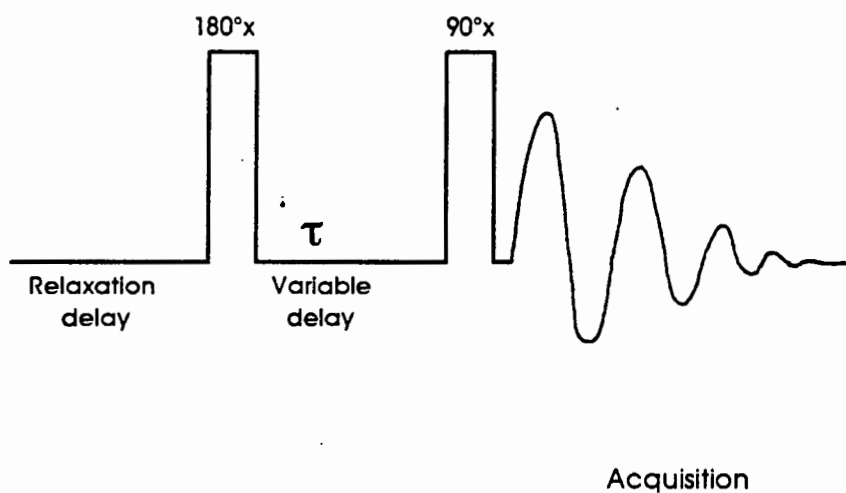


**Figure 2.11**

Pulse sequence for the inversion-recovery method

At the start of the sequence the nuclei are at equilibrium in the fixed magnetic field  $B_0$ , with a small excess population of the nuclei in the lower energy state. The

individual vectors precess about the  $B_0$  axis at the Larmour frequency, the result being a net magnetic vector  $M$  in the same direction as  $B_0$ . The rotating frame convention will be used in the following explanation which is shown schematically in Figure 2.9.

The  $180^\circ$  RF pulse causes  $M$  to rotate through  $180^\circ$  to the  $-z$  axis. Following the pulse there is a delay period,  $\tau$ , whose length is varied as the pulse is repeated. In the inversion-recovery experiment, eight or ten  $\tau$  values are used ranging from a small value up to four or five times  $T_1$ .

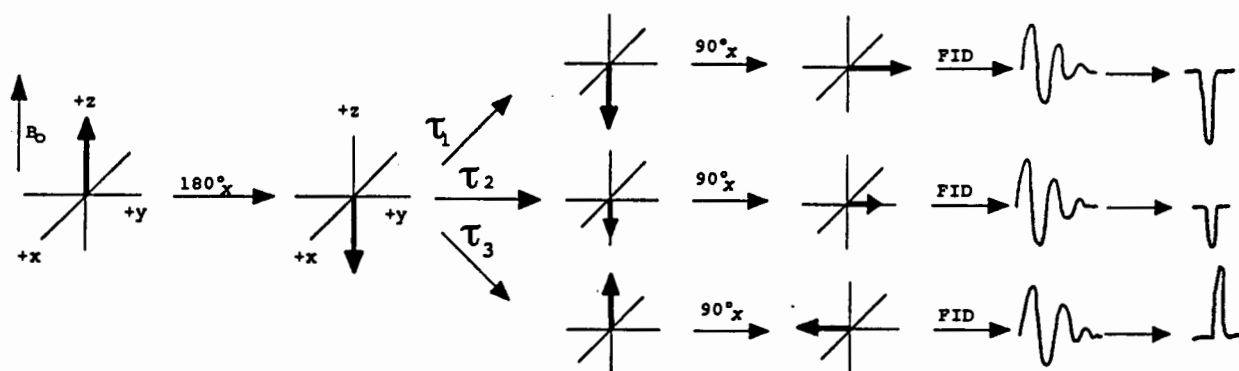


**Figure 2.9**

Vector description of the inversion-recovery method

During the  $\tau$  interval the system returns to equilibrium by the spin relaxation process. As the individual magnetic moments gradually return to their favoured orientation along the  $+z$  axis, the net magnetisation vector shortens in the  $-z$  direction. Depending on the length of the delay,  $M$  passes through zero and eventually recovers its full original magnetisation along the  $+z$  axis. To determine the extent of relaxation, a  $90^\circ$  pulse is applied which rotates  $M$  to lie along the  $y$  axis.

The pulse sequence (equilibration delay –  $180^\circ_x$  –  $\tau$  –  $90^\circ_x$  – acquisition) may be divided into three periods: preparation (the equilibration delay and the  $180^\circ$  pulse), evolution (the  $\tau$  delay), and detection (the  $90^\circ$  pulse and data acquisition).

$T_1$  values obtained of appropriate standards using the inversion-recovery method, are discussed and outlined in Section 2.3.2.

The potential problem of different  $T_1$  values may be overcome in the following ways:

*i*) lowering the pulse flip angle to very small values (a few degrees) has the effect of perturbing the spin population only very slightly *i.e.*, a large fraction of equilibrium longitudinal magnetisation is retained. This method however, results in a loss of sensitivity.

*ii*) the introduction of a delay between pulses sufficiently after data acquisition to ensure complete repolarisation (spins returning to their equilibrium distribution) of all nuclei. A delay of  $5T_1$  results in 99 % repolarisation but has the disadvantage of the experiment taking a significantly longer time.

*iii*) the use of paramagnetic substances, such as chromium acetylacetonate [ $\text{Cr}(\text{acac})_3$ ], as relaxation agents. This provides a very effective relaxation mechanism, however care must be taken in order to utilise concentrations of the relaxation agent of not more than 0.1 M, otherwise significant line broadening can occur.<sup>75,76</sup>

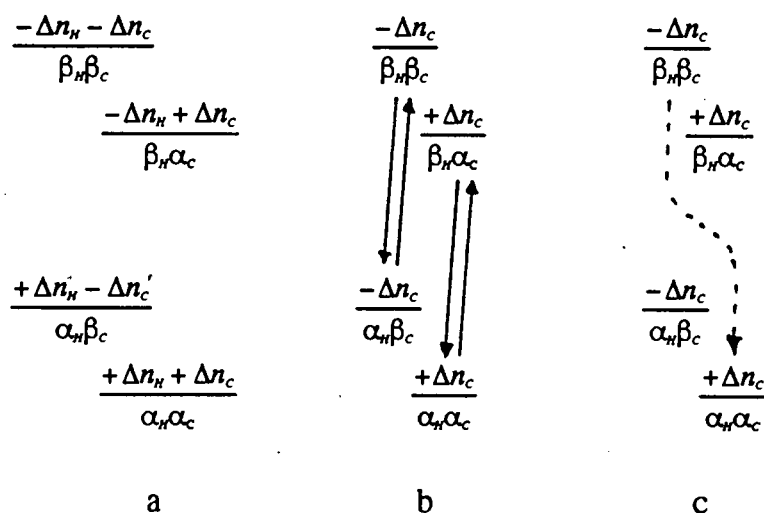
In this study it was decided to utilise the method involving the addition of a relaxation agent *viz.*  $\text{Cr}(\text{acac})_3$ . The measurements of  $T_1$  values will be discussed in more detail in Section 2.3.2.

b) Nuclear Overhauser effect, (nOe)

One of the consequences of decoupling is a change in the intensity of some peaks. This change is known as the nuclear Overhauser effect. When inducing decoupling of the hydrogen nuclei by irradiation of the proton spins, the excess population in the lower energy state of the  $^{13}\text{C}$  nuclei can be increased.<sup>75</sup> See Figure 2.13. This results in an increase in the signal by an additive factor called the nuclear Overhauser enhancement,  $\eta$ , which can approach 1.988 in the absence of other relaxation mechanisms, and zero in the absence of dipole-dipole relaxation.

**Figure 2.13**

Energy level diagram for a  $^{13}\text{C}/^1\text{H}$  pair ( $\alpha$  and  $\beta$  refer to  $m_I = +1/2$  and  $-1/2$ , respectively)



For clarity, only population differences  $\Delta n_H$  and  $\Delta n_C$  are shown. a) In the absence of any applied RF fields the levels are populated according to the requirements of the Boltzmann distribution. (b) When the protons are irradiated by the continuous RF source, the populations of the  $\alpha_H$  and  $\beta_H$  states are equalised. This means that the populations of the  $\alpha_H \alpha_C$  and  $\alpha_H \beta_C$  decrease by  $\Delta n_H$ , while the  $\beta_H \alpha_C$  and  $\beta_H \beta_C$  populations increase by the same amount. (c) The system attempts to return to the thermal equilibrium by  $T_1$  relaxation. If the dominant route is from  $\beta_H \beta_C$  to  $\alpha_H \alpha_C$  (as is usual for small molecules in nonviscous solvents), the result is a net increase in the number of  $^{13}\text{C}$  nuclei in the lower state and an enhancement in the intensity of the  $^{13}\text{C}$  resonance.<sup>75</sup>

The most effective way found so far to deal with the nOe is to make the factor,  $\eta$ , approach zero. This can be achieved by:

- i)* operation without proton decoupling thus reintroducing  $^{13}\text{C}$ - $^1\text{H}$  coupling information.
- ii)* use of gated decoupling. This is achieved by turning the decoupler off during the delay period while the nuclei are recovering from the pulse, and turning it on again only during acquisition, as shown in Figure 2.14.

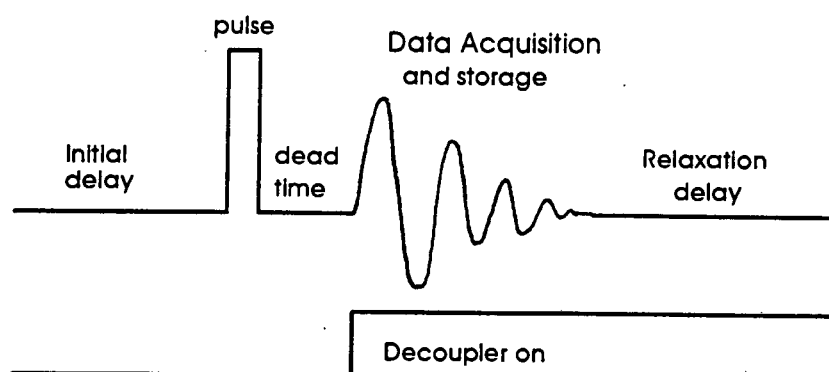


**Figure 2.14**

Schematic representation of the pulse sequence for gated decoupling.

If the delay is long enough compared with the acquisition time, the build up of nOe during acquisition will die away during the delay.

*iii)* chemically suppressing the nOe, as opposed to magnetic suppression, by the addition of a paramagnetic relaxation agent such as chromium acetylacetonate,  $[\text{Cr}(\text{acac})_3]$ , to the sample. This provides an alternative relaxation method by which the enhancement due to dipole-dipole relaxation can 'leak' away as it is generated.

In this study the method of gated decoupling in order to minimise the nuclear Overhauser enhancement was implemented.

## 2.3.2 Results and discussion

### 2.3.2.1 Characterisation of products by $^{13}\text{C}$ NMR spectroscopy

#### a) Standards

Initially  $^{13}\text{C}$  NMR spectra of standards were run in order to assign the individual spectra fully and to compare the experimental chemical shifts obtained with those reported in the literature. These include 1-octene, 1-decene, *n*-nonanal and 1-decanol. With the use of the DEPT pulse sequence (distortionless enhancement by polarisation transfer) which separately displays carbons with different numbers of attached hydrogens, the majority of the carbons in each compound could be unambiguously assigned. Figure 2.15 shows a typical DEPT NMR spectrum for the standard, 1-decanol. The assignments which are shown in Table 2.4, compared to within 0.2 ppm of those reported in the literature.<sup>72,76</sup>

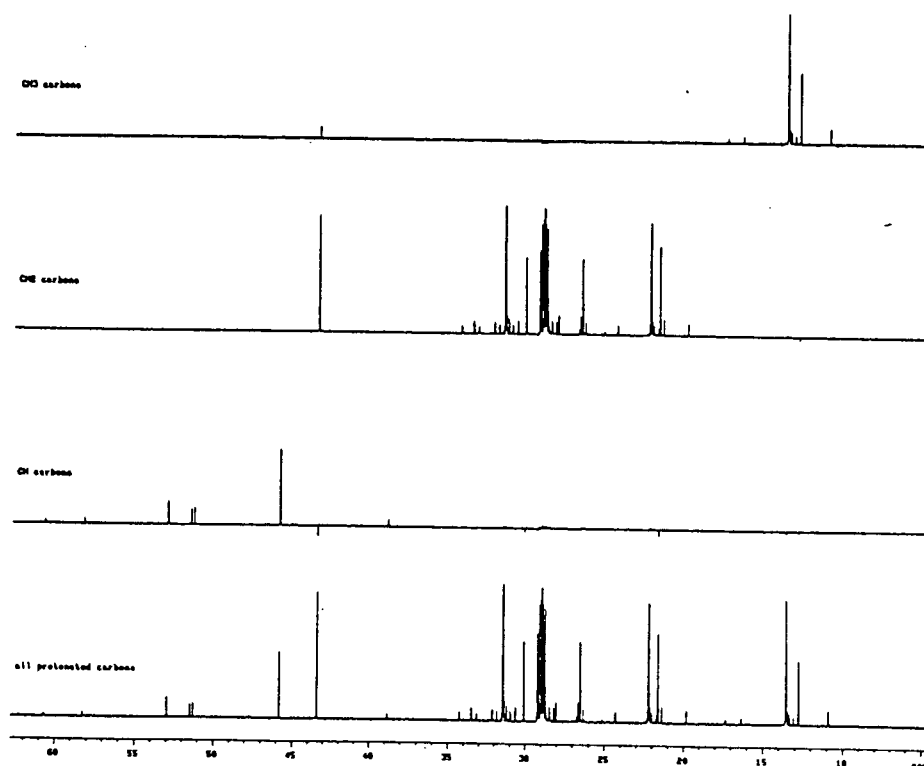


Figure 2.15

DEPT results for 1-decanol.

**Table 2.4**

$^{13}\text{C}$  chemical shifts of standards of compounds likely to be found in a mixture of hydroformylated products.<sup>a</sup>

Cpd	C <sub>1</sub>	C <sub>2</sub>	C <sub>3</sub>	C <sub>4</sub>	C <sub>5</sub>	C <sub>6</sub>	C <sub>7</sub>	C <sub>8</sub>	C <sub>9</sub>	C <sub>10</sub>
octene	114.1	139.1	33.9	28.9	29.0	31.9	22.7	14.0	–	–
decene	114.1	139.0	34.0	29.4	29.7	29.5	29.1	32.1	22.8	14.1
<i>n</i> -decanal	202.3	43.7	22.5	29.2	29.0	29.0	29.2	31.7	21.9	13.8
decanol	62.4	32.5	25.7	29.2	29.5	29.5	29.4	31.8	22.5	13.8

<sup>a</sup> Chemical shifts measured in ppm relative to internal TMS.

In hydrocarbons, olefinic nuclei appear over a span of about 65 ppm, in the chemical shift range  $\delta_{\text{C}}$ : 100 – 165 ppm. A hydroxyl group as found in alcohols causes an increased shielding effect which results in a pronounced upfield shift of between 36 and 52 ppm ( $\delta_{\text{C}}$ : 60 – 75 ppm) for the carbon to which it is bonded, and a definite but smaller shift of 5 – 10 ppm for the  $\beta$ -carbon. An even more pronounced upfield shift occurs for aldehydic carbons due to increased shielding effect of the oxygen atom. The chemical shifts of the carbonyl carbon is found typically in the range of  $\delta_{\text{C}}$ : 185 – 210 ppm.

#### b) Products of hydroformylation

$^{13}\text{C}$  NMR, spectra were then run for a number of mixtures of hydroformylation products. Mixtures 1 and 2 were products resulting from the hydroformylation of 1-decene and 1-octene respectively. The spectra of 1 and 2 are shown in Figure 2.16 and the assignments of the NMR spectra are outlined in Table 2.5. Only the particularly characteristic peaks of the individual products are assigned.

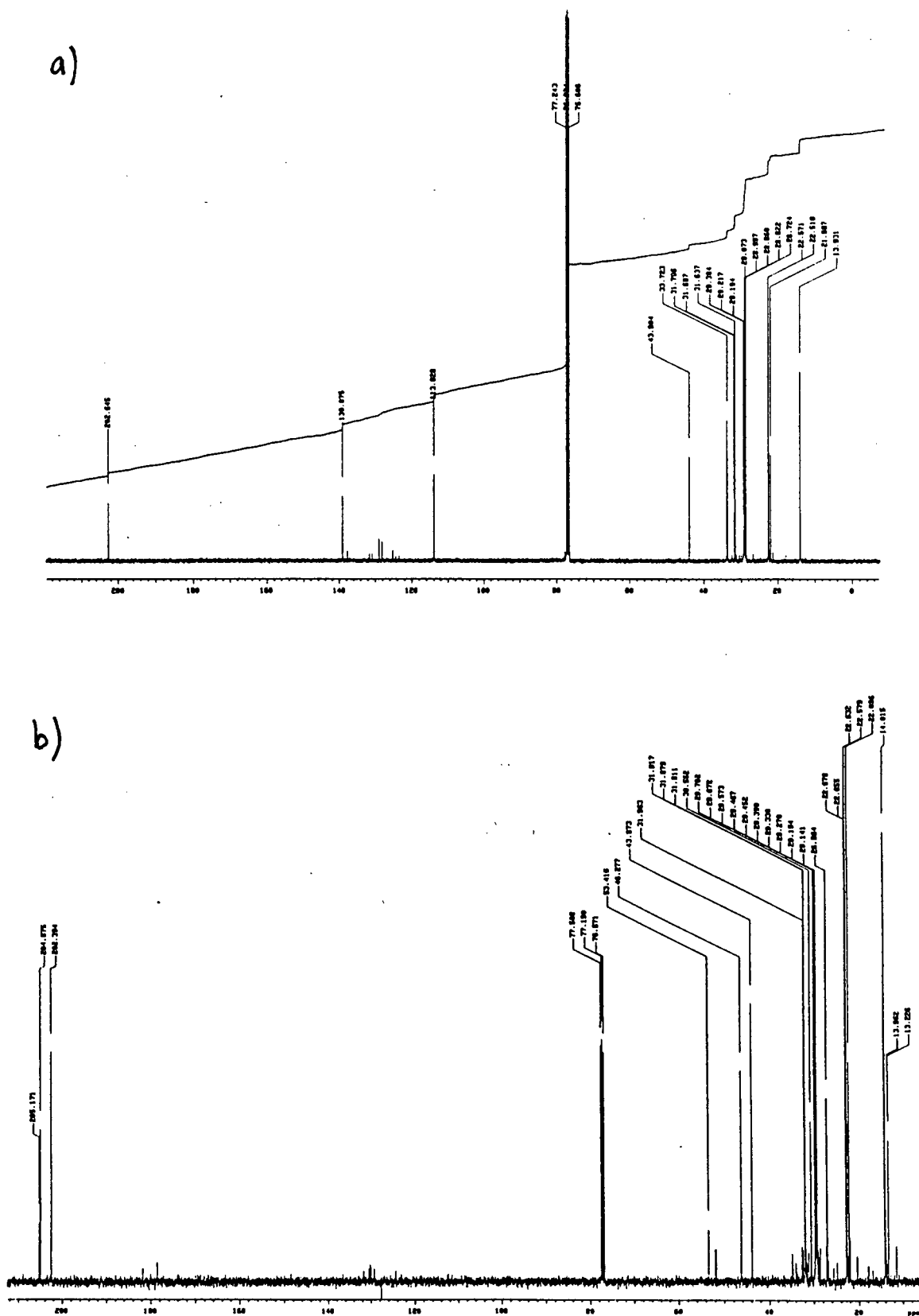


Figure 2.16

$^{13}\text{C}$  NMR spectra of hydroformylation products of a) 1-octene (1) and b) 1-decene (2)

**Table 2.5**

Table of  $^{13}\text{C}$  chemical shifts for hydroformylated products of 1-decene (1) and 1-octene(2)<sup>a,b,c</sup>

Mixture	Compound	C <sub>1</sub>	C <sub>2</sub>
1	1-decene	negligible amount - peaks of isomers indistinguishable	
	<i>n</i> -undecanal <sup>d</sup>	202.4 (~202)	43.9 (~45)
	<i>iso</i> -decenal <sup>e</sup>	204.9 (~206)	46.3 (~47)
2	1-octene	113.9 (115.0)	139.1 (139.2)
	<i>n</i> -nonanal	202.6 (~202)	43.8 (~45)

<sup>a</sup> Chemical shifts shown for characteristic carbons only.

<sup>b</sup> Chemical shifts measured in ppm relative to internal TMS with CdCl<sub>2</sub> as solvent.

<sup>c</sup> Literature chemical shifts of similar compound in brackets.

<sup>d</sup> Assignment of peak confirmed by a DEPT experiment, corresponds to a CH<sub>2</sub> carbon.

<sup>e</sup> Assignment of peak confirmed by a DEPT experiment, corresponds to a CH carbon.

### 2.3.2.2 Measurement of $T_1$ values for the application of quantitative $^{13}\text{C}$ NMR spectroscopy

The  $T_1$  values of appropriate standards were measured using the inversion-recovery method, as explained previously. A parallel experiment was run with the addition of a relaxation agent [Cr(acac)<sub>3</sub>] in order to ascertain if the different  $T_1$  values so produced were significantly lower.

Figure 2.17 shows a typical set of  $^{13}\text{C}$  NMR spectra obtained when measuring  $T_1$  values, and a plot of the heights of the transformed peaks as a function of  $\tau$  (delay time), for 1-decanol.

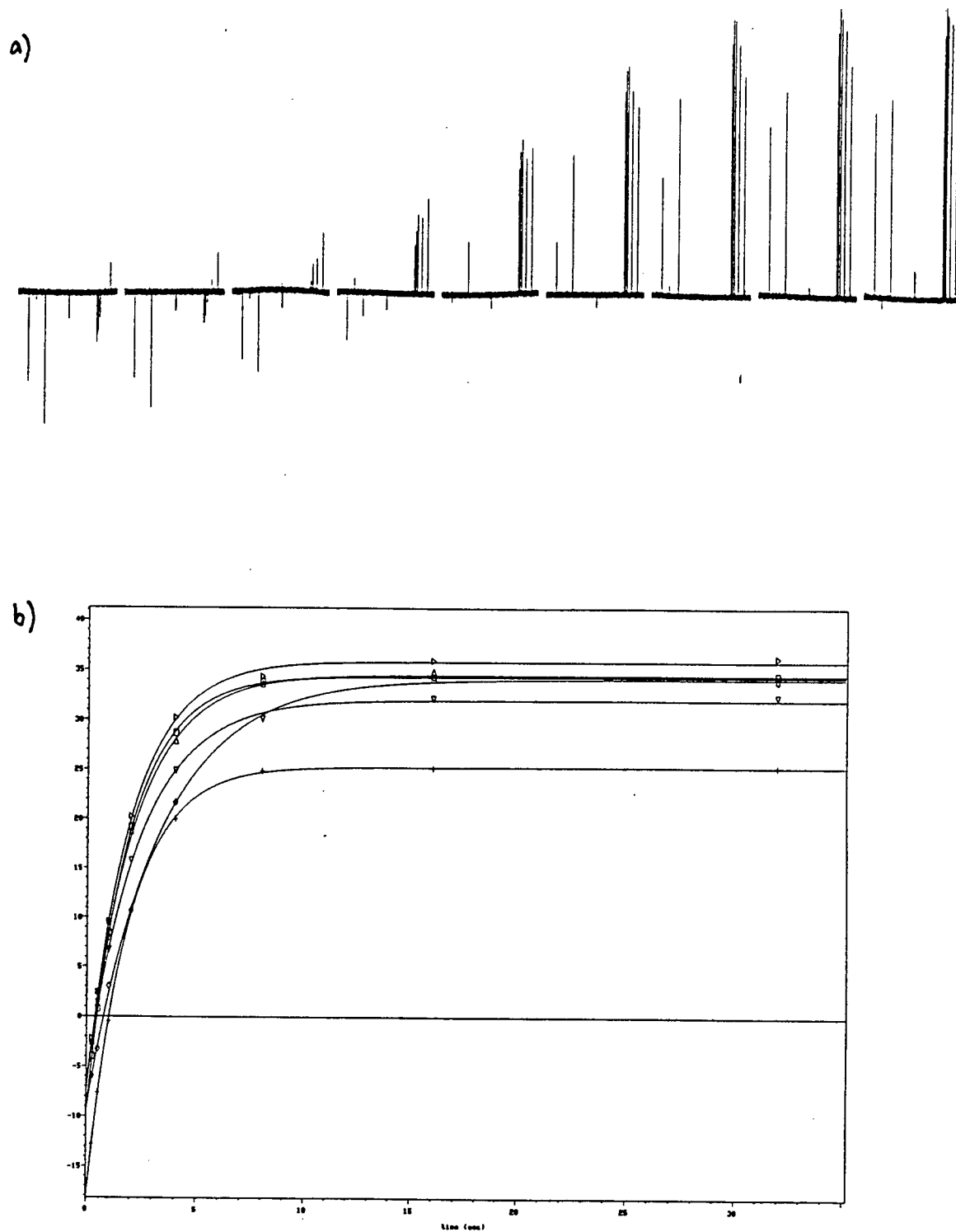


**Figure 2.17**

$T_1$  by inversion method a) set of  $^{13}\text{C}$  spectra for 1-decanol and b) plot of heights of transformed peaks as a function of  $\tau$ .

Table 2.6 below shows the resulting  $T_1$  values for 1-decene, measured by the inversion-recovery method with and without the addition of the relaxation agent  $\text{Cr}(\text{acac})_3$ .

**Table 2.6**

Spin lattice relaxation times ( $T_1$ 's) measured for 1-decene

peak	$T_1$ (sec) <sup>a</sup>	error (sec) <sup>b</sup>	$T_1$ (sec) <sup>c</sup>	error (sec)
1	13.56	0.32	6.88	0.19
2	5.758	0.16	4.00	0.06
3	5.790	0.13	4.14	0.13
4	5.839	0.07	4.32	0.07
5	4.736	0.16	3.66	0.06
6	4.987	0.08	3.90	0.15
7	4.994	0.24	3.60	0.12
8	5.316	0.09	3.85	0.06
9	6.711	0.18	4.75	0.07
10	6.053	0.45	4.89	0.2298

<sup>a</sup>  $T_1$  values measured without addition of  $\text{Cr}(\text{acac})_3$  as relaxation agent.

<sup>b</sup> Error derived by computer from numerical fit of trend.

$T_1$  values measured with the addition of  $\text{Cr}(\text{acac})_3$  (0.01 M) as relaxation agent.

The  $T_1$  values for 1-decanol without the addition of  $\text{Cr}(\text{acac})_3$  are shown below in Table 2.7.

As indicated by the  $T_1$  values obtained, the olefinic carbons of the alkene have the highest spin lattice relaxation time in a mixture of alkenes, alcohols and aldehydes

(which have similar  $T_1$  values to alcohols), and therefore taken as the limiting  $T_1$  value in the design of the quantitative  $^{13}\text{C}$  NMR experiments. It was also shown that the addition of  $\text{Cr}(\text{acac})_3$  to 1-octene results in a significant decrease in the value of  $T_1$  of about 50%. Thus due to the large differences in  $T_1$  values ranging from 1.9 to 13.6 seconds, it was decided to use  $\text{Cr}(\text{acac})_3$  (0.01 M) when performing quantitative  $^{13}\text{C}$  NMR spectroscopy.

**Table 2.7**Spin lattice relaxation times ( $T_1$ 's) measured for 1-decanol

peak	$T_1$ (sec)	error (sec) <sup>a</sup>
1	1.87	0.036
2	1.92	0.025
3	3.23	0.091
4	2.15	0.084
5	2.37	0.080
6	2.00	0.055
7	2.79	0.077
8	1.87	0.077
9	4.14	0.12
10	5.07	0.19

<sup>a</sup> Error derived by computer from numerical fit of trend.

*Comparison of quantitative results using GC and  $^{13}\text{C}$  NMR*

Together with the characterisation of the products by  $^{13}\text{C}$  NMR and information resulting from the use of GC-MS, unambiguous assignments of the GC peaks were made.

In order to compare quantitatively, results obtained from GC and  $^{13}\text{C}$  NMR spectroscopy, the necessary precautions were applied for the analysis of hydroformylated mixtures in order to carry out routine  $^{13}\text{C}$  NMR quantitative analysis. The problem involving the difference in the relaxation times,  $T_1$  was overcome by the addition of a paramagnetic relaxation agent [ $\text{Cr}(\text{acac})_3$ , (0.01 M)] and by introducing a pulse delay long enough to result in complete repolarisation of all the nuclei. The elimination of nOe was achieved with the use of gated decoupling, where the decoupler is on during data acquisition and off during pulse delay, as outlined previously.

A typical quantitative  $^{13}\text{C}$  NMR spectrum is shown in Figure 2.16(a). The relevant portion of the spectrum is expanded and the integration of the requisite peaks measured. The comparison of quantitative results obtained from the integration of the peak areas using quantitative  $^{13}\text{C}$  NMR spectra and gas chromatography (with capillary column) are outlined in Table 2.8 below.

**Table 2.8**

Comparison of quantitative results obtained by gas chromatography and  $^{13}\text{C}$  NMR respectively.

<b>mixture</b>	<b>compound</b>	<b>GC (%)</b>	<b><math>^{13}\text{C}</math> NMR (%)</b>
<b>1<sup>a</sup></b>	1-decene	~ 5	< 5
	<i>n</i> -undecanal	46	44
	<i>iso</i> -nonanal	49	50
<b>2<sup>a</sup></b>	1-octene	53	57
	<i>n</i> -nonanal	44	41
<b>3<sup>b</sup></b>	1-octene (+ isomers)	14	18
	<i>iso</i> -nonanal	35	38
	<i>n</i> -nonanal	31	35
	nonanoic acid	9	8
	other	11	

<sup>a</sup> Mixtures as mentioned previously in Table 2.5

<sup>b</sup> Complex mixture of products resulting after standing for a few weeks. Nonanoic acid formed as a result of condensation reactions of the hydroformylation products.

### Conclusion

Thus with the use of  $^{13}\text{C}$  NMR spectroscopy as a quantitative and qualitative technique, the problems associated with the ambiguous analysis of hydroformylation products by gas chromatography were overcome. Gas chromatography was therefore established as the principal analytical method with  $^{13}\text{C}$  NMR spectroscopy as a complimentary technique.

## **Chapter 3**

# **Catalytic Hydroformylation Reactions**

## Chapter 3

### Catalytic Hydroformylation Reactions

In this chapter the activity, and selectivity towards linear aldehydes of the two-phase heterogeneous rhodium-tri(*m*-sulfonatophenyl)phosphine (Rh-TPPTS) catalyst system for the hydroformylation of long-chain 1-alkenes, viz. 1-octene, 1-decene, and 1-dodecene, is reported. Due to the industrial value of straight-chain aldehydes, the establishment of experimental conditions for which one can expect high selectivity towards the linear aldehyde is of particular interest.

The active catalytic species are generated *in situ* from rhodium trichloride hydrate ( $\text{RhCl}_3 \cdot 3\text{H}_2\text{O}$ ) and excess water-soluble phosphine ligand, TPPTS, under standard hydroformylation conditions (carbon monoxide / hydrogen pressure of 5 MPa, and temperature of 100 °C).

Secondly for the purpose of comparison, the activity, selectivity and catalyst lifetime of the synthesised heterogeneous rhodium catalytic precursor,  $\text{RhH}(\text{CO})(\text{TPPTS})_3$ , and of the conventional homogeneous rhodium catalytic complex,  $\text{RhH}(\text{CO})(\text{PPh}_3)_3$ , for the hydroformylation of the long-chain 1-alkenes under similar hydroformylation conditions, is investigated.

The catalytic hydroformylation results will be discussed in detail in Chapter 5.

### 3.1 Reaction Procedure

The catalytic experiments were performed at a constant pressure and temperature of 5 MPa and 100 °C respectively, in a homebuilt stainless-steel reactor which had not been previously tested for catalytic performance. See Figure 3.1 below. The vessel was lined with a teflon cup in order to avoid contact of the gas mixture,  $H_2/CO$  with the stainless-steel walls of the reactor. The  $H_2/CO$  gas mixture was always in a ratio of 1:1.

The reactor containing the aqueous catalytic mixture plus the organic substrate was first purged with nitrogen and then flushed with the synthesis gas mixture. The pressure was increased to 5 MPa, before finally heating to the desired reaction temperature. The reaction mixture was stirred for 24 hours, cooled to between 0 and 5 °C, and the pressure released.

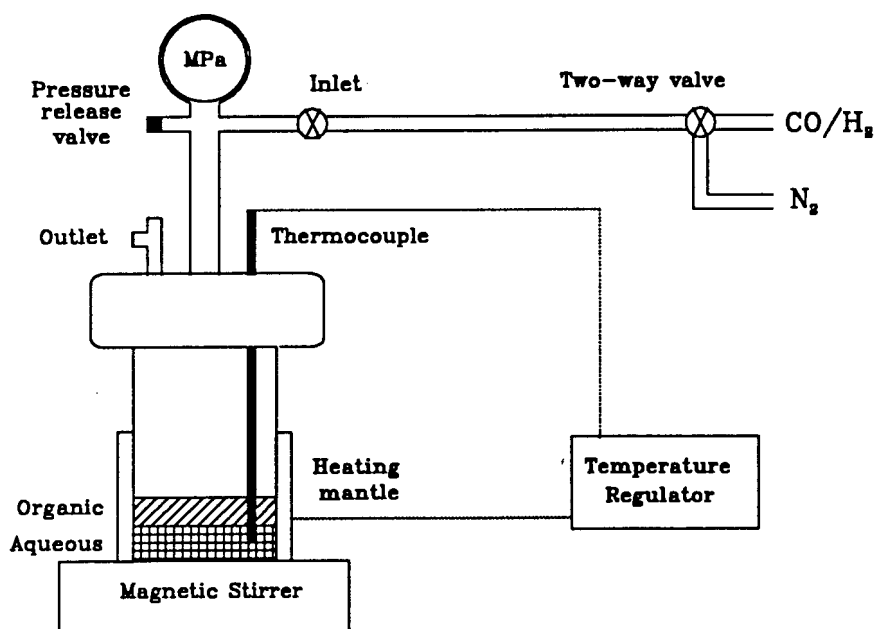


**Figure 3.1** Schematic representation of pressure vessel used for catalytic reactions

Due to the two distinct phases – the catalytic species in the aqueous phase and the reactants and products in the organic phase – separation of the catalyst from the products was easily facilitated. The resulting hydroformylation products were analysed using quantitative  $^{13}\text{C}$  NMR spectroscopy and gas chromatography. The aqueous phase containing the catalytic species was washed twice with toluene in order to extract any dissolved organic products, and then used for further catalytic reactions if desired.

## 3.2 Hydroformylation Reactions

### 3.2.1 Two-phase hydroformylation reactions

#### i) Rhodium catalytic species prepared *in situ*

The effect of the following variables on the catalytic hydroformylation of 1-octene, 1-decene and 1-dodecene using a number of two-phase catalyst systems of different composition, were considered:

- alkene chain-length
- rhodium/alkene ratio
- phosphine:rhodium ratio
- stirring rate

#### *Reaction conditions*

Two-phase hydroformylation reactions were typically performed by adding rhodium(III) (0.1–1.0 mmol) as the water-soluble rhodium trichloride,  $\text{RhCl}_3 \cdot 3\text{H}_2\text{O}$  to a buffered aqueous solution (20 ml) of the phosphine ligand, TPPTS, in the required mole ratios of rhodium:phosphine:olefin. It is well known that the

catalytically-active complex  $\text{RhH}(\text{CO})(\text{PPh}_3)_3$ , is thought to be formed under the action of CO and  $\text{H}_2$  under pressure with virtually any rhodium compound, in the presence of an excess of triphenylphosphine.<sup>77</sup> It is therefore reasonable to assume that the active catalytic species are similarly generated *in situ* in the aqueous phase under hydroformylation conditions (5 MPa  $\text{H}_2/\text{CO}$  and 100 °C).

It was thought advisable to buffer the aqueous phase to pH 5-7 [using a mixture of  $\text{Na}_2\text{HPO}_4$  (0.25 M) and  $\text{KH}_2\text{PO}_4 \cdot 2\text{H}_2\text{O}$  (0.25 M)], as the use of precursors containing chloride is known to liberate HCl which has a detrimental effect on the activity of the system.<sup>78</sup> This effect was demonstrated by Smith *et al.*<sup>65</sup> who reported that the heterogeneous hydroformylation of neat 1-hexene, using rhodium complexes of the water-soluble phosphine ligand  $\text{Ph}_2\text{PCH}_2\text{CH}_2\text{NMe}_3^+$ , proceeded in a 90% yield between pH 5.5 and 6.8, and dropped to 76% conversion at pH 5.0. Another reason for buffering the system is to ensure that the sulfonate groups of the TPPTS ligands remain deprotonated, since a low pH may well result in the deprotonation of the sulfonated phosphine ligand thereby forming the corresponding acid,  $\text{P}(\text{C}_6\text{H}_4\text{SO}_3^-\text{H}^+)_3$ . As the acid is soluble in the organic phase, significant loss of the phosphine ligand to the organic phase may result.

The nature and distribution of the rhodium tertiary-phosphine complexes present in the aqueous phase of a matching system is discussed in detail in Chapter 4.

In general, for comparative purposes similar rhodium:alkene ratios (Rh:alkene) of *ca.* 1:200 were used in this study, to those recorded in literature for similar systems.

#### *Catalytic hydroformylation results*

A series of catalytic systems for the hydroformylation of 1-octene, 1-decene, and 1-dodecene were prepared in the manner discussed above. The phosphine:rhodium

ratio ranged from 1:3 to 1:30, and the rhodium:alkene ratio was varied from 1:26 to 1:300.

Experimental details together with the catalyst compositions and results of catalytic hydroformylation reactions for the systems prepared, are contained in Tables 3.1 to 3.4.

*i) Catalytic activity in the hydroformylation of 1-octene, 1-decene, and 1-dodecene*

It was found that in general using rhodium:alkene ratios of *ca.* 1:200, fairly high conversions of up to 60% were achieved for the hydroformylation of 1-octene to the corresponding aldehyde, nonanal. However, the activity of the heterogeneous system reduced to a percentage conversion of *ca.* 10% for the hydroformylation of 1-decene, and *ca.* 5% for 1-dodecene. System 2 (Rh:P = 1:10) however, resulted in unusually high percentage conversion of 1-decene (69%) and 1-dodecene (52%) using similar rhodium:alkene ratios.

The aqueous phase for both systems 1 and 2 (Rh:P = 1:3 and 1:10 respectively, Tables 3.1 and 3.2) which was yellow at the beginning of the reaction, turned black after the first reaction. It was noted for these two systems, that colour was imparted to the organic phase during hydroformylation reactions resulting in a yellow organic phase. The activity of these two systems decreased to zero after four or five repeated uses of the catalytic mixture.

The colour of the aqueous phase for systems 3 and 4 (Rh:P = 1:20 and 1:30 respectively, Tables 3.3 and 3.4) however, remained yellow. The activity of systems 3 and 4 remained consistent for all reactions performed and the actual catalytic

lifetimes were not determined. Contrary to systems 1 and 2, little or no colour was imparted to the organic phase during hydroformylation reactions.

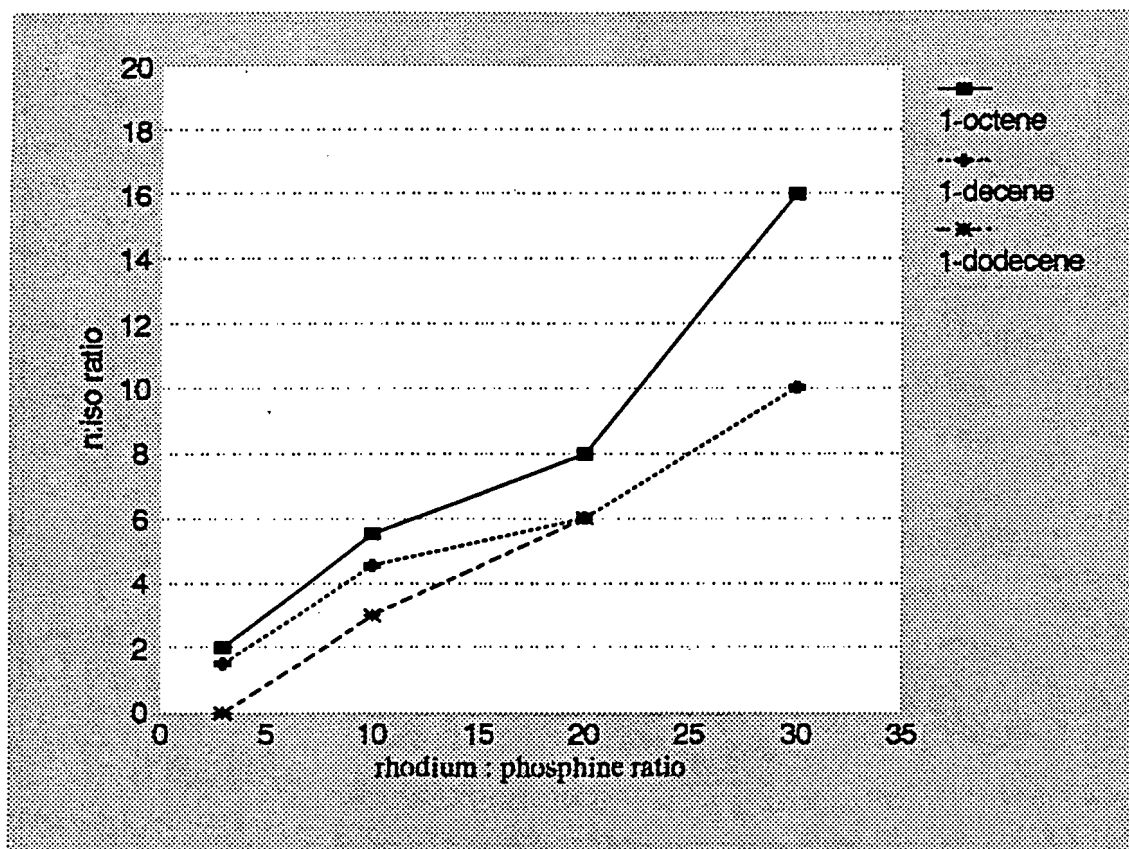
Increasing the rhodium concentration of the catalytic system (or decreasing the rhodium:alkene ratio) resulted in an increase in the percentage conversion of the 1-alkene to the corresponding aldehyde. A rhodium:alkene ratio of 1:26 for the hydroformylation of 1-decene resulted in 95% conversion to the aldehyde, undecanal, while a ratio of 1:64 corresponded to 71% conversion and 1:106 to 9% conversion. See Table 3.1.

On decreasing the stirring rate to 100 rpm (as opposed to 215 rpm usually used), the percentage conversion (activity) dropped significantly from *ca.* 45% to 12%, while a stirring rate of 0 rpm resulted in zero activity. An increase of the stirring rate from 215 rpm to 400 rpm produced negligible difference in the activity of the system. See Table 3.4.

Increase of the pressure from 5 to 7 MPa or the temperature from 100 to 150 °C did little to affect the percentage conversion of the heterogeneous system. See Table 3.1, runs 1 and 5).

*ii*) Selectivity to linear aldehydes in the hydroformylation of 1-octene, 1-decene, and 1-dodecene

Figure 3.1 shows the effect of the phosphine:rhodium ratio on the selectivity of the *n*-aldehydes (linear) to the *iso*-aldehydes (branched) produced.



Graph of the *n:iso* ratio versus rhodium:phosphine ratio

As outlined below the *n:iso* ratio of the aldehydes produced from the hydroformylation of 1-octene, 1-decene, and 1-dodecene increased from *ca.* 2:1 using a P:Rh ratio of 3:1, to *ca.* 15:1 with a P:Rh ratio of 30:1.

<b>P:Rh ratio</b>	<b><i>n:iso</i></b>
3:1	1:1 → 3:1
10:1	3:1 → 6:1
20:1	7:1 → 13:1
30:1	13:1 → 17:1

This ratio did not appear to be dependent on other factors such as pressure, temperature, stirring rate, or rhodium concentration.

**Table 3.1**

**Hydroformylation of 1-octene and 1-decene using catalyst<sup>a</sup> prepared *in situ*<sup>b</sup>**

1-alkene	run	Rh:alkene	T (°C)	P (MPa)	time (hr)	percentage composition of products					
						aldehyde <sup>c</sup>	alkene <sup>d</sup>	'n'	'iso'	n:iso	TON <sup>e</sup>
decene	1	1:106	100	7	24	8.5	91.5	6.4	2.1	3:1	0.4
decene	2	1:26	100	5	24	94.5	5	46	48.5	1:1	1.1
decene	3	1:64	100	5	24	71	29	35.6	35.5	1:1	1.9
octene	4	1:128	100	5	24	65	33.5	42	23	2:1	3.5
decene	5	1:106	150	5	24	5.5	93.5	3.5	2.5	1.5:1	0.3
decene	6	1:106	100	5	24	0	100	-	-	-	-
octene	7	1:128	100	5	48	0	100	-	-	-	7.2 <sup>f</sup>

<sup>a</sup> Composition of System 1 : 0.2616 g (0.9932 mmol) RhCl<sub>3</sub>.3H<sub>2</sub>O + 2.1620 g TPPTS in 20 ml aqueous buffer. Rh:TPPTS = 1:3.

<sup>b</sup> Note that the hydroformylation reactions are tabulated chronologically.

<sup>c</sup> *n* and *iso* aldehydes generated.

<sup>d</sup> Unreacted 1-alkene plus possible alkene isomers.

<sup>e</sup> Turnover number = no. moles of alkene per mole of rhodium converted to aldehydes per hour.

<sup>f</sup> Total TON

Table 3.2

Hydroformylation of 1-octene, 1-decene and 1-dodecene using rhodium catalyst<sup>a</sup> prepared *in situ*<sup>b</sup>

run	1-alkene	Rh:alkene	T °C	P (MPa)	time (hr)	Percentage composition of products					
						aldehyde <sup>c</sup>	alkene <sup>d</sup>	'n'	'iso'	n:iso	TON <sup>e</sup>
1	octene	1:300	100	24	5	44	56	37	7	5.3:1	5.6
2	decene	1:263	100	24	5	68.5	31.5	54.5	14	4:1	6.9
3	dodecene	1:215	100	24	5	51.5	45	36	15.5	2.5:1	4.6
4	octene	1:300	100	24	5	40	60	33.5	5.5	6:1	5.1
5	octene	1:300	100	24	5	9	90	7.5	1.5	5:1	1.1
6	decene	1:263	100	24	5	0	100	-	-	-	-
											22.2 <sup>f</sup>

<sup>a</sup> Composition of System 2 : 0.0572 g (0.209 mmol) RhCl<sub>3</sub>·3H<sub>2</sub>O + 2.1 mmol TPPTS in 20 ml aqueous buffer. Rh:TPPTS = 1:10.

<sup>b</sup> Note that the hydroformylation reactions are tabulated chronologically.

<sup>c</sup> *n* and *iso* aldehydes generated.

<sup>d</sup> Unreacted 1-alkene plus possible alkene isomers.

<sup>e</sup> Turnover number = no. moles of alkene per mole of rhodium converted to aldehydes per hour.

<sup>f</sup> Total TON.

**Table 3.3**

**Hydroformylation of 1-octene, 1-decene and 1-dodecene using rhodium catalyst<sup>a</sup> prepared *in situ*<sup>b</sup>**

run	1-alkene	Rh:alkene	T °C	P (MPa)	time (hr)	Percentage composition of products					TON <sup>c</sup>
						aldehyde <sup>c</sup>	alkene <sup>d</sup>	'n'	'iso'	n:iso	
1	octene	1:303	100	24	5	47	53	43.5	3.5	12.5:1	5.9
2	octene	1:303	100	24	5	54	46	47.5	6.5	7.3:1	5.7
3	octene	1:151	100	24	5	46	54	41	5	8.2:1	3.4
4	decene	1:263	100	24	5	8.5	91	7	~1.5	~6:1	0.9
5	decene	1:131	100	24	5	5	94	3.5	<0.5	6:1	0.3
6	dodecene	1:108	100	24	5	3.5	96	4	<1	~6:1	—
7	octene	1:151	100	24	5	28	61.5	24.5	3.5	7:1	4.1

<sup>a</sup> Composition of System 3 : 0.0553 g (0.211 mmol) RhCl<sub>3</sub>.3H<sub>2</sub>O + 4.2 mmol TPPTS in 20 ml aqueous buffer. Rh:TPPTS = 1:20.

<sup>b</sup> Note that the hydroformylation reactions are tabulated chronologically.

<sup>c</sup> *n* and *iso* aldehydes generated.

<sup>d</sup> Unreacted 1-alkene plus possible alkene isomers.

<sup>e</sup> Turnover number = no. moles of alkene per mole of rhodium converted to aldehydes per hour.

**Table 3.4**

**Hydroformylation of 1-octene, 1-decene and 1-dodecene using rhodium catalyst<sup>a</sup> prepared *in situ*<sup>b</sup>**

1-alkene	Rh:alkene	stirring rate (rpm) <sup>c</sup>	T °C	P (MPa)	time (hr)	Percentage composition of products					
						aldehyde <sup>d</sup>	alkene <sup>e</sup>	'n'	'iso'	n:iso	TON <sup>f</sup>
decene	1:263	215	100	5	24	~4	95	~3	<0.5	~10:1	0.4
decene	1:131	215	100	5	24	3.5	94	3.5	<0.5	~10:1	0.2
octene	1:160	215	100	5	24	43.5	53	43.5	2.5	17:1	3
octene	1:160	0	100	5	24	0	100	—	—	—	—
octene	1:160	100	100	5	24	11.5	84	11.5	1	12:1	0.8
octene	1:160	400	100	5	24	42.5	54	42.5	2.5	17:1	2.8
decene	1:131	215	100	5	24	5	94	5	<0.5	~10:1	—
dodecene	1:108	215	100	5	24	~2	98	—	—	—	—
octene	1:160	215	100	5	24	42	57	39.5	2.5	16:1	2.8

<sup>a</sup> Composition of System 4 : 0.0553 g (0.201 mmol) RhCl<sub>3</sub>.3H<sub>2</sub>O + 2.1 mmol TPPTS in 20 ml aqueous buffer. Rh:TPPTS = 1:30.

<sup>b</sup> Note that the hydroformylation reactions are tabulated chronologically.

<sup>c</sup> Stirring-rate used in all other reaction is 215 rpm, unless otherwise stated.

<sup>d</sup> *n* and *iso* aldehydes generated.

<sup>e</sup> Unreacted 1-alkene plus possible alkene isomers.

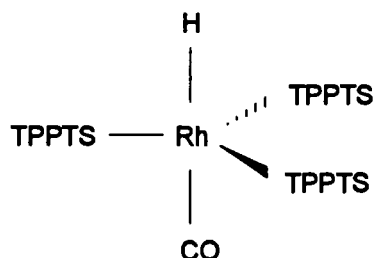
<sup>f</sup> Turnover number = no. moles of alkene per mole of rhodium converted to aldehydes per hour.

ii) Heterogeneous hydroformylation using a synthesised catalyst precursor,



A study was carried out in order to compare the performance of the system discussed above in which the catalytically active species are created *in situ*, with that of a system which utilizes the transition-metal catalyst precursor,  $\text{RhH}(\text{CO})(\text{TPPTS})_3$ .

The water-soluble complex  $\text{RhH}(\text{CO})(\text{TPPTS})_3$  is based on the well-known homogeneous hydroformylation catalyst,  $\text{RhH}(\text{CO})(\text{PPh}_3)_3$ . The trigonal bipyramidal rhodium(I) complex shown below, was synthesised through a modification of the method used for the preparation of the homogeneous complex  $\text{RhH}(\text{CO})(\text{PPh}_3)_3$ , which is discussed in the Experimental Section.



Schematic representation of the catalytic precursor,  $\text{RhH}(\text{CO})(\text{TPPTS})_3$

*Reaction Procedure*

An appropriate amount of the complex  $\text{RhH}(\text{CO})(\text{TPPTS})_3$  required to yield 0.21 mmole of rhodium, corresponding to the amount generally used for previous reactions, was dissolved in 20 ml aqueous buffer solution, and the same procedure followed as described previously in part (i). The catalytic reactions were carried out under exactly the same conditions as used formerly *i.e.*, stirred for 24 hours under a  $\text{CO}/\text{H}_2$  pressure of 5 MPa, at a temperature of 100 °C.

*Catalytic results*

Lower percentage conversions for the hydroformylation of 1-octene to nonanal of *ca.* 30% resulted, compared to *ca.* 50% obtained for the reactions under the same conditions where the catalytic species are generated *in situ*. See Table 3.5 and 3.6. The conversion of 1-decene and 1-dodecene to aldehydes was below the detection limit (< 0.5%).

The aqueous phase of System 5 [no added excess phosphine ligand (Table 3.5)], which was initially orange, turned black after the first reaction, and the activity dropped to zero after four runs. Higher *n:iso* ratios of *ca.* 7:1 were obtained for this system with a Rh:P ratio of 1:3, than the analogous '*in situ*' system using the same Rh:P ratios.

The aqueous phase of System 6 [with the addition of excess phosphine ligand (Rh:P =1:20), Table 3.6] turned from orange to yellow after the initial run, and remained yellow during all further reactions. The actual catalytic lifetime was not determined but the activity of the system remained consistent during all reactions performed. The percentage conversion of 1-octene to nonanal was as low as that obtained using System 5 however, and again the conversion of 1-decene and 1-dodecene was below the detection limit. Similar *n:iso* ratios of 6:1 were obtained in System 6 as those found for the "*in situ*" systems with the same Rh:P ratios (1:20).

Table 3.5

Hydroformylation reactions of 1-octene and 1-decene using synthetically prepared heterogeneous catalyst,  $\text{RhH}(\text{CO})(\text{TPPTS})_3^{\text{a, b}}$

run	1-alkene	Rh:alkene	T (°C)	P (MPa)	time (hr)	Percentage conversion of products					
						aldehyde <sup>c</sup>	olefin <sup>d</sup>	'n'	'iso'	n:iso	TON <sup>e</sup>
1	octene	1:303	100	5	24	26.5	73.5	24	2.5	10:1	3.3
2	octene	1:303	100	8	24	13	87	11	2	6:1	1.6
3	octene	1:151	100	5	24	11	87.5	10	~1	10:1	1.4
4	decene	1:125	100	5	24	4	96.5	~3.5	~0.5	7:1	0.2
5	octene	1:151	100	5	24	—	100	—	—	—	—

<sup>a</sup> System 5 : heterogeneous (water-soluble) catalyst  $\text{RhH}(\text{CO})(\text{TPPTS})_3$  synthetically prepared. Rh:TPPTS = 1:3 (see experimental)

<sup>b</sup> Note that the hydroformylation reactions are tabulated chronologically.

<sup>c</sup> n and iso aldehydes generated

<sup>d</sup> Unreacted 1-alkene plus possible alkene isomers.

<sup>e</sup> Turnover number = no. moles of alkene per mole of rhodium converted to aldehydes per hour.

Table 3.6

Hydroformylation reactions of 1-octene and 1-decene using synthetically prepared heterogeneous catalyst,  $\text{RhH(CO)(TPPTS)}_3$ <sup>a, b</sup>

run	1-alkene	Rh:alkene	T (°C)	P (MPa)	time (hr)	Percentage composition of products					
						aldehyde <sup>c</sup>	alkenes <sup>d</sup>	'n'	'iso'	n:iso	TON <sup>e</sup>
1	octene	1:160	100	5	24	22	76	19	~3	6:1	1.5
2	octene	1:160	100	5	24	16	83.5	14	~2.5	6:1	1.1
3	decene	1:131	100	5	24	<1	~100	—	—	—	—
4	octene	1:319	100	5	24	15	84	13	~2	7:1	2.0
5	octene	1:160	100	5	24	21	75	17	4	4:1	1.4

<sup>a</sup> System 6 : heterogeneous (water-soluble) catalyst  $\text{RhH(CO)(TPPTS)}_3$  synthetically prepared. Rh:TPPTS = 1:20 (see experimental)

<sup>b</sup> Note that the hydroformylation reactions are tabulated chronologically.

<sup>c</sup> n and iso aldehydes generated

<sup>d</sup> Unreacted 1-alkene plus possible alkene isomers.

<sup>e</sup> Turnover number = no. moles of alkene per mole of rhodium converted to aldehydes per hour.

### 3.2.2 Homogeneous hydroformylation

In order to make an objective comparison of the heterogeneous and homogeneous hydroformylation systems under the same conditions used in this study, the transition-metal complex,  $\text{RhH}(\text{CO})(\text{PPh}_3)_3$  was synthesised and used as the catalytic precursor for the homogeneous hydroformylation of 1-octene, 1-decene, and 1-dodecene under the same conditions of temperature (100 °C), pressure (5 MPa) and reaction time (24 hours).

The results obtained shown in Table 3.7 are far superior to those obtained for the heterogeneous system. Conversions of 100% for all three substrates (1-octene, 1-decene, and 1-dodecene) were obtained, with *n:iso* ratios of up to 10:1 depending on the Rh:P ratios used, which corresponded closely to those reported in the literature.<sup>19</sup>

Table 3.7

Hydroformylation reaction of 1-octene, 1-decene, and 1-dodecene using synthetically prepared homogeneous catalyst,  $\text{RhH}(\text{CO})(\text{PPh}_3)_3$ <sup>a</sup>

catalyst	1-alkene	[Rh] (mmol)	Rh:alkene	T (°C)	P (MPa)	time (hr)	percentage composition of products					
							aldehyde <sup>b</sup>	alkene <sup>c</sup>	'n'	'iso'	n:iso	TON <sup>d</sup>
CAT 1 <sup>e</sup>	octene	0.21	1:303	100	5	24	100	—	67	33	2:1	12.6
CAT 2 <sup>f</sup>	octene	0.10	1:640	100	5	24	100	—	75.0	25	3:1	25.2
	decene	0.10	1:528	100	5	24	100	—	72	28	2.5:1	22.0
	dodecene	0.10	1:450	100	5	24	100	—	73	27	2.5:1	18.8
CAT 3 <sup>g</sup>	octene	0.10	1:640	100	5	12	100	—	89	11	9:1	25.2

<sup>a</sup> Note that the hydroformylation reactions are tabulated chronologically.

<sup>b</sup> *n* and *iso* aldehydes generated.

<sup>c</sup> Unreacted alkene added as reactant plus possible alkene isomers.

<sup>d</sup> Turnover number = no. moles of alkene per mole of rhodium converted to aldehydes per hour.

<sup>e</sup> Homogeneous catalyst  $\text{RhH}(\text{CO})(\text{PPh}_3)_3$  synthetically prepared. (Rh:TPP = 1:3).

<sup>f</sup> Homogeneous catalyst  $\text{RhH}(\text{CO})(\text{PPh}_3)_3$ , excess  $\text{PPh}_3$  added (Rh: $\text{PPh}_3$  = 1:10).

<sup>g</sup> Homogeneous catalyst  $\text{RhH}(\text{CO})(\text{PPh}_3)_3$ , excess  $\text{PPh}_3$  added (Rh: $\text{PPh}_3$  = 1:50).

## **Chapter 4**

### **Catalyst Speciation**

## Chapter 4

### Catalyst Speciation

Phosphorous NMR spectroscopy is a powerful and well utilised tool in the study of the structure of transition-metal tertiary-phosphine complexes, and factors affecting the metal–phosphorous coupling constants which contribute useful information on the nature of the complex, have been well investigated.<sup>71,79</sup> However, there has been little research using NMR spectroscopy in the study of catalytically-active transition-metal complexes formed *in situ* in the aqueous phase.

In order to gain a better understanding of the nature and distribution of the transition-metal species formed in the aqueous phase, while attempting to generate the active catalytically-active complex for the hydroformylation of 1-alkenes using a two-phase system, a study of  $\text{RhCl}_3 \cdot 3\text{H}_2\text{O}$  and free water-soluble phosphine ligand (TPPTS) in water, has been undertaken. This system under different conditions (*i.e.*, with and without being exposed to hydroformylation conditions of a  $\text{CO}/\text{H}_2$  pressure of 5 MPa and temperature of 100 °C), is compared to an aqueous solution of the synthesised catalytic precursor,  $\text{RhH}(\text{CO})(\text{TPPTS})_3$ .

This study will be divided into three parts.

- i)* Review of the chemistry of  $\text{RhCl}_3 \cdot 3\text{H}_2\text{O}$  in the aqueous phase, and the nature of rhodium(I) and rhodium(III) tertiary-phosphine complexes formed in the organic phase.
- ii)* Review of the factors affecting the rhodium–phosphorous and phosphorous–phosphorous coupling constants in  $^{31}\text{P}$  NMR spectroscopy.
- iii)* Discussion of the results obtained from the  $^{31}\text{P}$  NMR spectroscopic study undertaken in the aqueous phase.

## 4.1 Rhodium Speciation

### 4.1.1 Rhodium(III) complexes

#### *Chloro-aqua species*

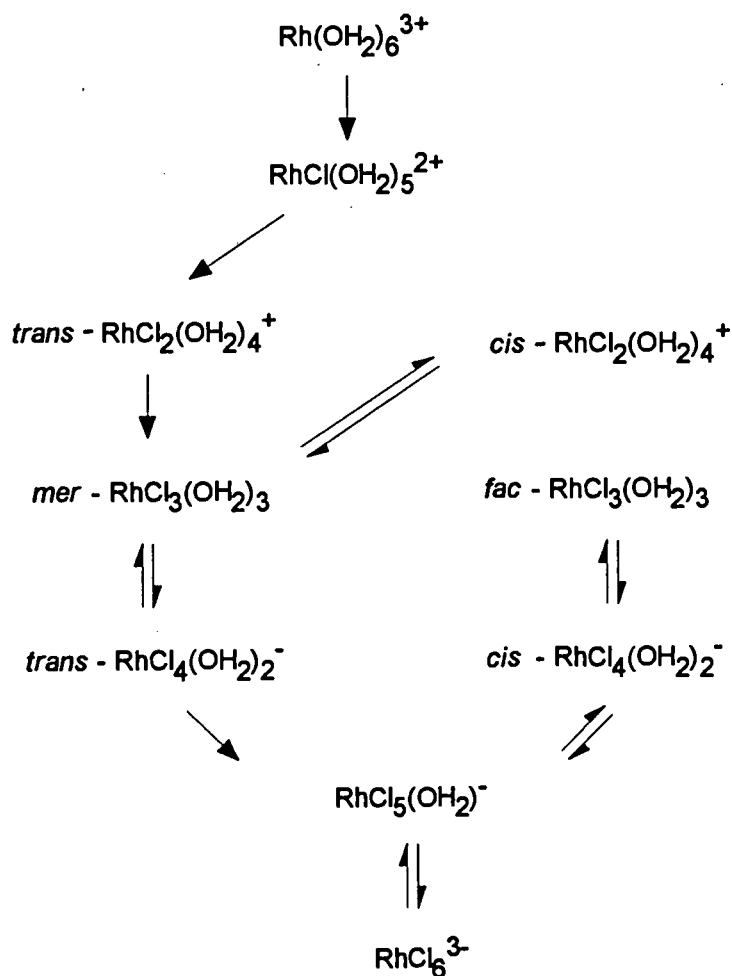
One of the most important of rhodium(III) compounds, and the usual starting material for the preparation of rhodium complexes is the dark red, crystalline, deliquescent trichloride,  $\text{RhCl}_3 \cdot n\text{H}_2\text{O}$ ; where  $n$  is usually 3 or 4. This octahedral complex is very soluble in water and alcohols, giving red-brown solutions.

$\text{RhCl}_3 \cdot 3\text{H}_2\text{O}$  undergoes a series of complex reactions when dissolved in water since it undergoes a succession of aquation (displacement of Cl by  $\text{H}_2\text{O}$ ) and anation reactions (displacement of  $\text{H}_2\text{O}$  by Cl) to yield, depending on the pH of the solution, a mixture of chloroaquorhodium(III) species of the general formula  $[\text{Rh}(\text{H}_2\text{O})_{6-n}\text{Cl}_n]^{(3-n)+}$ , as shown in Scheme 4.1.<sup>80</sup> This distribution of species applies to acidic solutions where negligible amounts of hydroxo species are present. One of the most outstanding features of these reactions is that their steric course is dictated mainly by the *trans* effect of the chloride ligands on each reactant species. The *trans* effect is defined as the influence of a particular ligand to facilitate substitution in the position *trans* to itself.<sup>78</sup>

The actual species present in the solution and their distribution is dependent upon factors such as chloride ion concentration, acidity, ionic strength, age and temperature.

Although formation constant values reported by various researchers are not always in agreement, the general consensus of opinion,<sup>78,81</sup> is that cationic and neutral

Catalyst Speciation



**Scheme 4.1**

Reaction Scheme for the chloroaquorhodium(III) system at 50 °C <sup>80</sup>

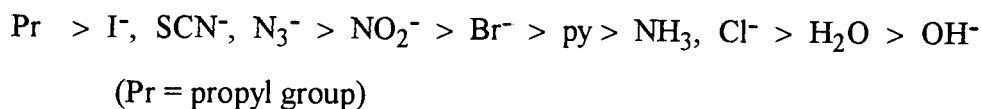
complexes are present in solutions up to an acidity of 2 M hydrochloric acid and that ionic complexes only are present in solutions of greater than 2 M hydrochloric acid. It is noted that the lability of the coordinated hydroxy groups in  $[\text{RhCl}_n(\text{H}_2\text{O})_{6-n}]^{(3-n)+}$  increases sharply with  $n$  (i.e., the number of substituted chloride ions).<sup>78,81</sup>

With a chloride ion concentration of 0.43 M as used in the current study, it can be expected that in an aqueous solution of  $\text{RhCl}_3 \cdot 3\text{H}_2\text{O}$  at 25 °C there would be a predominance of the *mer* and *fac*- $[\text{RhCl}_3(\text{OH}_2)_3]$  isomers; the *cis* and *trans*-

$[\text{RhCl}_4(\text{OH}_2)_2]^-$ , and the *cis* and *trans*  $[\text{RhCl}_2(\text{OH}_2)_4]^+$  isomers. It can be assumed that hydrolysis is too slow for the formation of any notable amount of other hydroxy species.

### Phosphine complexes

The addition of tertiary-phosphine ligands to the solution of rhodium(III) complexes results in a number of phosphine-substituted rhodium complexes formed as a result of the preferable substitution of the  $\text{OH}^-$ ,  $\text{H}_2\text{O}$  or  $\text{Cl}^-$  ligands (depending on the composition of the solution) by the phosphine ligand. This is due to the difference in nucleophilicity of the entering phosphine ligands from that of the other ligands, towards the transition-metal, rhodium. The order of nucleophilicity of some ligands, which is substantially invariant whatever the other ligands may be, is as follows:<sup>78</sup>



This can result in a myriad of species whose equilibria depend on the nature of the phosphine ligand, the chloride ion concentration, the age and pH of the solution.

Some common examples of non-water-soluble rhodium(III) phosphine complexes which have been isolated<sup>82</sup> are summarised below.

On treatment with triethylphosphine, alcoholic  $\text{RhCl}_3 \cdot 3\text{H}_2\text{O}$  gives *mer*- $[\text{RhCl}_3(\text{PEt}_3)_3]$ .<sup>78</sup> Analogous reactions occur with other tertiary phosphines. With many tertiary-phosphines, a small amount of the *fac*-complex is formed along with a majority of the *mer*-isomer. The isomerisation of *mer*- $[\text{Rh}(\text{PEt}_3)_3\text{Cl}_3]$  to the *fac*-isomer on irradiation of the solution has been reported.<sup>83</sup> Reactions of phosphines such as triethylphosphine with  $\text{RhCl}_3 \cdot 3\text{H}_2\text{O}$  in 2:1 ratio yield the presumably

dimeric  $\text{Rh}_2\text{Cl}_6(\text{PEt}_3)_4$ ; this is also formed from appropriate ratios of  $\text{RhCl}_3 \cdot 3(\text{H}_2\text{O})$  and *mer*- $\text{RhCl}_3(\text{PEt}_3)_3$ .<sup>78</sup>

#### 4.1.2 Rhodium(I) complexes

Rhodium(I), which is a  $d^8$  species, forms both square-planar (four coordination) and trigonal bipyramidal (five coordination) complexes, with the former complexes being the most common.

##### *Phosphine complexes*

Complexes of rhodium(I) with phosphine ligands are readily obtained by refluxing  $\text{RhCl}_3 \cdot 3\text{H}_2\text{O}$  with excess phosphine ligand in ethanolic solution. The best known example is the dark-red crystalline square-planar complex,  $[\text{RhCl}(\text{PPh}_3)_3]$ .<sup>84</sup> A large excess of triphenylphosphine is essential to prevent the formation of a bridged dimer, and to further the reduction of the  $\text{Rh}^{\text{III}}$  species formed initially. Since reduction of  $\text{Rh}^{\text{III}}$  to  $\text{Rh}^{\text{I}}$  does not occur in ethanol heated under reflux, unless an excess of phosphine ligand is present, and since acetone-water mixtures can be used in place of ethanol as a solvent, the triphenylphosphine is alleged to be the actual reducing agent, with triphenylphosphine oxide formed as a by-product.<sup>84</sup>

The five-coordinate complexes of stoichiometry  $\text{RhXL}_4$  (where X is a halide and L a tertiary-phosphine ligand) seem too unstable for alkyl or aryl-phosphines, despite the existence of other five-coordinate species such as  $\text{RhH}(\text{CO})(\text{PPh}_3)_3$ . It is assumed that this is a result of steric factors.<sup>84</sup>

It is also well-known that the  $\text{Rh}^{\text{I}}$  catalytic precursor,  $\text{RhH}(\text{CO})(\text{PPh}_3)_3$ , is formed under the action of CO and  $\text{H}_2$  under pressure with virtually any  $\text{Rh}^{\text{I}}$  or  $\text{Rh}^{\text{III}}$  compound in the presence of excess tertiary-phosphine.<sup>78</sup>

It is presumed that the analogous water-soluble phosphine ligand, TPPTS, will behave in a similar way to the non-water-soluble phosphine ligands discussed above. Thus depending on the composition of the aqueous solution, a distribution of a number of different rhodium(I) and rhodium(III) tertiary-phosphine species is expected to occur when treating a rhodium(III) solution with a water-soluble phosphine such as TPPTS.

## 4.2 Phosphorous NMR Spectroscopy of Rhodium Complexes

### 4.2.1 Factors affecting rhodium – phosphorous coupling constants

Since the  $^{103}\text{Rh}$  nucleus is 100% abundant with spin  $I = 1/2$ ,  $J(^{103}\text{Rh}-^{31}\text{P})$  coupling is expected to occur in rhodium-phosphine complexes.

#### *Differences in coupling in rhodium(I) and rhodium(III) complexes*

Inspection of coupling constant data for  $\text{Rh}^{\text{I}}$  and  $\text{Rh}^{\text{III}}$  complexes indicates that all the coupling constants are larger for complexes of  $\text{Rh}^{\text{I}}$  than for those of  $\text{Rh}^{\text{III}}$ .<sup>79,85</sup>

It is believed that the Rh–P coupling constants depend on the electron densities at both nuclei, and since the current consensus of opinion is that the metal–phosphorous bond is composed of both a sigma ( $\sigma$ ) and a pi ( $\pi$ ) component with the former dominating, increased s ( $\sigma$ ) character of the valence orbitals on either atom should lead to an increase in the coupling constant.<sup>86</sup> However, another argument is that the greater  $\pi$ -bonding may also indirectly increase the coupling constant by strengthening the bond.<sup>87</sup>

The larger Rh–P coupling constant for Rh<sup>I</sup> complexes than for Rh<sup>III</sup> complexes can be predicted almost as well by either mechanism. A larger fraction of both s (σ) and π character of the rhodium bonding orbitals is predicted for the lower valence rhodium(I) complexes, which leads to an increase in the strength of the bond and therefore higher values of the coupling constants.

This leads to the useful ratio:  $\frac{{}^1J(\text{Rh}^{\text{III}}-\text{P})}{{}^1J(\text{Rh}^{\text{I}}-\text{P})}$

The "theoretical" value of  ${}^1J(\text{Rh}^{\text{III}}-\text{P})/{}^1J(\text{Rh}^{\text{I}}-\text{P})$  is calculated to be 0.67.<sup>85</sup> The Rh–P coupling constants of a number of analogous Rh<sup>III</sup> and Rh<sup>I</sup> complexes have been recorded in the literature,<sup>79</sup> and their ratios agree satisfactorily with the "theoretical" value. (See Table 4.1).

*Effect of the nature of the ligand trans to phosphine*

Several research groups have also observed that for compounds of both oxidation states (I and III), the rhodium–phosphorous coupling constant is always larger for a phosphorous *trans* to a halogen,  ${}^1J(\text{Rh}-\text{P}_A)$ , than for two phosphorous atoms mutually *trans* to each other,  ${}^1J(\text{Rh}-\text{P}_B)$ <sup>88,89</sup>. See Figure 4.1.

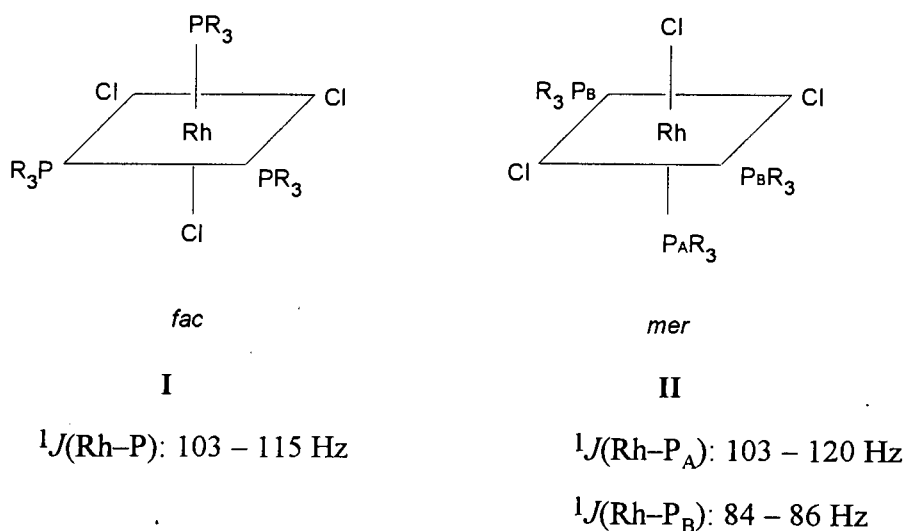


**Figure 4.1**

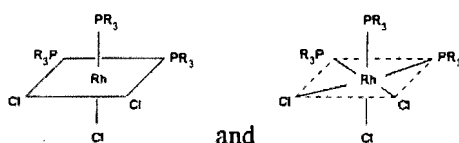
Coupling constants of the *mer* and *fac*-[RhCl<sub>3</sub>(PR<sub>3</sub>)<sub>3</sub>] isomers<sup>79</sup>

In the octahedral triphosphine rhodium(III)<sup>a</sup> complexes,  $\text{RhCl}_3\text{P}_3$ , both the *facial*, I, and the *meridional*, II, complexes have been isolated and several studies have reported their  $^{31}\text{P}$  NMR characteristics,<sup>79</sup> showing that there is relatively little change in  $^1J(\text{Rh}-\text{P})$  for different phosphine ligands.

This feature of a greater  $^1J(\text{Rh}-\text{P})$  coupling constant for the the phosphorous *trans* to the chloride than for mutually *trans* phosphorous atom in transition-metal complexes, can be explained in terms of the strength of the metal–ligand bonds. Phosphines have a strong tendency to weaken metal-halogen  $\sigma$ -bonds in *trans* relationships, due to the strong '*trans* influence' (*i.e.*, the influence of one ligand on the strength of the bond to the ligand that is *trans* to it) and a smaller coupling constant therefore results. It is probable that  $\sigma$ -bonds of other ligands (*viz.* phosphines) *trans* to phosphines are similarly affected to some degree. Thus metal-phosphine bonds are expected to be longer (*i.e.*, weaker) when mutually *trans* to each other, than when *trans* to chloride, and as coupling constants are proportional to the strength of the bond, this leads to a decrease in the magnitude of the coupling constants. This results in the coupling constants of mutually *trans* phosphorous atoms ( $\text{P}_\text{B}$ ) being substantially smaller than those for phosphorous atoms *trans* to chloride ( $\text{P}_\text{A}$ ).

The ratio  $\frac{{}^1J(\text{Rh}-\text{P}_\text{A})}{{}^1J(\text{Rh}-\text{P}_\text{B})}$  (where  $\text{P}_\text{A}$  is the phosphorous atom *trans* to the halide, and

$\text{P}_\text{B}$  the phosphorous atoms which are mutually *trans* to each other) can be useful in the determination of the structures of transition-metal complexes. Generally the value of this ratio lies in the range of 1.3–1.5.<sup>90</sup>



<sup>a</sup> Note that the structures and are equivalent, where the solid equatorial lines of the former structure do not imply bonds between the atoms. This depiction will be used in the discussion to represent the geometry of the transition-metal complexes.

Some representative phosphorous-metal coupling constants are given for certain species of Rh<sup>I</sup> and Rh<sup>III</sup>,<sup>90</sup> and the ratios,  $^1J(\text{Rh}-\text{P}_A)/^1J(\text{Rh}-\text{P}_B)$ , calculated as shown in Table 4.1.

**Table 4.1** Phosphorous-rhodium NMR coupling constants

Complex	<i>trans</i> ligand	$^1J(\text{P}-\text{M})^a$	$\frac{^1J(\text{Rh}-\text{P}_A)}{^1J(\text{Rh}-\text{P}_B)}^b$	$\frac{^1J(\text{Rh}^{\text{III}}-\text{P})}{^1J(\text{Rh}^{\text{I}}-\text{P})}$	ref.
Rh <sup>III</sup> <i>mer</i> -[RhCl <sub>3</sub> (PBU <sub>3</sub> ) <sub>3</sub> ]	Cl	113		0.60	79,86
	Bu <sub>3</sub> P	84	1.36	0.59	
Rh <sup>I</sup> [RhCl(PPh <sub>3</sub> ) <sub>3</sub> ] [Rh(PPh <sub>3</sub> ) <sub>2</sub> COCl]	Cl	189			79,88
	Bu <sub>3</sub> P	142	1.33		
	CO	124			86

<sup>a</sup> Coupling constants (*J*) measured in Hertz.

<sup>b</sup> The small differences in the  $^1J(\text{Rh}-\text{P})$  for PPh<sub>3</sub> and PBU<sub>3</sub> are considered negligible.<sup>79</sup>

In contrast to the influence of a halogen on the coupling of rhodium to phosphorous, the substitution of a carbonyl for a phosphine group produces a marked decrease in the value of the coupling constant of the phosphorous atom *trans* to the carbonyl group.<sup>86</sup> (See Table 4.1).

### 4.3 Speciation Experiments

In order to attempt to establish the nature and distribution of the species formed on the addition of RhCl<sub>3</sub>·3H<sub>2</sub>O and the tertiary-phosphine, TPPTS in the aqueous phase, a number of experiments monitored by <sup>31</sup>P NMR spectroscopy were performed.

The following experiments were undertaken:

- Examination of the nature and distribution of species in the aqueous phase on addition of  $\text{RhCl}_3 \cdot 3\text{H}_2\text{O}$  and TPPTS. Three different systems were studied, where the ratios of Rh:P:Cl were as follows:

*i)* Rh:TPPTS:Cl = 1:2:0 (system 1)

*ii)* Rh:TPPTS:Cl = 1:2:5 (system 2)

*iii)* Rh:TPPTS:Cl = 1:4:5 (system 3)

The ratios were chosen carefully in order to compare the effect of *i)* the addition of excess chloride ions (systems 1 and 2), and *ii)* the addition of excess phosphine ligand (systems 2 and 3).

The  $^{31}\text{P}$  NMR spectra of these mixtures were recorded initially after 15 minutes and then at different time intervals thereafter.

- Determination of the species present after being subjected under the hydroformylation conditions of a  $\text{CO}/\text{H}_2$  pressure of 5 MPa and temperature of 100 °C.
- The comparison by  $^{31}\text{P}$  NMR spectroscopy of the synthesised catalyst precursor,  $\text{RhH}(\text{CO})(\text{TPPTS})_3$ , with the species found in the aqueous solution of  $\text{RhCl}_3 \cdot 3\text{H}_2\text{O}$  and free TPPTS.

## Results and Discussion

### 4.3.1 Tertiary-phosphine rhodium complexes formed in aqueous solution

#### *System 1*

The phosphorous NMR spectrum of system 1 (Rh:TPPTS:Cl = 1:2:0) in a 50:50 D<sub>2</sub>O/H<sub>2</sub>O solution resulted in a fairly simple spectrum as shown in Figure 4.3.

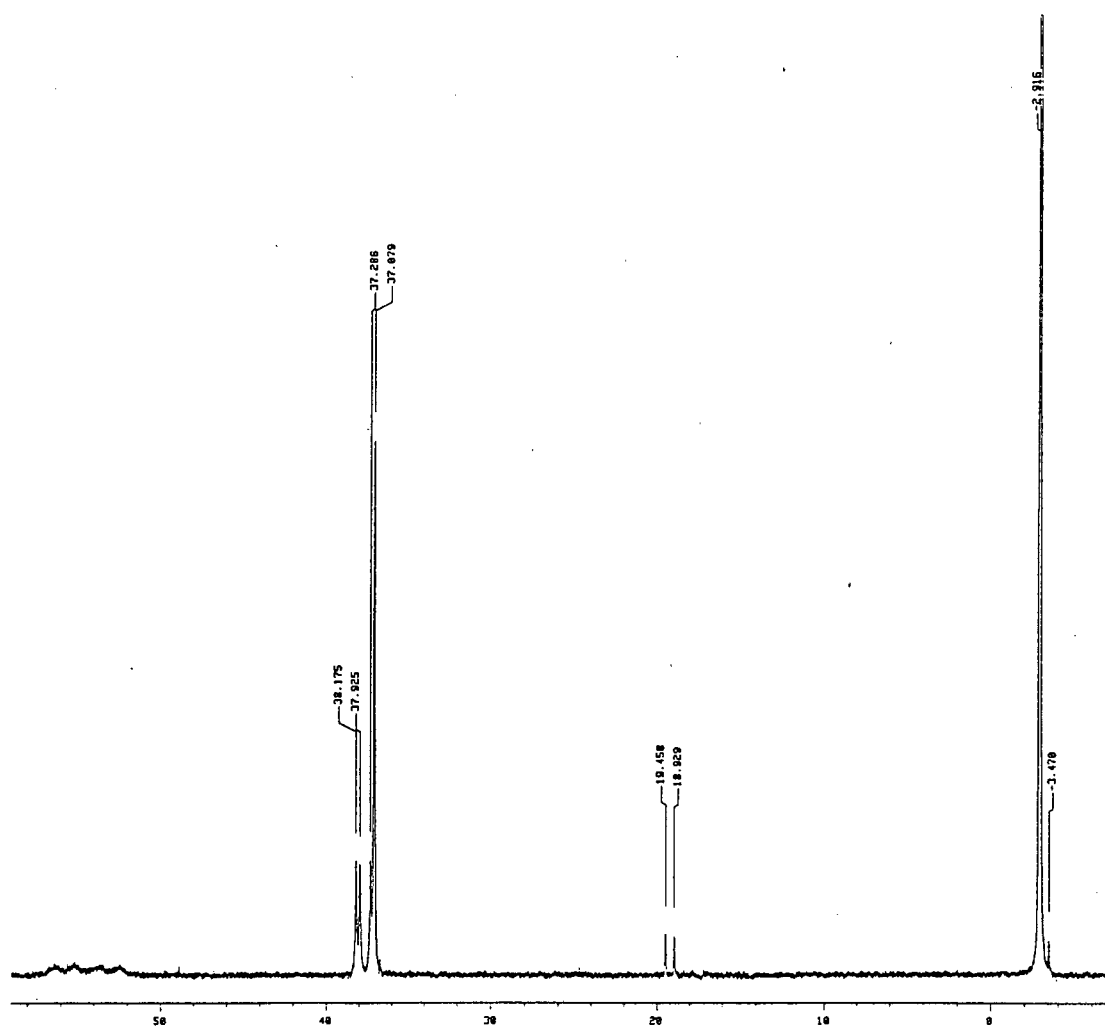
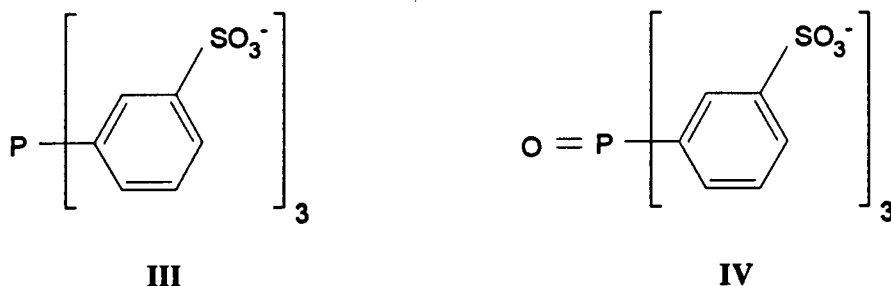


**Figure 4.3** <sup>31</sup>P NMR spectrum of System 1 (Rh:P:Cl = 1:2:0) after 15 minutes

The characteristic singlet at  $\delta_p = -2.9$  ppm is assigned to the unbound phosphine ligand, TPPTS, (III) and the singlet resulting at  $\delta_p = 37.1$  ppm to the corresponding phosphine oxide, TPPOTS (IV). The oxide is thought to be generated as a result of

oxidation of the free phosphine ligand, TPPTS by dissolved oxygen in the solution, possibly mediated or catalysed by rhodium(III).



The broad doublet of triplets at  $\delta_p = 53.1$  ppm [ $^1J(\text{Rh}-\text{P}) = 187.5$  Hz] and doublet of doublets at  $\delta_p = 37.7$  ppm [ $^1J(\text{Rh}-\text{P}) = 142$  Hz,  $^2J(\text{P},\text{P}) = 38.5$  Hz] supports a structure entailing three phosphorous atoms in two chemically different environments,  $\text{P}_A$  and two magnetically equivalent  $\text{P}_B$ s, where the resonance integral of  $\text{P}_B$  is twice that of  $\text{P}_A$ . See Figure 4.2. This can either be ascribed to the octahedral rhodium(III) structure, *mer*- $\text{RhCl}_3(\text{TPPTS})_3$  (V), or to the square-planar rhodium(I) structure,  $\text{RhCl}(\text{TPPTS})_3$  (VI).

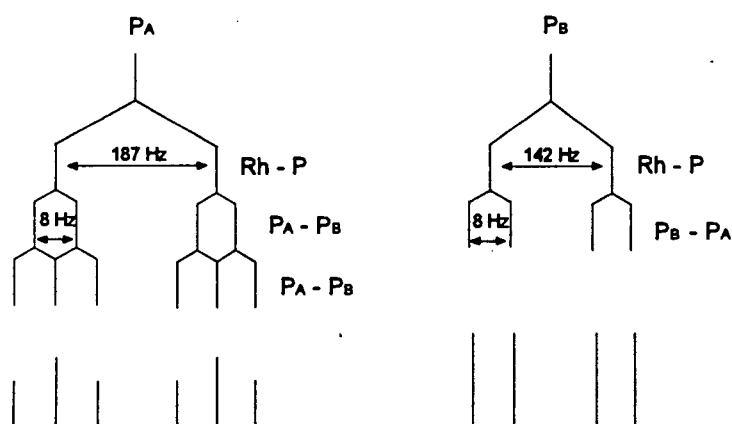
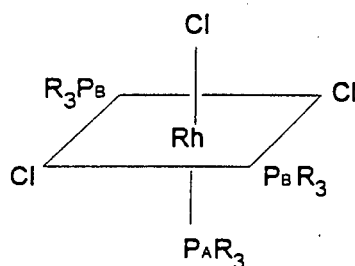


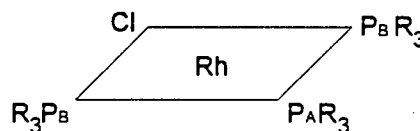
**Figure 4.2** Pattern resulting from the  $^{31}\text{P}$  resonances of an  $\text{AMX}_2$  system

Catalyst Speciation



V

*mer*-RhCl<sub>3</sub>(TPPTS)<sub>3</sub>



VI

RhCl(TPPTS)<sub>3</sub>

Inspection of the experimental data, in particular the Rh–P coupling constants obtained here and of analogous compounds reported in the literature (Table 4.2), supports the presence of a rhodium(I) species rather than a rhodium (III) species. The coupling constants fall into the reported range of  $^1J(\text{Rh}^{\text{III}}\text{--P}) = 103 - 120$  Hz for similar rhodium(III) complexes with the phosphorous atom *trans* to the chloride (labeled P<sub>A</sub>), and 84–86 Hz for the mutually trans phosphorous atoms (labeled P<sub>B</sub>). The  $^2J(\text{P}_A, \text{P}_B)$  coupling constant (38 Hz) is also too high for a rhodium(III) complex, which is expected to be *ca.* 23 Hz<sup>79,86</sup> but appropriate for a rhodium(I) complex.

**Table 4.2** Chemical shifts and coupling constants of analogous rhodium(I) and rhodium(III) complexes

complex	$\delta\text{P}_A$ <sup>a</sup>	$\delta\text{P}_B$	$^1J(\text{Rh--P}_A)$ <sup>b</sup>	$^1J(\text{Rh--P}_B)$	$^2J(\text{P,P})$	ref.
RhCl(PPh <sub>3</sub> ) <sub>3</sub>	48	31.5	189	142	38	79,86
<i>mer</i> -RhCl <sub>3</sub> (PBU <sub>3</sub> ) <sub>3</sub>	15.1	-0.5	113	84	23	79,86

<sup>a</sup> Chemical shifts are stated in ppm relative to external 85 % H<sub>3</sub>PO<sub>4</sub>.

<sup>b</sup> coupling constants (*J*) measured in Hertz.

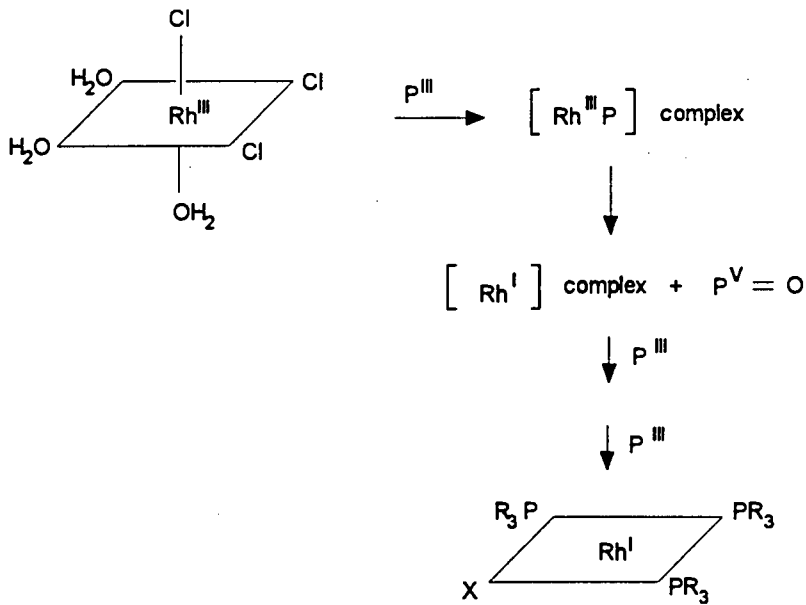
The Rh–P coupling constant of the triplet,  $J = 189$  Hz is due to the phosphorous atom trans to the halide, Cl, and the lower coupling constant  $J = 142$  Hz, due to the mutually trans phosphorous atoms. The ratio  ${}^1J(\text{Rh-P}_A)/{}^1J(\text{Rh-P}_B) = 1.32$  agrees closely with literature values (shown previously in Table 4.1).

The  $\text{AMX}_2$  pattern is therefore assigned to the square-planar rhodium(I) complex  $\text{RhCl}(\text{TPPTS})_3$  (VI), where the chemical shifts and the coupling constants  ${}^1J(\text{Rh-P}_B)$ ,  ${}^1J(\text{Rh-P}_A)$  and  ${}^2J(\text{P}_A, \text{P}_B)$  compare remarkably closely with the literature values of analogous complexes.

As the complex  $\text{RhCl}(\text{PPh}_3)_3$  forms readily from solutions of  $\text{RhCl}_3 \cdot 3\text{H}_2\text{O}$  and triphenylphosphine (discussed previously in Section 4.1.2), a similar reaction is postulated in the case of the TPPTS system, where the reduction of  $\text{Rh}^{\text{III}}$  to  $\text{Rh}^{\text{I}}$  is presumably facilitated by the phosphine ligand (TPPTS), resulting in the formation of a square-planar rhodium(I) complex and the corresponding phosphine oxide formed as a by-product. See Scheme 4.2.

Without addition of excess chloride, as is the case in this system, exchange between the solvent ( $\text{H}_2\text{O}$ ) and the chloride ligand may occur which results in the equilibria of the complex  $\text{RhCl}(\text{TPPTS})_3$  in aqueous solution as outlined below, accounting for the broad resonance in the  ${}^{31}\text{P}$  NMR spectrum at  $\delta_{\text{p}} = 53.1$  ppm (Figure 4.3).

Catalyst Speciation

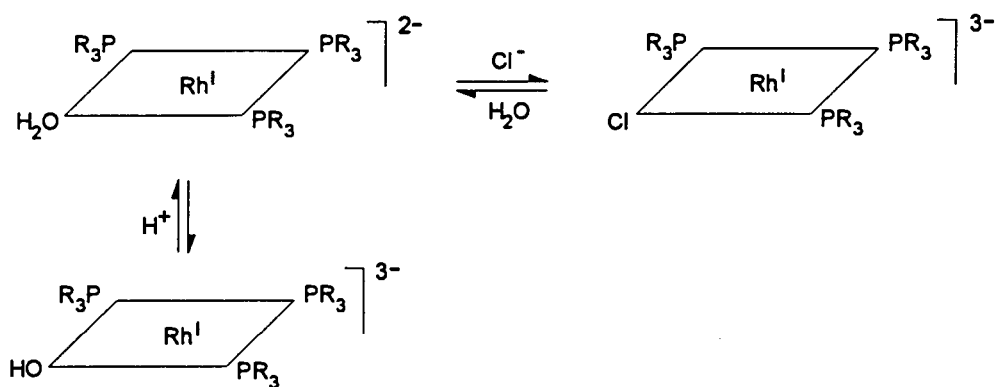


$\text{X} = \text{Cl} \text{ or } \text{H}_2\text{O}$

$\text{PR}_3 = \text{TPPTS}$

**Scheme 4.2**

Formation of the square-planar  $\text{RhCl}(\text{TPPTS})_3$  from the addition of  $\text{RhCl}_3 \cdot 3\text{H}_2\text{O}$  and TPPTS in water.



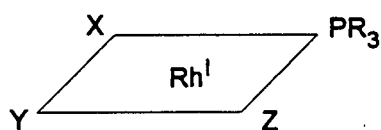
$\text{PR}_3 = \text{TPPTS}$

**Scheme 4.3**

Equilibria of complex  $\text{RhCl}(\text{TPPTS})_3$  without excess chloride ions

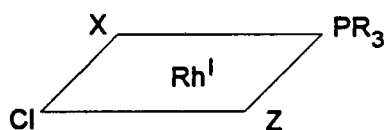
The effect of rapid ligand exchange (Scheme 4.3) would serve as an explanation for the broadness of the two peaks assigned as a doublet of triplets in the  $AMX_2$  pattern. The high ratio of the integration intensities for the dt:dd of 1:2.7 (expected 1:2) may be a result of the difficulty to integrate broad lines accurately, or due to incomplete relaxation of the nuclei due to an altered spin relaxation time,  $T_1$ , caused by the chloride/solvent ligand exchange.

Inspection of the spectrum in Figure 4.3 shows another doublet at  $\delta_p = 55.1$  ppm [ $^1J(\text{Rh-P}) = 195$  Hz], which is tentatively assigned as a  $\text{Rh}^{\text{I}}$  complex with only one coordinated TPPTS ligand (VII). This possible assignment of a rhodium(I) species is made because of the high Rh-P coupling constant, and the fact that a doublet results suggests that only one phosphine is coordinated to the rhodium.



VII

$X, Y, Z = \text{Cl}, \text{H}_2\text{O}, \text{ or } \text{OH}^-$



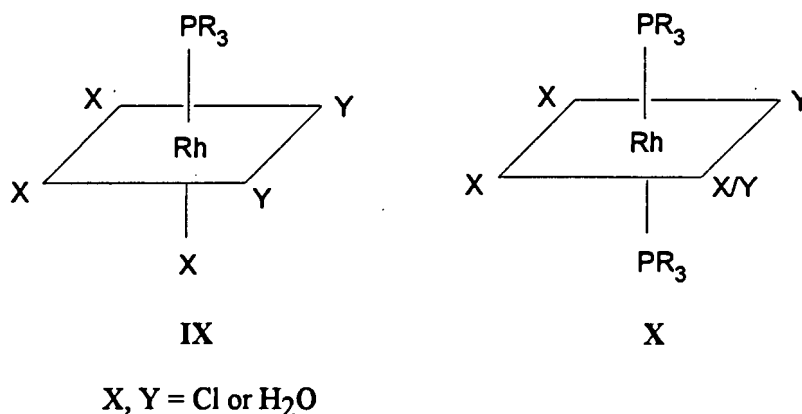
VIII

$X, Z = \text{Cl}, \text{H}_2\text{O} \text{ or } \text{OH}^-$

The small doublet at  $\delta_p = 19.2$  ppm, [ $^1J(\text{Rh-P}) = 87.3$  Hz] must remain unassigned, although it is reasonable to suggest a rhodium(III) complex on the basis of the relatively small coupling constant of 87 Hz. Possible assignments include:

- i)* the dimer  $\text{Rh}_2\text{Cl}_6(\text{TPPTS})_4$  where the doublet arises from coupling of the chemically equivalent phosphorous to rhodium.
- ii)* a mono- or di-substituted rhodium(III) complex, IX and X respectively.

## Catalyst Speciation



The relative rate of complex formation and the time dependence of the spectral change were of interest. Hence the integrated intensities of the different species present in solution were followed over a period of time. The data for Systems 1, 2 and 3 are outlined in Table 4.3 and the corresponding spectra shown in Figures 4.3 and 4.4 (System 1), 4.5 and 4.6 (System 2) and 4.7 and 4.8 (System 3).

The concentrations of the species present, which were indirectly estimated by the resonance intensities of the <sup>31</sup>P NMR spectra, were measured over a period of time. The resonance corresponding to the unbound phosphine ligand (TPPTS) decreased substantially, while the resonances corresponding to the other species present were of a similar intensity as found initially. It therefore appears that the rhodium-phosphine complexes formed at the expense of the unbound phosphine ligand. The increase in the resonance intensity of the phosphine oxide present (*i.e.* an increase in concentration), may be as a result of the formation of the rhodium(I) complex, RhCl(TPPTS)<sub>3</sub>, in which the phosphine oxide is a by-product, or due to the oxidation of free TPPTS by dissolved oxygen in the solution.

Table 4.3

Distribution of species in system 1 as a function of time

System	time lapsed	species present (%) <sup>a</sup>						
		d1	dt	(dd)	oxide	d2	TPPTS	other
1	15 minutes	3.1	4.1	10.8	9.8	1.3	70.8	
	16 hours	19.5	13	36.4	39.6		0	3.2
	2–3 days							
2	15		8.1	(17.7)	12.9	0.8	60.5	
	205		11.1	(23.0)	16.8	1.1	48.3	
	>1000		0	(0)	78.9	0	0	13.8
3	15		3.5	(7.6)	8.8	0.6	79.4	
	40		5.1	(11.2)	10.7	0.5	72.4	
	>1000		12.4	(26.0)	36.2	<0.5	24.9	

<sup>a</sup> Concentration of species present calculated indirectly from resonance intensities.

d1 – doublet at  $\delta_p = 55.1$  ppm

dt – doublet of triplets ( $\delta_p = 53.1$  ppm)

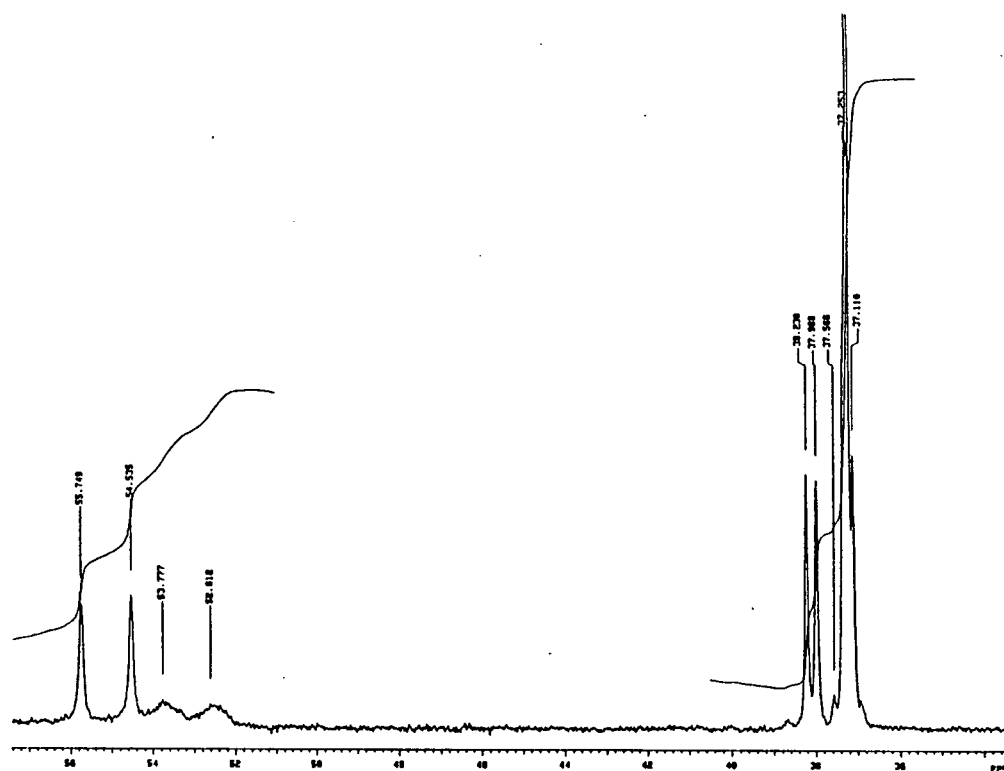
(dd) – doublet of doublets ( $\delta_p = 37.7$  ppm) associated with the doublet of triplets

d2 – doublet at  $\delta_p = 19.2$  ppm

After a period of 2–3 days the doublet of triplets and the associated doublet of doublets increased significantly. The concentration of the free ligand was below the detection limit, while the peak assigned to the phosphine oxide increased significantly, suggesting slow oxidation of the TPPTS ligand in the NMR tube.

# Catalyst Speciation

a)



b)

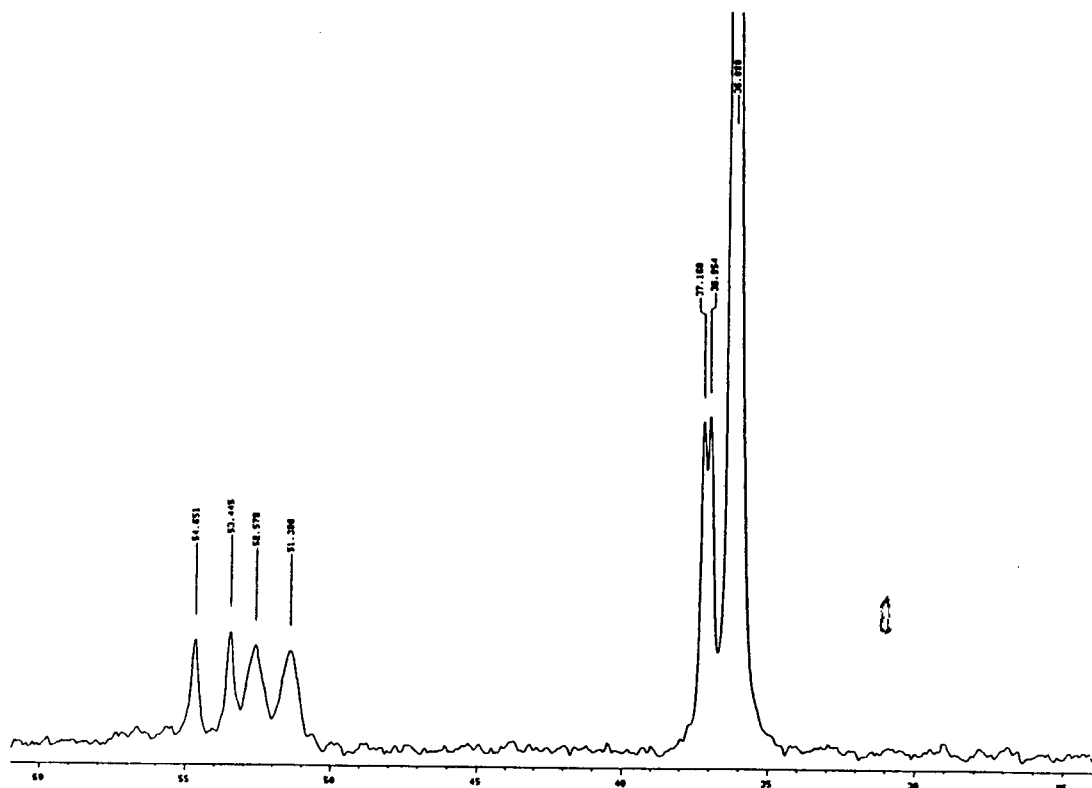


**Figure 4.4**  $^{31}\text{P}$  NMR spectrum of System 1 (Rh:P:Cl = 1:2:0) after *a)* 16 hours and *b)* 3 days.

*System 2*

The  $^{31}\text{P}$  NMR spectrum of system 2 (Rh:TPPTS:Cl = 1:2:5) in a 50:50  $\text{D}_2\text{O}/\text{H}_2\text{O}$  solution, shown in Figure 4.5 resulted in a fairly similar distribution of species as found in system 1.

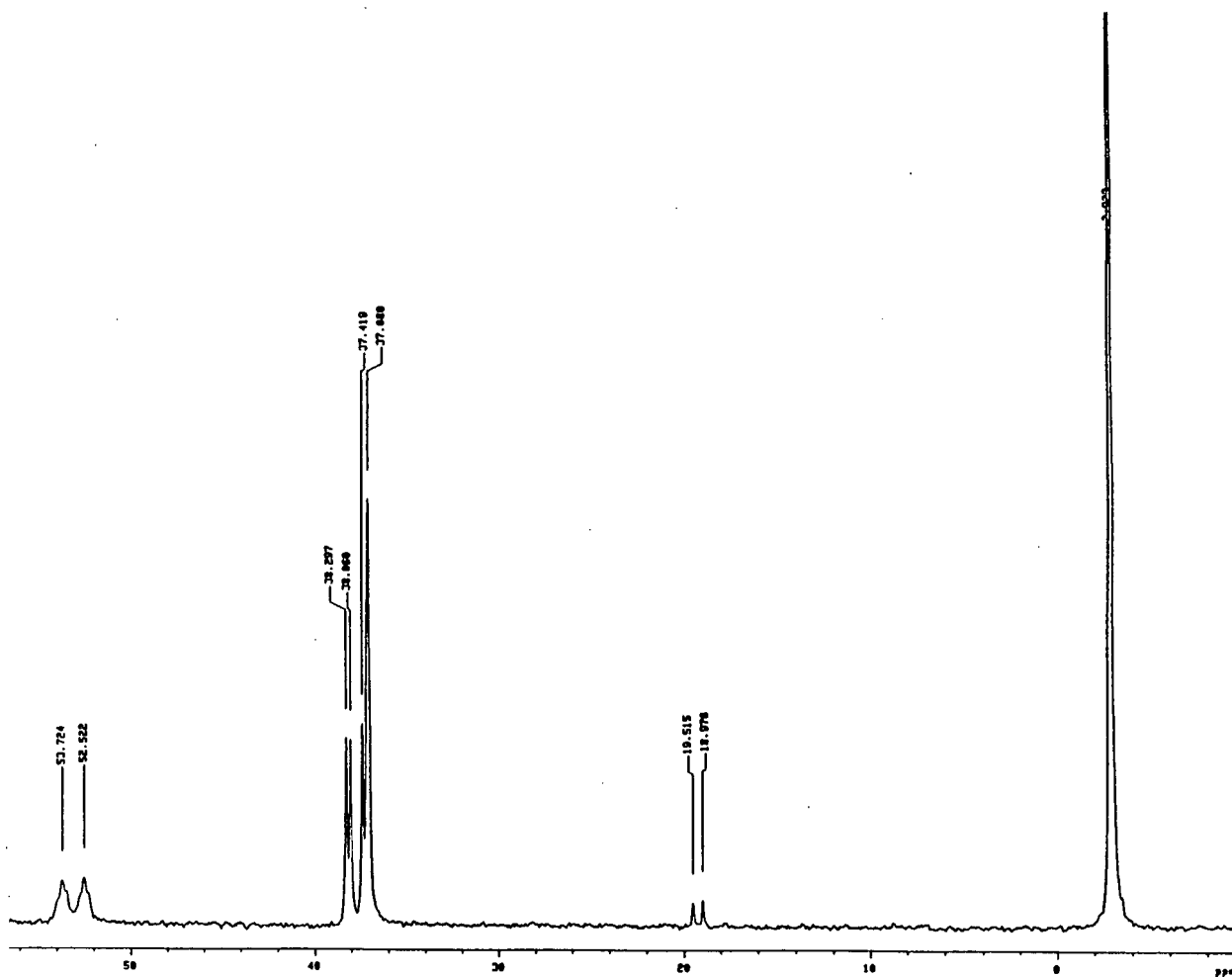
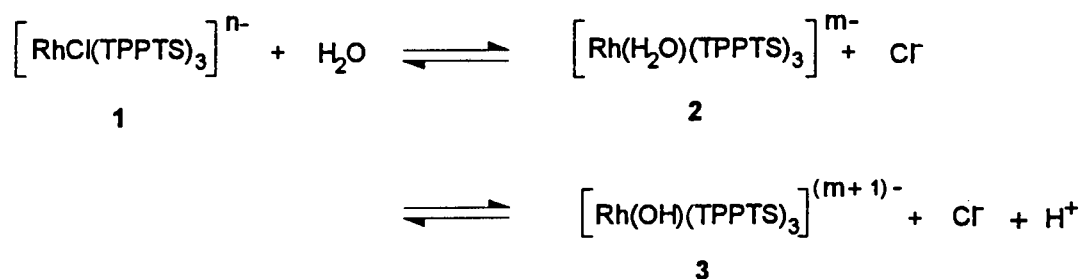


**Figure 4.5**  $^{31}\text{P}$  NMR spectrum of System 2 (Rh:P:Cl = 1:2:5) after 15 minutes

The singlet at  $\delta_p = -2.9$  ppm is assigned to the free phosphine ligand, TPPTS, and the singlet occurring at  $\delta_p = 37.1$  ppm to the corresponding phosphine oxide, TPPOTS. Again a doublet of triplets and a doublet of doublets appeared at very similar chemical shifts and coupling constants ( $\delta_p = 53.1$  ppm [ $^1J(\text{Rh-P}) = 194.3$  Hz,  $^2J(\text{P-P}) = 38.5$  Hz] and  $\delta_p = 37.7$  ppm [ $^1J(\text{Rh-P}) = 142$  Hz,  $^2J(\text{P,P}) = 38.5$  Hz] respectively) as found in system 1, which again supports the structure of the square-planar rhodium(I) complex  $\text{RhCl}(\text{TPPTS})_3$ .

However, in this system with excess chloride, the doublet of triplets are more clearly resolved and the phosphorous to phosphorous coupling information is apparent  $^2J(\text{P,P}) = 38$  Hz. The relative integrated intensities for the doublets and triplets are 2:1 respectively as required for the proposed structure. Due to the presence of excess chloride,  $\text{RhCl}(\text{TPPTS})_3$ , ligand exchange between  $\text{H}_2\text{O}$  and  $\text{Cl}^-$  is presumed to be negligible which results in the stabilisation of the complex.  $\text{RhCl}(\text{TPPTS})_3$ . The presence of chloride also inhibits the production of the doublet found in system 1 at  $\delta_p = 55.1$  ppm. This is probably as a result of mass action which directs the equilibrium towards the formation of  $[\text{RhCl}(\text{TPPTS})_3]^{n-}$  (1) as shown in the scheme below. Negligible formation of the complexes 2 and 3 which would result in the formation of another doublet is expected, due to the excess chloride added.



The nature and distribution of species was again followed over a period of time by the change in the integrated intensities, as shown in Table 4.3. The corresponding spectra are shown in Figure 4.6.

Catalyst Speciation

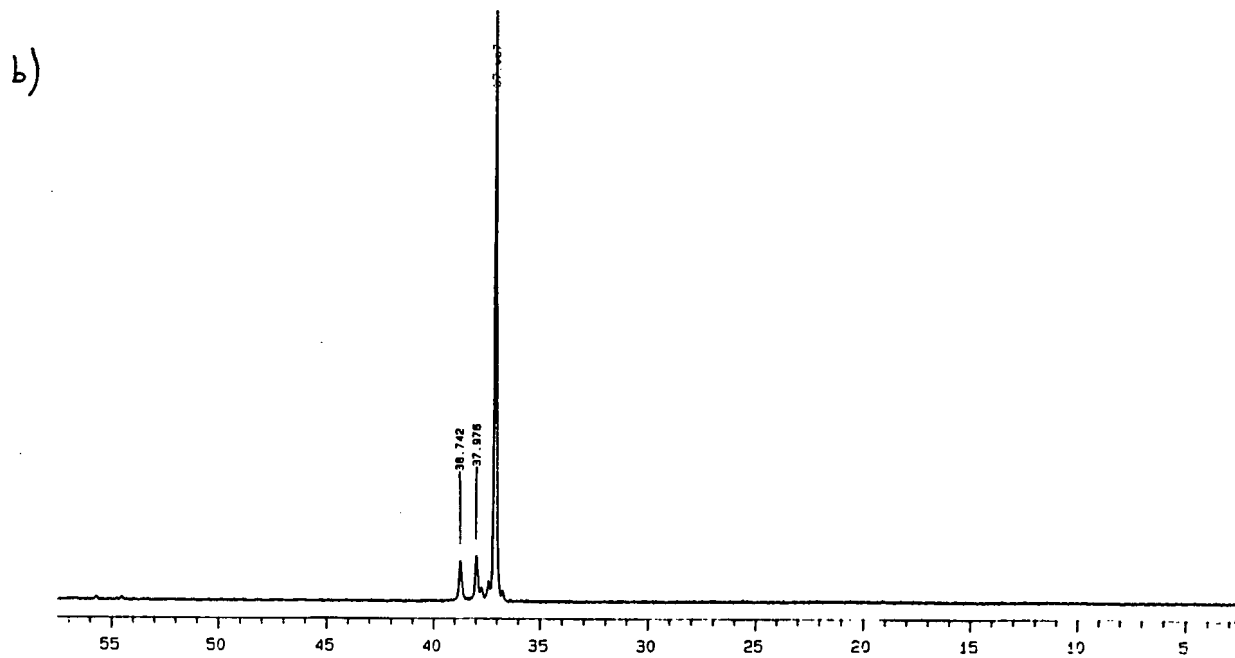
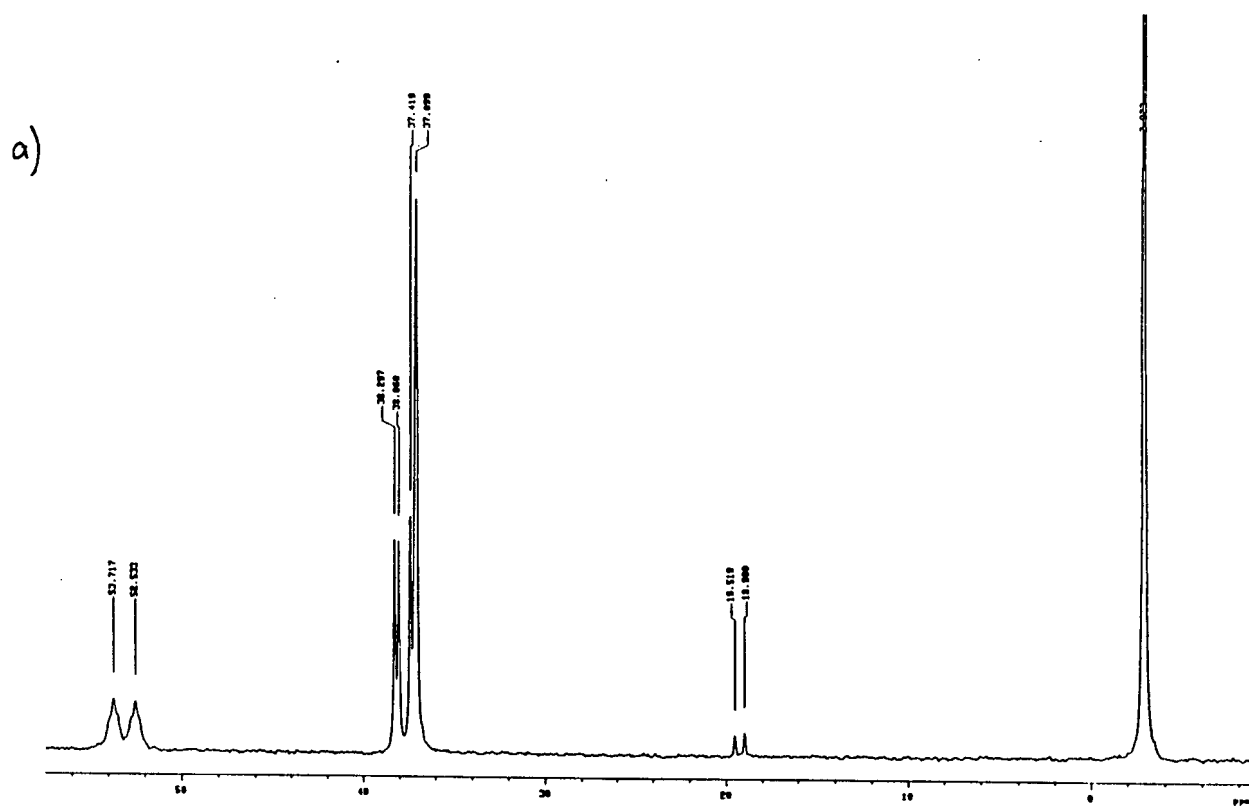


Figure 4.6  $^{31}\text{P}$  NMR spectrum of System 2 (Rh:P:Cl = 1:2:5) after a) 3 hours and

• b) one week.

It was noted that after a week the species corresponding to the doublet of triplets and doublet of doublets had disappeared almost entirely. A small trace of the triplets was observed at  $\delta_p = 53.1$  ppm [ $^1J(\text{Rh-P}) = 195.3$  Hz] but the concentration was below the observable integrated intensity limit. The doublet at  $\delta_p = 19.3$  ppm [ $^1J(\text{Rh-P}) = 87.3$  Hz] was also below the detection limit. An additional doublet appeared at  $\delta_p = 38.4$  ppm [ $^1J(\text{Rh-P}) = 124.0$  Hz] which remains unassigned.

*System 3 (Rh:P:Cl = 1:4:5)*

This system resulted in a similar distribution of species in the initial spectrum as found in system 2 (Rh:P:Cl = 1:2:5). See Figure 4.7. The assignments of the peaks remain as before in systems 1 and 2.

The resonance intensities of the resulting species were again measured over a period of time using  $^{31}\text{P}$  NMR spectroscopy. (See Table 4.3). Again the results show an increase in the concentration of the species corresponding to the doublet of triplets and the doublet of doublets over time, at the expense of the free phosphine ligand, TPPTS. See Figure 4.8. The concentration of phosphine oxide also increased significantly. No extra peaks appeared and the solution remained dark red and no precipitation occurred which is most probably due to the stabilisation of the square-planar rhodium(I) complex by the excess phosphine.

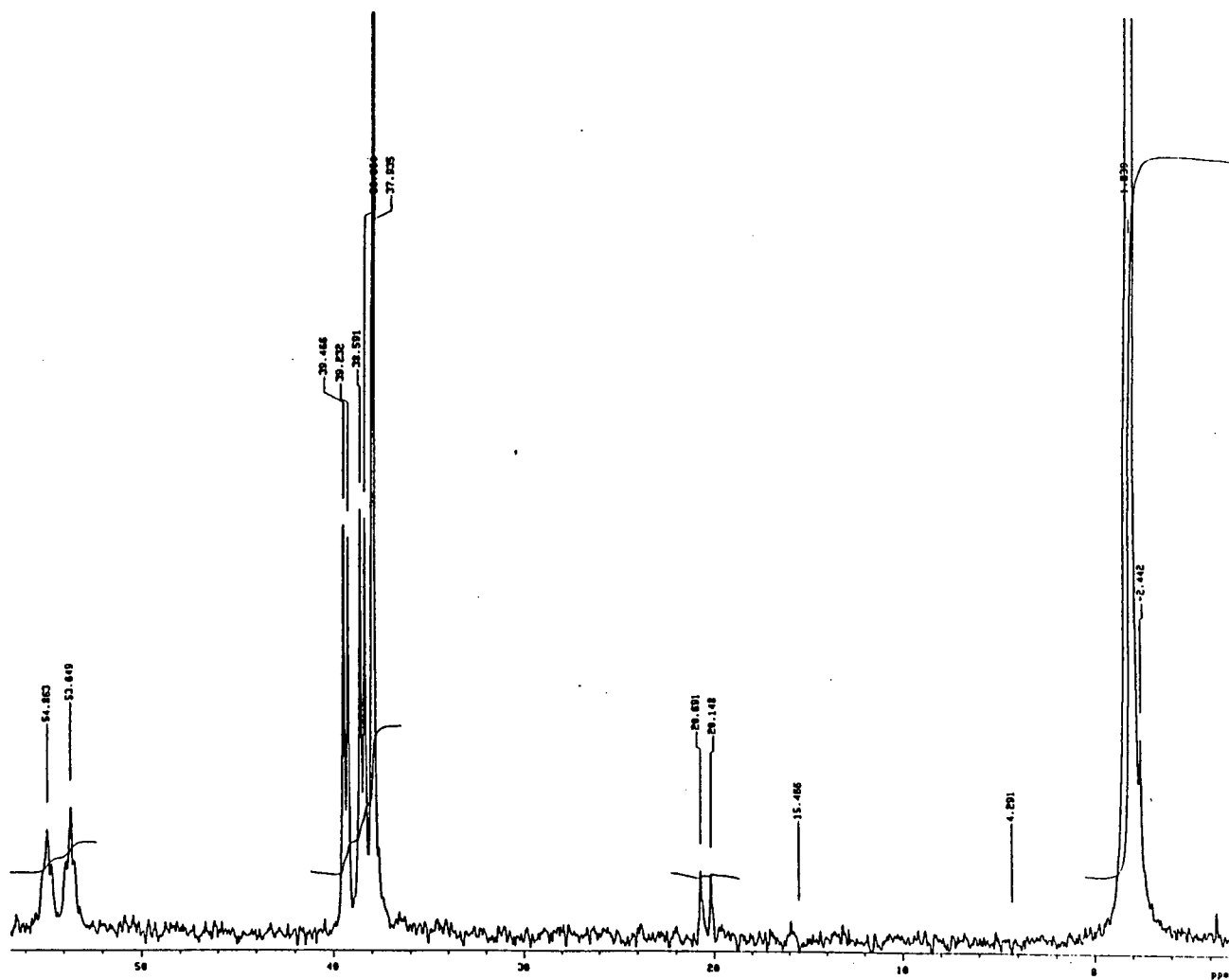
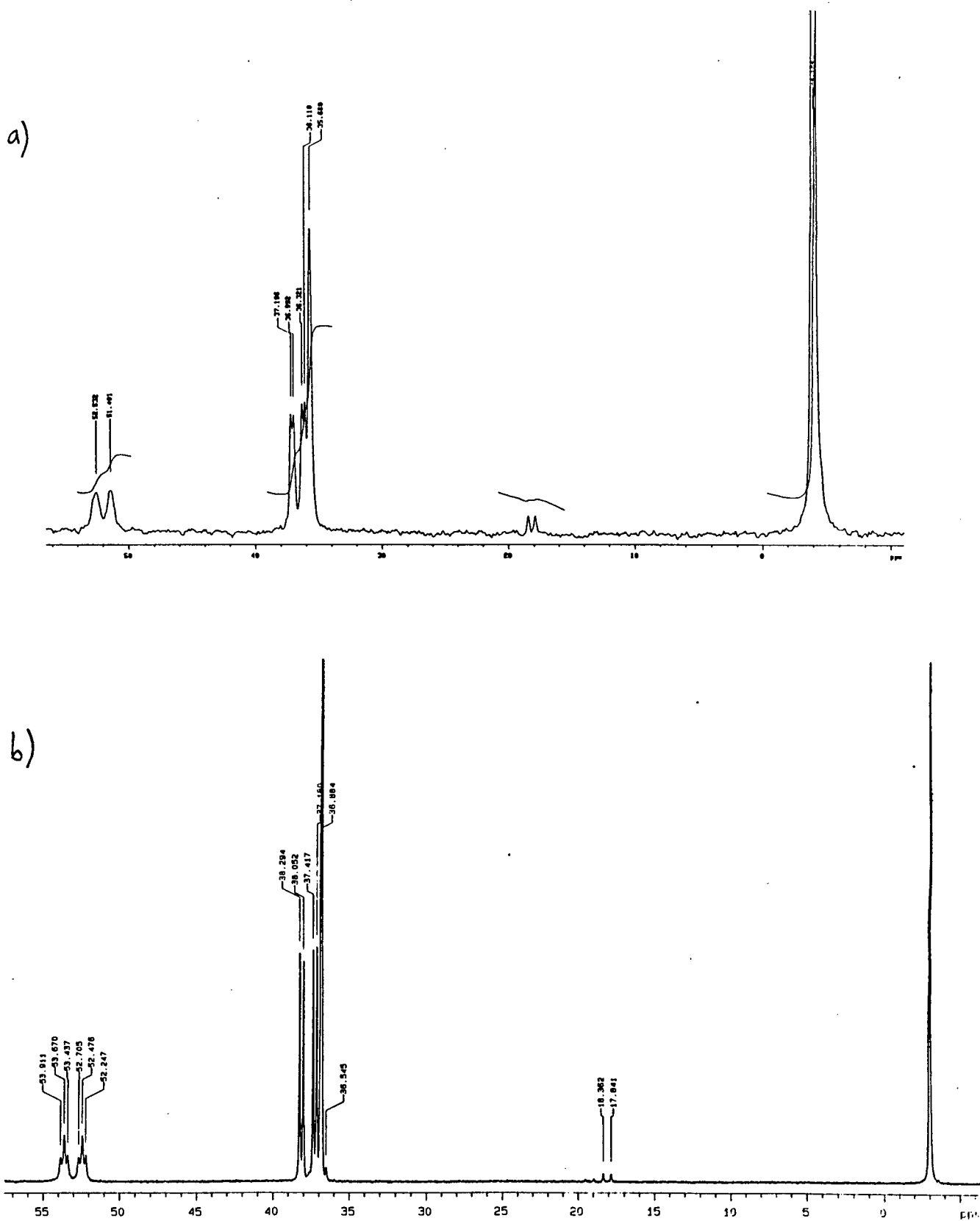


Figure 4.7  $^{31}\text{P}$  NMR spectrum of System 3 (Rh:P:Cl = 1:4:5) after 15 minutes.

Catalyst Speciation



**Figure 4.8**  $^{31}\text{P}$  NMR spectrum of System 3 (Rh:P:Cl = 1:4:5) after *a)* 40 minutes and *b)* one week.

### 4.3.2 Distribution of species under hydroformylation conditions

An aqueous solution of Rh:P:Cl = 1:4:5 was stirred for 16 hours under a CO/H<sub>2</sub> pressure of 5 MPa, at 100 °C. The NMR spectrum showed in Figure 4.9 resulted. The singlet at  $\delta_p = 36.1$  ppm is again assigned to the phosphine oxide, TPPOTS. No unbound ligand, TPPTS remained but two very broad peaks appeared at  $\delta_p = 24.5$  ppm and  $\delta_p = 11.6$  ppm.

The percentage intergrated intensities of the three peaks are as follows:

$\delta_p = 37$	$\delta_p = 24$	$\delta_p = 11.5$
18 %	50 %	32 %

Unfortunately all the coupling information is lost in the broadness of the peaks which most probably due to rapid ligand exchange. The chemical shifts of the two unknown peaks do not correlate to those of any other complexes found in the study under discussion, and as yet the peaks remain unassigned.

### 4.3.3 <sup>31</sup>P NMR spectrum of the synthesised complex, RhH(CO)(TPPTS)<sub>3</sub>

The synthesis of the water-soluble catalytic precursor, RhH(CO)(TPPTS)<sub>3</sub> is discussed in the Experimental section.

The <sup>31</sup>P NMR spectrum, Figure 4.10, compared very closely with that obtained for the same complex by Davies *et al.*<sup>34</sup> The doublet at  $\delta_p = 45.9$  ppm [ $^1J(\text{Rh-P}) = 155.5$  Hz] supports the assignment of a rhodium(I) trigonal bipyramidal structure

where the three equivalent phosphorous atoms lie in the equatorial plane and the CO and H in axial positions. This assignment is also suggested by Davies *et al.* The fairly low Rh<sup>I</sup>-P coupling constant of 155.5 Hz is in agreement with the predicted values of coupling constants for phosphorous ligands in a rhodium(I) complex which lie mutually *trans* to each other.

In this <sup>31</sup>P NMR spectrum, some phosphine oxide is shown ( $\delta_p = 37$  ppm) which results from the oxidation of the free ligand TPPTS during the synthesis of the catalytic precursor, RhH(CO)(TPPTS)<sub>3</sub>.

A doublet also appears at  $\delta_p = 28.3$  ppm [ $^1J(\text{Rh-P}) = 100.2$  Hz) which remains unassigned. This doublet, which is most likely a Rh<sup>I</sup> complex, was also mentioned by Davies *et al.*, but was not assigned.

Catalyst Speciation

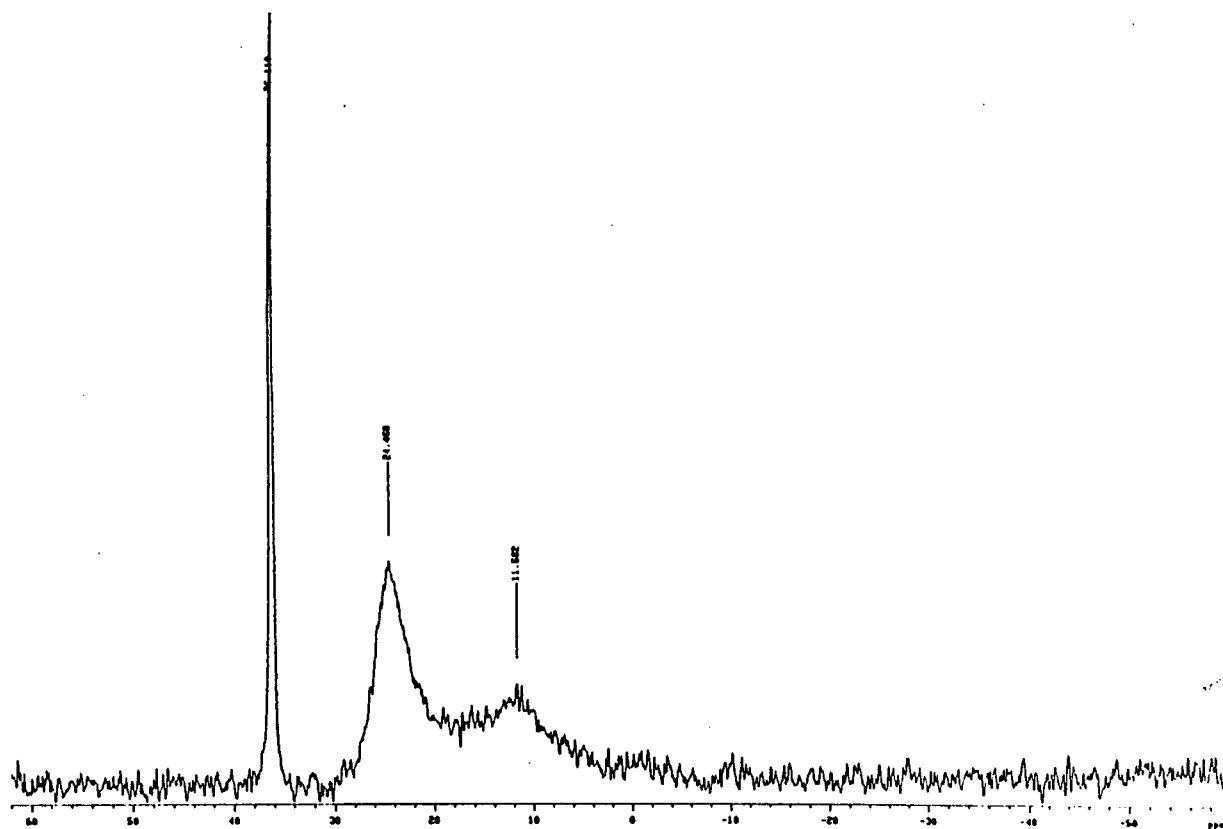


**Figure 4.9**  $^{31}\text{P}$  NMR spectrum of System 4 (Rh:P:Cl = 1:4:5) after hydroformylation conditions (CO/H<sub>2</sub> pressure of 5 MPa and temperature of 100 °C).

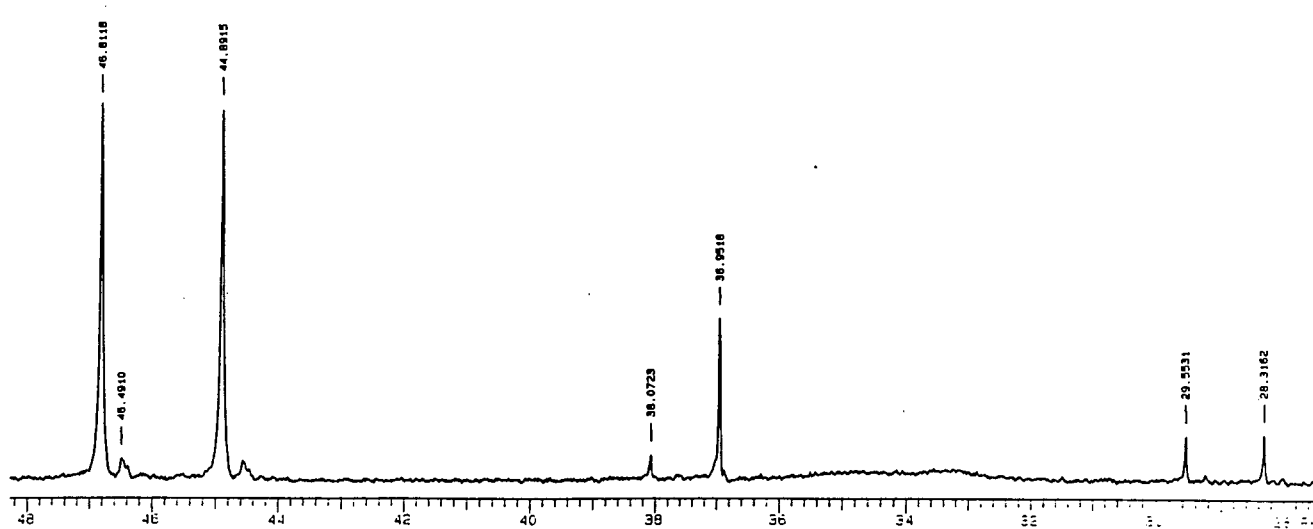


**Figure 4.10**  $^{31}\text{P}$  NMR spectrum of RhH(CO)(TPPTS)<sub>3</sub>

#### 4.4 Conclusion

It can be seen that the number of complexes formed during *in situ* generation of catalytically-active species, can be quite extensive and highly dependent on the conditions of the aqueous solution. None of the complexes found in the  $\text{RhCl}_3 \cdot 3\text{H}_2\text{O}$ / TPPTS system however, could be correlated with the catalytic precursor,  $\text{RhH}(\text{CO})(\text{TPPTS})_3$  which was synthesised separately, even after being subjected to high  $\text{CO}/\text{H}_2$  pressures and temperatures. However,  $\text{RhH}(\text{CO})(\text{TPPTS})_3$  may not necessarily be the active catalytic species. Nevertheless it is expected that the equilibria of the complex  $[\text{RhH}(\text{CO})(\text{TPPTS})_3]$ , with excess phosphine ligand in the aqueous phase under high  $\text{CO}/\text{H}_2$  pressures and temperatures is fairly complex, which is suggested by the number of species found in the organic phase of the corresponding homogeneous catalytic precursor  $\text{RhH}(\text{CO})(\text{PPh}_3)_3$  which has been studied thoroughly by Wilkinson *et al.*<sup>84</sup>

As oxidation of the unbound phosphine ligand (TPPTS) to the corresponding phosphine oxide (TPPOTS) does not seem completely reversible under  $\text{H}_2/\text{CO}$  pressure, the rhodium:phosphine ratio in the catalyst formulation remains unknown and is undoubtedly less than the nominal Rh:P ratio. This limitation is very important since ultimately the effective Rh:P ratio is critical in determining the *n:iso* ratio of the aldehyde products produced from the hydroformylation reaction.

However, the success of the hydroformylation system using the water-soluble catalyst generated *in situ* from  $\text{RhCl}_3 \cdot 3\text{H}_2\text{O}$  and TPPTS in a buffered aqueous solution leads to the irrefutable conclusion that the catalytically-active species are indeed generated under hydroformylation conditions. It is recognised that for a greater understanding of the exact distribution and equilibria of these species during

hydroformylation reactions, a comprehensive study of the system has to be undertaken.

This particular study however, has procured an insight into the nature and distribution of certain rhodium(I) and rhodium(III) tertiary-phosphine complexes, under particular conditions in the aqueous phase. From extended studies of this aqueous system, interesting and valuable information for the design of water-soluble hydroformylation catalysts can be gleaned.

## **Chapter 5**

### **Discussion**

## Chapter 5

### Discussion

In this chapter the results obtained for the hydroformylation of long-chain 1-alkenes, *viz.* 1-octene, 1-decene, and 1-dodecene using a two-phase heterogeneous rhodium–tri(*m*-sulfonatophenyl)phosphine (Rh–TPPTS) catalyst system (outlined in Chapter 3), are discussed.

For the purpose of comparison, the activity and selectivity of the synthesised heterogeneous rhodium catalytic precursor,  $\text{RhH(CO)(TPPTS)}_3$ , and of the conventional homogeneous rhodium catalytic complex,  $\text{RhH(CO)(PPh}_3)_3$ , for the hydroformylation of long-chain 1-alkenes under similar hydroformylation conditions, will also be discussed.

The simplicity of the system used, where the active catalytic species are generated *in situ* from rhodium trichloride ( $\text{RhCl}_3 \cdot 3\text{H}_2\text{O}$ ) and excess water-soluble phosphine ligand, TPPTS, under standard hydroformylation conditions, is considered highly advantageous for industrial applications.

Due to the two distinct phases – the catalytic species in the aqueous phase and the reactants and products in the organic phase – separation of the catalyst from the products was easily facilitated. The hydroformylated products were analysed using quantitative  $^{13}\text{C}$  NMR spectroscopy and gas chromatography. In general, little or no colour was imparted to the organic phase which implied that catalyst loss by leaching into the organic phase was negligible. The aqueous phase containing the catalytic species was washed twice with toluene in order to dissolve any dissolved organic products, and then used for further catalytic reactions if desired.

## 5.1 Two-phase hydroformylation reactions

In this section the results obtained for the two-phase hydroformylation catalytic system which incorporates the use of rhodium catalytic species generated *in situ*, and a synthetically prepared catalytic precursor  $\text{RhH}(\text{CO})(\text{TPPTS})_3$  will be discussed. As these results have already been outlined in detail in Chapter 3, only representative data will be used in this discussion.

### 5.1.1 Rhodium catalytic species prepared in situ

The catalyst system was typically prepared by adding rhodium(III) as the water-soluble  $\text{RhCl}_3 \cdot 3\text{H}_2\text{O}$  to a buffered aqueous solution of the phosphine ligand in the required rhodium:alkene and rhodium:phosphine ratios. The catalytic species are generated in situ under hydroformylation conditions (5 MPa  $\text{H}_2/\text{CO}$  and 100 °C). Each 'catalyst mixture' was reused for hydroformylation reactions a number of times with the limiting factor being the deactivation of the catalyst.

Four different catalytic systems were studied in which the rhodium:phosphine ratios varied from 1:3 to 1:30.

System 1 : Rh:P = 1:3

System 2 : Rh:P = 1:10

System 3 : Rh:P = 1:20

System 4 : Rh:P = 1:30

The following variables of the '*in situ*' catalytic systems were considered:

- alkene chain-length
- rhodium:alkene ratio
- rhodium:phosphine ratio
- stirring rate

*i) Influence of alkene chain-length on activity*

The activity of the heterogeneous system was highly dependent on the chain-length of the 1-alkene used as the substrate. Fairly high conversions of up to 60% were achieved for the hydroformylation of 1-octene to the corresponding aldehyde, nonanal, using a rhodium:alkene ratio of *ca.* 1:200. (In general negligible amounts of alcohols or products resulting from alkene isomerisation or hydrogenation were observed). However, the activity of the system reduced to *ca.* 10% for the hydroformylation of 1-decene, and *ca.* 5% for 1-dodecene. See Table 5.1 below. [The unusually high percentage conversion of 1-decene and 1-dodecene for systems 1 and 2, (Tables 3.1 and 3.2) will be discussed later].

The decrease in the percentage conversion as the molecular weight of the 1-alkene increases is most likely as a result of the hydrophobicity of the long-chain alkenes resulting in extremely low solubilities in water. The solubility of the 1-alkene

**Table 5.1**

Influence of chain-length on the percentage conversion of 1-alkene to the corresponding aldehyde.

1-alkene	Rh:alkene	Percentage composition of products		
		aldehyde	alkene	<i>n:iso</i>
octene	1:151	54	46	7:1
decene	1:133	8.5	91	6:1
dodecene	1:108	3.3	96	6:1

Conditions of hydroformylation: Rh:TPPTS = 1:20,  $P_{\text{CO/H}_2}$  = 5 MPa, T = 100 C, stirred for 24 hours.

decreases as the carbon-chain length (molecular weight) increases. The limited solubility of the alkene in the aqueous phase probably confines the hydroformylation reaction solely to the interface of the organic and aqueous phases (as opposed to the bulk fluid phase in the homogeneous system). The area of contact therefore between the substrate and catalyst is severely reduced, which results in a lower catalytic activity, and therefore lower percentage conversion of the 1-alkene to the corresponding aldehyde.

In order to test this hypothesis, a series of reactions were performed where the stirring rate, and therefore the area of contact of the two phases, was varied. See Table 5.2 below. As is shown by the results, the percentage conversion is dependent on the mixing of the two phases, where a maximum was achieved for this particular reactor, at a stirring-rate of *ca.* 215 rpm. This stirring rate was used for all other hydroformylation reactions, unless otherwise stated.

Table 5.2

Influence of the stirring rate on the percentage conversion of 1-octene.

stirring rate (rpm)	Percentage composition of products				
	aldehyde	alkene	'n'	'iso'	<i>n:iso</i>
0	—	100	—	—	—
100	11.5	84	11.5	<1	~15:1
215	43.5	53	43.5	2.5	17:1
400	42.5	54	42.5	2.5	17:1

Conditions of hydroformylation reactions:  $P_{\text{CO/H}_2} = 5\text{MPa}$ ,  $T = 100\text{ }^\circ\text{C}$ , stirred for 24 hours. Rh:P = 1:30; Rh:olefin = 1:160.

Davies and co-workers introduced a novel family of heterogeneous catalysts, *viz.* supported liquid phase catalysts (SAPC's)<sup>34</sup> in an attempt to increase the activity of the heterogeneous system by providing a large interfacial area for the hydroformylation reaction to take place at. These catalysts consist of a water-soluble organometallic complex supported on a thin film of water residing on a high-surface-area hydrophilic solid support. High conversions of up to 95% and *n:iso* ratios of *ca.* 2:1 were obtained for the hydroformylation of 1-octene with similar Rh:olefin ratios as used in this study. A comparison made by Davies using a similar two-phase system as in this study for the hydroformylation of 1-octene, resulted in <1% conversion in a reaction time of 5.5 hours.<sup>34</sup> However, a system where a 25 wt-% octene solution was subjected to hydroformylation conditions in the presence of solid  $\text{RhH}(\text{CO})(\text{TPPTS})_3$ , resulted in a 98.7% conversion with similar *n:iso* ratios obtained as those with the supported catalysts, *viz.* 2:1. (In the

current study, reactions using the synthesised catalyst precursor,  $\text{RhH(CO)(TPPTS)}_3$  are discussed in part *ii*) in this section). As the complex,  $\text{RhH(CO)(TPPTS)}_3$  is completely insoluble in 1-octene/cyclohexane, Davies concluded that the reaction must occur at the solid/liquid interface.

This leads to the conclusion that the contact area between the catalyst and substrate is a crucial factor in the activity of the heterogeneous system for the hydroformylation of long-chain 1-alkenes.

Horváth, who reports the first comparative study of the biphasic and supported aqueous phase (SAP) catalyst systems,<sup>91</sup> obtains 23% conversion of 1-octene to nonanal, and 4% conversion of 1-decene to the corresponding aldehyde, undecanal, under similar conditions of temperature, pressure and reaction time as used in the current study. The higher olefin:rhodium ratio in Horváth's investigation explains the slightly lower percentage conversion of 1-octene than obtained in this study. An increase in the reaction time did result in a proportional increase in the percentage conversion.

Russel<sup>32</sup> conducted a study on the biphasic heterogeneous hydroformylation of long-chain 1-alkenes using a water-soluble carboxylated phosphine ligand and rhodium system. Although initially the hydroformylation of 1-hexene, 1-dodecene, and 1-hexadecene resulted in less than 3% conversion to the corresponding aldehydes, Russel reports that the conversion increased to as much as 70%, with *n:iso* ratios of up to 1:20 (rhodium:phosphine = 1:10) with the addition of an appropriate phase-transfer agent (rhodium: transfer agent = 1:20). However the use of the phase-transfer agent caused a significant increase in leaching of rhodium into the organic phase, thereby leading to loss of the catalyst.

*ii) Influence of the rhodium concentration (rhodium:alkene ratio)*

The percentage conversion (activity) and selectivities obtained for the hydroformylation of 1-octene, 1-decene, and 1-dodecene, where the rhodium:alkene ratio ranged from 1:26 to 1:263, are shown for a number of catalytic systems in Tables 3.1–3.4. Outlined below in Table 5.3 is some representative data for the percentage conversions obtained with the variation of the rhodium:alkene ratio.

<b>Rh:alkene</b>	<b>alkene</b>	<b>aldehyde</b>	<b>'n'</b>	<b>'iso'</b>	<b>n:iso</b>
1:26	5	94.5	46	49	1:1
1:64	29	71	36	36	1:1
1:106	91.5	8.5	6.5	2	1:3

**Table 5.3**

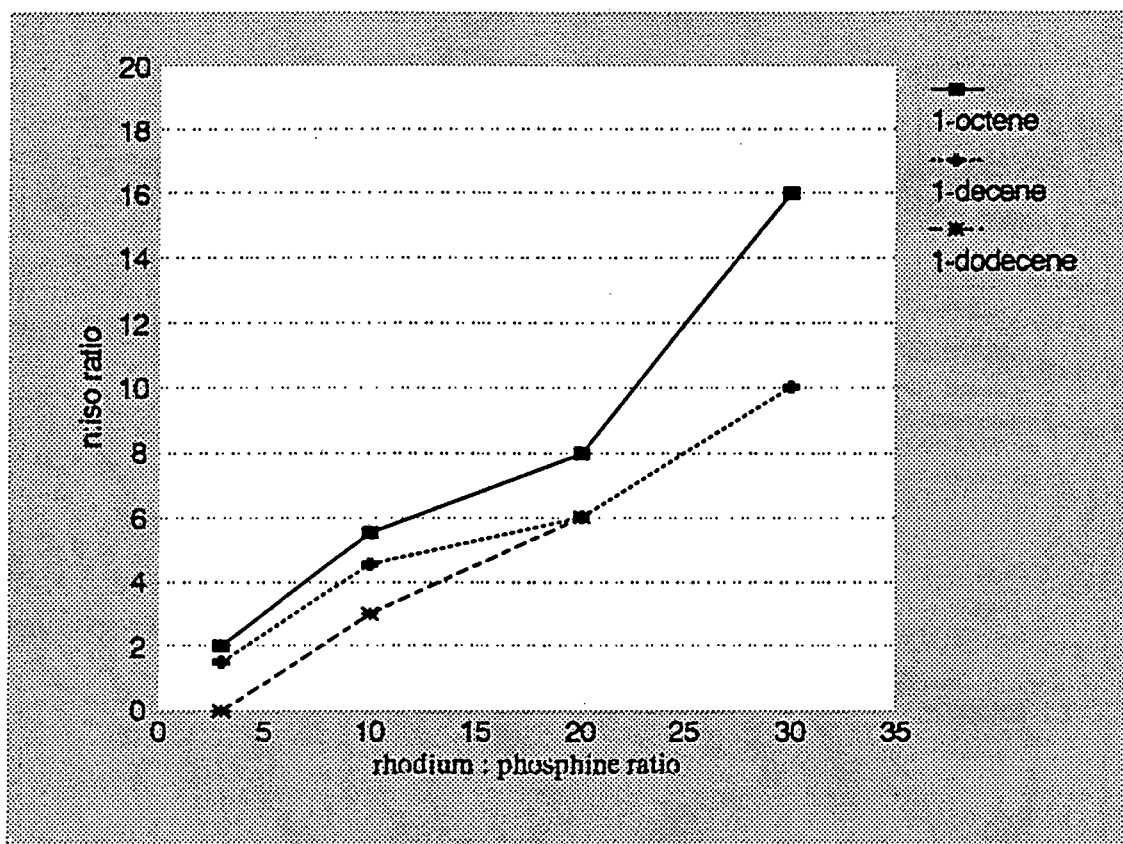
Dependence of percentage conversion (activity) on the rhodium:alkene ratio for the hydroformylation of 1-decene using System 1 (Rh:P = 1:3).

As expected, the activity depended strongly on the rhodium metal concentration *i.e.*, percentage conversion increased as the rhodium:alkene ratio increased. The increase in the effective rhodium concentration did not appear to affect the *n:iso* (linear:branched) ratio of the corresponding aldehydes produced.

*iii) Effect of excess phosphine ligand (Rh:P)*

On increasing the phosphine:rhodium ratio (ratios used ranged from 3:1 to 30:1), the *n:iso* ratios of the aldehydes produced increased significantly, as outlined below:

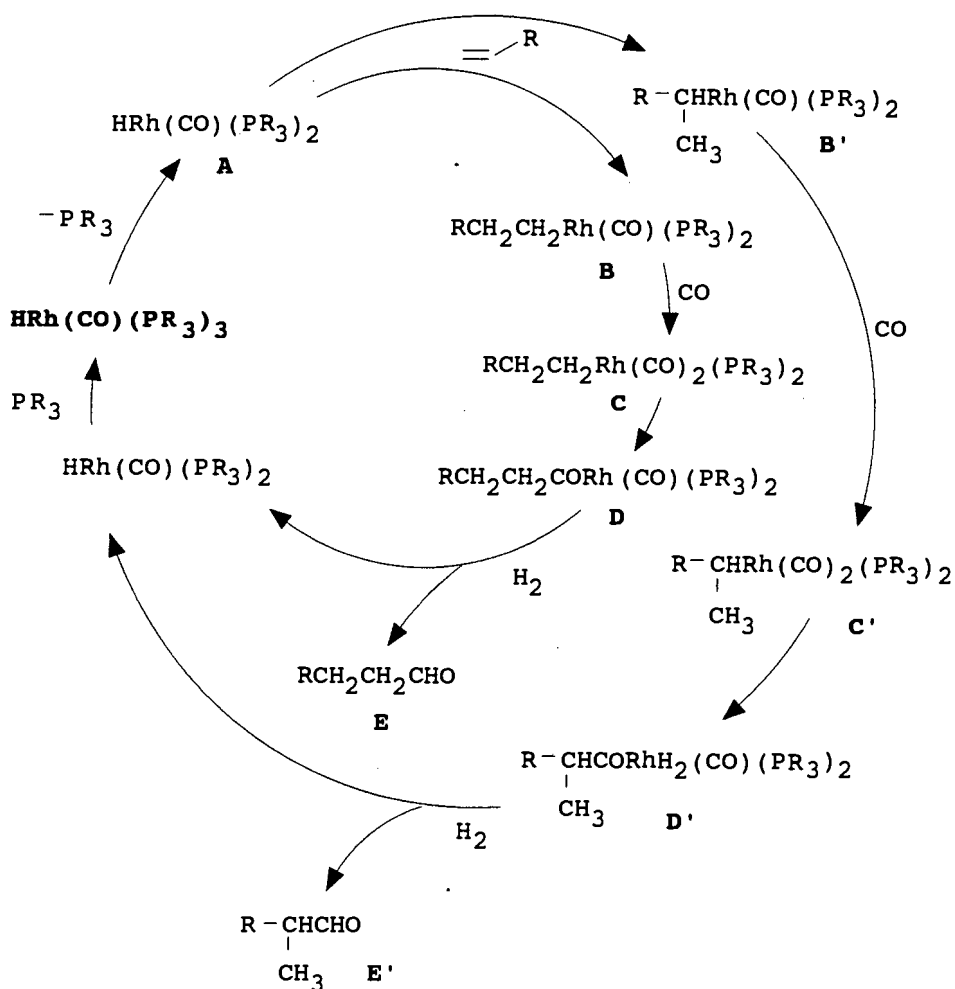
P:Rh ratio	<i>n:iso</i>
3:1	1:1 → 3:1
10:1	3:1 → 6:1
20:1	7:1 → 13:1
30:1	13:1 → 17:1



Graph of the *n:iso* ratio versus rhodium:phosphine ratio

This trend is in agreement with the postulate proposing that a high concentration of the tertiary-phosphine ligand leads to the predominance of rhodium species substituted by more than one bulky phosphine ligand. This species (A) (shown in the catalytic cycle below) presents a more crowded environment for the

approaching alkene substrate, which results in the anti-Markovnikov addition of the CHO (formyl group) and H across the double bond of the alkene, resulting in a coordinated linear alkyl group **B** as opposed to the coordinated branched alkyl group **B'** which is the result of Markovnikov addition of H and CHO.



R = aryl or alkyl group e.g.,  $\text{Ph}_3$

**Scheme 5.1**

Simplified proposed catalytic cycle for hydroformylation using a triphenylphosphine-modified rhodium catalyst.<sup>3</sup>

Oxidative addition of hydrogen ( $H_2$ ) results in the formation of the  $\sigma$ -acyl complex **D** (and **D'**). This is followed by reductive elimination of the acyl group to yield the linear or branched aldehyde, **E** and **E'** respectively, and regenerate the catalytically active rhodium hydride.

High *n:iso* ratios of up to 1:17 were obtained for the catalytic system where the phosphine ligand was thirty times in excess ( $Rh:P = 1:30$ ). The *n:iso* ratios obtained are higher than generally reported for the hydroformylation of shorter-chain alkenes ( $C_3-C_6$ ), although Horváth<sup>91</sup> has reported *n:iso* ratios of as high as 25:1 using a  $Rh:P$  ratio of 1:18 in a two-phase system for the hydroformylation of 1-octene, with  $RhH(CO)(TPPTS)_3$  as the catalytic precursor under similar reaction conditions.

It may be noted with interest that the SAP catalytic system investigated by Davies results in a fairly low *n:iso* ratio of 2.3:1, for the hydroformylation of 1-octene with a  $Rh:P$  ratio of as high as 1:33.<sup>11</sup> This corresponds well with the hydroformylation of 1-alkenes with homogeneous solutions of  $RhH(CO)(PPh_3)_3$  at similar  $Rh:P$  ratios.

It appeared that using  $Rh:P$  ratios of less than 1:20 resulted in rapid deactivation of the catalytic complex. The aqueous catalyst solutions **1** and **2** with a  $Rh:P$  ratio of 1:3 and 1:10 respectively, (Tables 3.1 and 3.2) turned dark brown after 24 hours under hydroformylation conditions, indicating decomposition of the transition-metal catalytic complex. This was also noted in the study of a similar two-phase system by Davies and coworkers using a  $Rh:P$  ratio of 1:8.<sup>11</sup> The activity of both Systems **1** and **2** decreased significantly and reached zero after about the fifth catalytic run (reuse of catalyst) in each case:

Systems 3 and 4, using a P:Rh ratio of 20:1 or greater, resulted in a clear yellow aqueous phase after the first reaction, which indicates reduction of rhodium(III) to rhodium(I). Even after *ca.* ten repeated runs using the same catalyst mixture, the aqueous solution containing the catalytic species of the two systems remained yellow. This is probably due to the effect of stabilisation of the rhodium catalytic species by the excess phosphine ligand, which is in accord with theory.<sup>5</sup> In systems 3 and 4, with Rh:P = 1:20 and Rh:P = 1:30 respectively, the catalyst was still active when the last reaction was performed and a study of the actual catalyst life-time under these conditions of excess phosphine ligand was not conducted.

When comparing each catalytic system (*i.e.* all the reactions using one catalyst mixture), the total turnover number, *i.e.* the total number of moles of hydroformylation products (aldehydes and alcohols) formed per mole of rhodium used, was significantly higher in the cases where the phosphine:rhodium ratio was greater than 10:1. The actual values of the the overall turn-over number (TON) for the different catalytic systems are not truly comparative as the total TON for catalytic systems 3 and 4 where Rh:P = 1:20 and 1:30, was not determined.

It was also noted that the organic phase was more coloured (brown/yellow) in systems with a low P:Rh ratio ( $\leq 10:1$ ) after 24 hours under hydroformylation conditions, than when operating with higher P:Rh ratios. The colour can be attributed to the leaching of some water-soluble rhodium species into the organic phase.

An interesting observation of the activity of the systems with low P:Rh ratios (*i.e.*,  $\leq 1:10$ ) was made. Although deactivation of the entire catalytic system was rapid (activity of the system after five consecutive runs was zero), a high percentage conversion of up to 69% for the hydroformylation of 1-decene and 52% for that of

1-dodecene to the corresponding aldehydes resulted during the first few repeated runs. This was particularly noticeable for system 2 (Rh:P = 1:30); after which reactions the organic phase was the most coloured. (See Table 3.2). It is suggested that the unusually high activity is due to the "homogeneous" activity of rhodium catalytic species leached into the organic phase, *i.e.*, corresponding to a homogeneous hydroformylation reaction. However, as the activity of the two-phase system decreased very quickly after the third or fourth run due to the deactivation of the rhodium catalytic solution, this is obviously an unbeneficial feature.

It was found in studies of the catalytic species present (discussed in Chapter 4), that the majority of the excess phosphine ligand is oxidised, apparently irreversibly, to the corresponding phosphine oxide, TPPTOS, under hydroformylation conditions. The effective P:Rh ratio therefore remains unknown but is undoubtedly less than the nominal P:Rh ratio. Being a phosphorous(V) compound, the phosphine oxide probably does not coordinate to the transition-metal complex which effectively results in a decrease in the concentration of the coordinating phosphine ligand. However, this does not seem to affect the activity or 'stability' of the system where the phosphine ligand is present in an excess of twenty times or more. In fact there is an interesting report by Onada<sup>92</sup> of a commercial system for the hydroformylation of 1-octene, which claims that the use of an oxidised phosphine ligand (triphenylphosphine oxide) increases the activity of the system due to its weak ligand effect on rhodium.

It is important to note that in the literature, cases where the amount of phosphine ligand is excessive *i.e.*, greater than 100 times that of rhodium, a decrease in the activity of the system is noted<sup>17</sup>. This results in a necessity for compromise between the effect of increased stability of the catalytic complex and therefore a longer catalyst lifetime, and the effect of a decrease in activity due to the excessive

concentration of the phosphine ligand. However, in the current study the greatest P:Rh ratio used was only 30:1 and no definite trend of a decrease in activity was observed when comparing the results of the percentage conversions obtained for systems with low P:Rh ratios (3:1, 10:1) to those with higher P:Rh ratios (20:1, 30:1).

### Conclusion

The two-phase hydroformylation catalytic systems discussed above demonstrated poor conversions (activity) of 1-decene and 1-dodecene which are not comparable to conversions obtained using the homogeneous hydroformylation system with the catalyst precursor,  $\text{RhH}(\text{CO})(\text{PPh}_3)_3$ , reported in Section 3.2.2. However, the activity of the system for the hydroformylation of 1-octene was significantly higher, and very good *n:iso* ratios of 1:17 using Rh:P ratios of 1:30, were obtained, which are higher than most reported in similar systems. Overall the percentage conversions were lower than those reported for the heterogeneous hydroformylation of short-chain 1-alkenes ( $\text{C}_3 - \text{C}_6$ ) using biphasic or supported catalytic systems as discussed previously.

The reason proposed for the fairly low activity, particularly for the higher molecular weight alkenes ( $\text{C}_{10}-\text{C}_{12}$ ), is twofold.

The main cause of the reduced activity compared to that of the homogeneous system, is the very nature of the heterogeneous system where the area of contact between the catalyst and substrate is much smaller than in the homogeneous system. The activity is further reduced by the extremely low solubilities of the long-chain 1-alkenes ( $\text{C}_8 - \text{C}_{12}$ ), as compared to those of shorter-chain alkenes, in the aqueous phase. As the hydroformylation reaction is thought to take place solely at the interface of the two phases where the catalyst and substrate come into contact, the

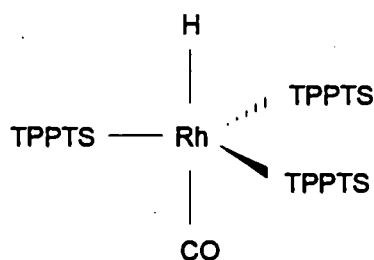
result is a very small contact surface-area which leads to a reduction in the activity of the two-phase system.

When comparing reported biphasic and supported catalyst systems, the activity of the latter system for the hydroformylation of 1-alkenes is usually higher than that of the biphasic system under similar conditions. (This trend becomes more pronounced as the molecular weight of the alkene increases). This higher activity can be attributed to the higher surface area presented to the alkene substrate by the supported catalyst. A similar two-phase catalytic system to that used in this study is reported using rhodium and ruthenium complexes of the water-soluble phosphine ligand  $[\text{Na}(m\text{-SO}_3\text{C}_6\text{H}_4\text{PPh}_2)]$ ,<sup>33</sup> in which these systems are virtually inactive for the hydroformylation of similar long-chain 1-alkenes, unless a water-soluble organic solvent is added.

### 5.1.2 Heterogeneous hydroformylation using a synthesised catalyst precursor, $\text{RhH}(\text{CO})(\text{TPPTS})_3$

This study was carried out in order to compare the performance of the system discussed above in which the catalytically active species are created *in situ*, with that of a system which utilizes the transition-metal catalyst precursor,  $\text{RhH}(\text{CO})(\text{TPPTS})_3$ .

The water-soluble complex  $\text{RhH}(\text{CO})(\text{TPPTS})_3$  is based on the well-known homogeneous hydroformylation catalyst,  $\text{RhH}(\text{CO})(\text{PPh}_3)_3$ . The trigonal bipyramidal rhodium(I) complex shown below, was synthesised through a modification of the method used for the preparation of the homogeneous complex  $\text{RhH}(\text{CO})(\text{PPh}_3)_3$ , which is discussed in the Experimental Section.



Schematic representation of the  
catalytic precursor,  $\text{RhH(CO)(TPPTS)}_3$

### *Reaction Procedure*

An appropriate amount of the complex  $\text{RhH(CO)(TPPTS)}_3$  required to yield 0.21 mmole of rhodium, corresponding to the amount used for previous reactions, was dissolved in 20 ml aqueous buffer solution resulting in an orange solution, and the same procedure followed as described previously in part (i). The catalytic reactions were carried out under exactly the same conditions as used previously *i.e.*, stirred for 24 hours under a  $\text{CO/H}_2$  pressure of 5 MPa, at a temperature of 100 °C.

### *Results and Discussion*

Poorer conversions for the hydroformylation of 1-octene to nonanal of *ca.* 30% resulted, compared to *ca.* 50% obtained for the reactions under the same conditions where the catalytic species are generated *in situ*. See Table 3.7 and 3.8. The conversion of 1-decene and 1-dodecene to aldehydes was below the detection limit (< 0.1%).

A system was examined without excess phosphine ligand (Table 3.7), and as before it was noted that the activity of the system dropped to a negligible amount after four repeated runs. The aqueous phase which was initially orange, turned black after the first reaction, indicating decomposition of the catalyst due to the lack of stabilisation of the catalytic species by the phosphine ligand.

Stabilising the system with the addition of excess phosphine ligand (Rh:P =1:20) resulted in similar activity of *ca.* 30% but showed the advantage of an increased catalyst life-time. After the initial run the solution turned yellow, indicating the formation of other rhodium species by the action of CO and H<sub>2</sub> under pressure. The percentage conversion of 1-octene to nonanal, remained similarly low however, and again the conversion of 1-decene and 1-dodecene was below the detection limit. Similar *n:iso* ratios were obtained as those resulting in the "*in situ*" systems with the same Rh:P ratios.

## 5.2 Homogeneous hydroformylation

Secondly for comparative purposes, the analogous homogeneous catalytic precursor, RhH(CO)(PPh<sub>3</sub>)<sub>3</sub> was investigated under similar conditions.

The homogeneous hydroformylation process using modified rhodium catalysts implemented in the 1970's by Union Carbide, operates at the relatively low pressures (2-3 MPa) and temperatures (60-120 °C) in the presence of synthesis gas and produces *n:iso* ratio of 15:1.<sup>5</sup>

In order to make an objective comparison of the heterogeneous and homogeneous hydroformylation systems under the same conditions used in this study, the transition-metal complex, RhH(CO)(PPh<sub>3</sub>)<sub>3</sub> was synthesised and used as the catalytic precursor for the homogeneous hydroformylation of 1-octene, 1-decene, and 1-dodecene under the same conditions of temperature (100 °C), pressure (5 MPa) and reaction time (24 hours).

The results obtained (shown in Table 3.9) are far superior to those obtained for the heterogeneous system. Conversions of 100% for all three substrates resulted, with *n:iso* ratios of up to 1:10 depending on the Rh:P ratios used which corresponded to those reported in the literature.<sup>19</sup>

### 5.3 Conclusion

The application of a two-phase rhodium-tri(*m*-sulfonatophenyl)phosphine system for the hydroformylation of long-chain 1-alkenes ( $C_8 - C_{12}$ ) was investigated.

Compared to the highly successful heterogeneous hydroformylation reactions performed on short-chain 1-alkenes ( $C_3 - C_6$ ) which has been commercialised by Rhône-Poulenc,<sup>67</sup> little success has been achieved in the conversion of higher molecular weight alkenes ( $C_8 - C_{12}$ ) to the corresponding aldehydes, using two-phase heterogeneous systems. In fact, the commercial hydroformylation of higher olefins ( $C_6$  or larger) is currently performed exclusively using homogeneous cobalt carbonyl-derived catalysts<sup>93</sup>. The complexity of the two-phase reaction system leads to the prediction that the design of an industrial plant for the hydroformylation of high molecular weight 1-alkenes will not be trivial.

However, fairly good conversions of *ca.* 60% with unexpectedly high *n:iso* ratios of 1:17, for the hydroformylation of 1-octene to nonanal were obtained. Moreover, the system utilised, where the catalytically-active species are generated *in situ* from  $RhCl_3 \cdot 3H_2O$  and excess phosphine ligand under standard hydroformylation conditions, has the advantage of simplicity which is extremely beneficial in the application of this system to an industrial scale. It is no less superior in terms of

activity and selectivity than the two-phase system using the synthesised catalyst precursor,  $\text{RhH}(\text{CO})(\text{TPPTS})_3$ . Unfortunately the extremely low solubility of 1-decene, 1-dodecene and to a lesser extent, 1-octene, proved to be a crucial and limiting factor in the conversion of the alkenes to the corresponding aldehydes.

Although superior activities are achieved with the analogous SAPC system reported by Davies and coworkers<sup>34</sup>, the production of linear aldehydes (*i.e.* high *n:iso* ratios) which is a most important factor in the hydroformylation of 1-alkenes, is substantially lower than that found for the two-phase system under study.

Another expedient feature of this system is the lower phosphine ligand excess necessary for the attainment of high *n:iso* ratios. Thus the necessity to compromise between high *n:iso* ratios and a decreased activity as a result of a high phosphine concentration is not an important consideration.

With an improved reactor design and possible use of surfactants (phase-transfer agents) the limitation imposed by the insolubility of the alkene in the aqueous phase can possibly be overcome, and comparably high activities may be combined with the beneficial feature of high *n:iso* ratios and a simple catalytic system, in the production of industrially valuable linear aldehydes.

## **References**

## REFERENCES

1. *Homogeneous Catalysis with Metal Phosphine Complexes*, Ed. L.H. Pignot, Plenum Press, New York, 1983.
2. R.L. Dickson, *Homogeneous Catalysis with Complexes of Rhodium and Iridium*, D. Reidel Publishing Company, Dordrecht, Holland, 1985.
3. G.W. Parshall, *Homogeneous Catalysis – the applications and chemistry of catalysis by soluble transition-metal complexes*, John Wiley and Sons, New York, 1980
4. O. Roelen, German Patent, AG 849 548, Ruhrchemie, 1938.
5. C. Masters, *Homogeneous Transition-metal Catalysis*, Chapman and Hall, London, 1981.
6. R.F. Heck and D.S. Heslow, *J. Am. Chem. Soc.*, 1961, **83**, 4023.
7. L.H. Slaugh and R.D. Mullineaux, US Patents, 3, 239, 569 and 3, 239, 570, 1966.
8. R.L. Pruett, *Ann. N. Y. Acad. Sci.*, 1977, **295**, 239.
9. G. Yagupsky, D. Evans, and G. Wilkinson, 1970, *J. Chem. Soc. A*, 1392.
10. G.F. Pregaglia, A. Andreetta, G.F. Ferrari, and R. Ugo, *J. Organomet. Chem.*, 1972, **2**, 554.
11. D.E. Morris and H.B. Tinker, *Chem. Technol.*, 1972, **2**, 554.
12. G. Henrici-Olivé and S. Olivé, *Transition Met. Chem.*, 1976, **1**, 77.
13. C.A. Tolman, *Chem. Rev.*, 1977, **77**, 313.
14. A.A. Oswald, D.E. Hendriksen, R.V. Kastrup, and E.J. Mozeleski, *Adv. Chem. Ser.*, 1992, **230**, 395.
15. R.L. Pruett and J.A. Smith, *J. Org. Chem.*, 1969, **34**, 327.
16. P.W.N.M. Van Leeuwen and C.F. Roobeek, *J. Organomet. Chem.*, 1983, **258**, 343.

## References

17. C.F. Roobeek and P.W.N.M. Van Leeuwen, U.S. Patent, 4 467 116, 1984.
18. T. Yoshida, T. Okano, Y. Ueda, and S. Otsuka, *J. Am. Chem. Soc.*, 1981, **103**, 3411.
19. M.A. Freeman and D.A. Young, *Inorg. Chem.*, 1986, **25**, 1556.
20. K. A. Alekseeva, M.D. Vysotski, N.S. Imayanitov, and V.A. Rybakov, *Zh. Vses. Khim. Ova im D.I. Mendeleeva*, 1977, **22**, 45.
21. G. Montservat, G. Muller, D. Sainz, and J. Sales, *Organometallics*, 1991, **10**, 4036.
22. A. Scrivanti, S. Pagnelli, U. Matteoli, and C. Botteghi, *J. Organomet. Chem.*, 1990, **385**, 439.
23. L. Kollár, J. Bakos, I. Toth, and B. Heil, *J. Organomet. Chem.*, 1988, **350**, 277.
24. P.W.N.M. van Leeuwen, C.F. Roobeek, R.L. Wife, and H.G. Frijns, *J. Chem. Soc., Chem. Commun.*, 1986, 31.
25. A.G. Abatjoglou, E. Billig, and D.R. Bryant, *Organometallics*, 1984, **3**, 923.
26. M.K. Markiewicz and M.C. Baird, *Inorg. Chim. Acta*, 1986, **113**, 95.
27. R.T. Smith and M.C. Baird, *Inorg. Chim. Acta*, 1982, **62**, 135.
28. F. Joó and Z. Tóth, *J. Mol. Catal.*, 1980, **8**, 369.
29. E. G. Kuntz, *Chemtech*, 1987, **17**, 570.
30. J.P. Arhancet, M.E. Davies, J.S. Merola, and B.E. Hanson, *Nature*, 1989, **339**, 454.
31. Ph. Kalck, P. Escaffre, F. Serein-Spiran, and A. Thorez, *New J. Chem.*, 1988, **12**, 687.
32. M.J.H. Russel, *Platinum Met. Rev.*, 1988, **32**, 179.
33. A.F. Borowski, D.J. Cole-Hamilton, and G. Wilkinson, *Nouv. J. Chim.*, 1978, **2**, 137.
34. J.P. Arhancet, M.E. Davies, J.S. Merola, and B.E. Hanson, *J. Catal.*, 1990, **121**, 327.
35. J.P. Arhancet, M.E. Davies, J.S., and B.E. Hanson, *J. Catal.*, 1991, **129**, 94.

## References

36. J.P. Arhancet, M.E. Davies, and B.E. Hanson, *J. Catal.*, 1991, **129**, 100.
37. I. Guo, B. E. Hanson, I. Tóth, and M.E. Davis, *J. Organomet. Chem.*, 1991, **403**, 221.
38. J. P. Collman, J.A. Belmont, and J. I. Brauman, *J. Am. Chem. Soc.*, 1983, **105**, 7288.
39. S. Naito and M. Tanimoto, *J. Chem. Soc., Chem. Commun.*, 1989, 1403.
40. K. Asakura, K. Kitamura-Bando, K.I. Sobe, H. Arakawa, and Y. Iwasawa, *J. Am. Chem. Soc.*, 1990, **112**, 3242.
41. D.C. Bailey and S.H. Langer, *Chem. Rev.*, 1981, **81**, 109.
42. R.E. Davis, J.A. Rossin, and M.E. Davis, *J. Catal.*, 1986, **98**, 477.
43. D.F. Taylor, B.E. Hanson, and M.E. Davis, *Inorg. Chim. Acta*, 1987, **128**, 55.
44. K. S. Ro and S.I. Woo, *J. Mol. Catal.*, 1990, **61**, 27.
45. K. S. Ro and S.I. Woo, *Appl. Catalysis*, 1991, **69**, 169.
46. N.A. de Munck, M.W. Verbruggen, J.E. de Leur, and J.J.F. Scholten, *J. Mol. Catal.*, 1981, **11**, 331.
47. L. Alrila, T.A. Pakkanen, and T.T. Pakkanen, *J. Mol. Catal.*, 1992, **71**, 281.
48. H.J. Zong, X.Y. Guo, Q. Tang, and Y. Jin, *J. Macromol. Sci., Chem.*, 1987, **A24**, 277.
49. P. Terreros, E. Pastor, J.M. Palacios, and J.L.G. Fierro, *Surf. Interface Anal.*, 1990, **15**, 279.
50. F. Ciardelli, G. Braca, C. Carlini, G. Sbrana, and G. Valentini, *J. Mol. Catal.*, 1982, **14**, 1.
51. W.H. Lang, A.T. Jurewicz, W.O. Haag, D.D. Whitehurst, and L.D. Rollmann, *J. Organomet. Chem.*, 1977, **134**, 85.
52. R.H. Grubbs and E.M. Sweet, *J. Mol. Catal.*, 1977, **3**, 259.
53. S.C. Tang, T.E. Paxson, and L. Kim, *J. Mol. Catal.*, 1980, **9**, 313.
54. M.H.J.M. De Croon, and J.W.E. Coenen, *J. Mol. Catal.*, 1981, **11**, 301.

## References

55. L. Bemis, H.C. Clark, J.A. Davies, C.A. Fyfe, and R.E. Washington, *J. Am. Chem. Soc.*, 1982, **104**, 438.
56. W. Strohmeier and M. Michel, *J. Catal.*, 1981, **69**, 209.
57. P. Barbier, *Comptes Rendus*, 1899, **128**, 110.
58. V. Grignard, *C.R. Hebd. Seances Acad. Sci.*, 1900, **130**, 1322.
59. K. Ziegler, *Angew. Chem.*, 1955, **65**, 426.
60. M.S. Spencer and D.A. Dowden, US Patent, 3,009 969, 1961.
61. J.K. Kwiatek, I.L. Madok, and J.K. Syeler, *J. Am. Chem. Soc.*, 1962, **84**, 304.
62. J. Chatt, G.J. Leigh, and R.M. Slade, *J. Chem. Soc. Dalton Trans.*, 1973, 2021.
63. E.G. Kuntz, French Patent, 2 314 910, Rhône-Poulenc, 1975; and US Patent, Re 31812, 1982.
64. S. Ahland, J. Chatt, N.R. Davies, and A.A. Williams, *J. Chem. Soc.*, 1958, 276, 88.
65. R.T. Smith, R.K. Ungar, L.J. Sanderson, and M.C. Baird, *Organometallics*, 1983, 1138.
66. M.C. Markiewicz and M.C. Baird, *Inorg. Chim. Acta*, 1986, **113**, 95.
67. Ruhrchemie, German Patent, 3235030, 1982.
68. E.G. Kuntz, French Patent, 2 314 910, Rhône-Poulenc, 1975.
69. S.S. Bath and L. Vaska, *J. Am. Chem. Soc.*, 1963, **85**, 3500.
70. N. Ahmed, S.D. Robinson, and M.M. Uttley, *J. Chem. Soc. A*, 1968, 2600.
71. J.N. Schoolery, *Prog. Nucl. Magn. Reson. Spectrosc.*, 1977, **11**, 79.
72. G.C. Levy, R.L. Lichter, and G.L. Nelson, *Carbon-13 Nuclear Magnetic Resonance Spectroscopy*, John Wiley and Sons, New York, 1980.
73. K.R. Williams and R.W. King, *J. Chem. Educ.* 1990, **67**, A93.
74. G.N. LaMar, *J. Am. Chem. Soc.*, 1971, **93**, 1040
75. R.W. King and K.R. Williams, *J. Chem. Educ.*, 1989, **66**, A243.

## References

76. J.B. Stothers, *Carbon-13 NMR Spectroscopy*, Academic Press, New York, 1972.
77. C. O'Connor and G. Wilkinson, *J. Chem. Soc. A*, 1968, 2665.
78. F.A. Cotton and G. Wilkinson, *Advanced Inorganic Chemistry*, John Wiley and Sons, New York, 1988.
79. P.S. Pregosin and R.W. Kunz, *<sup>31</sup>P and <sup>13</sup>C NMR of transition-metal complexes*, Springer-Verlag, Berlin, 1979, p. 9.
80. D.A. Palmer and G.M. Harris, *Inorg. Chem.*, 1975, **14**, 1316.
81. W. Robb and G.M. Harris, *J. Am. Chem. Soc.*, 1965, **87**, 4472.
82. S.A. Cotton and F.A. Hart, *The Heavy Transition Elements*, The MacMillan Press Ltd, London, 1975.
83. P.R. Brooks and B.L. Shaw, *Chem. Commun.*, 1968, 919.
84. J.A. Osborn, F.H.J. Jardine, J.F. Young, and G. Wilkinson, *J. Chem. Soc. A*, 1966, 1711.
85. T.G. Appleton, H.C. Clark, and L.E. Manzer, *Coord. Chem. Rev.*, 1973, **10**, 335.
86. T.H. Brown and P.J. Green, *J. Am. Chem. Soc.*, 1970, **92**, 2359.
87. P.A.W. Dean and R.J. Gillespie, *J. Am. Chem. Soc.*, 1970, **92**, 2359.
88. B.E. Mann, C. Masters, and B.L. Shaw, *J. Chem. Soc. Dalton*, 1974, 704.
89. S.O. Grim and L.C. Satek, *J. Coord. Chem.*, 1974, **3**, 307.
90. C.A. McAuliffe, *Transition-metal complexes of Platinum, Arsenic, and Antimony ligands*, The MacMillan Press Ltd, London, 1973.
91. I.T. Horváth, *Catal. Lett.*, 1990, **6**, 43.
92. T. Onada, *Chemtech*, 1993, **23**, 34.
93. L.H. Slaugh and R.D. Mullineaux, *J. Organomet. Chem.*, 1968, **13**, 469.